

NO-A166 111

TESTS OF BURIED LIFELINES AND  
INSTRUMENTATION/COMMUNICATION CONDUITS(U) HERRITT CASES  
INC REDLANDS CA H C DAVIS ET AL. 01 JAN 84

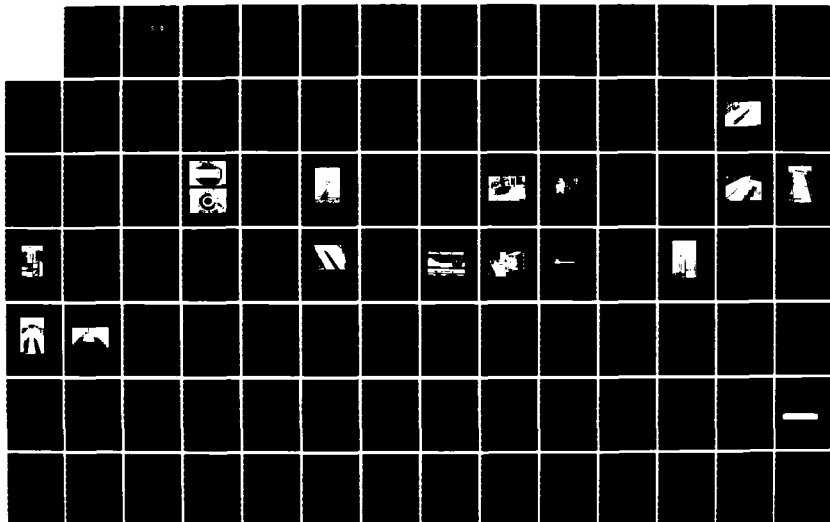
1/2

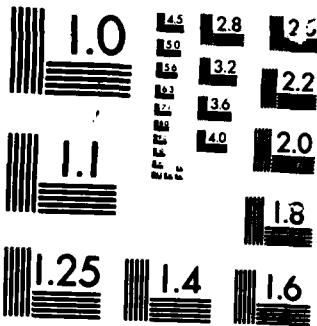
UNCLASSIFIED

DNA-TR-84-442 DNA001-81-C-0242

F/G 17/2

NL





MICROCOPY RESOLUTION TEST CHART

**AD-A166 111**

12

**DNA-TR-84-442**

**TESTS OF BURIED LIFELINES AND  
INSTRUMENTATION/COMMUNICATION CONDUITS**

**H.C. Davis  
G.L. Wintergerst  
K.B. Morrill  
J.L. Merritt  
Merritt CASES, Inc.  
P.O. Box 1206  
Redlands, CA 92373-0401**

**DTIC  
ELECTE  
S D  
APR 10 1984  
D**

**1 January 1984**

**Technical Report**

**CONTRACT No. DNA 001-81-C-0242**

**GRANT No. NSF CEE-81-05791**

**Approved for public release;  
distribution is unlimited.**

THIS WORK WAS SPONSORED BY THE DEFENSE NUCLEAR AGENCY  
UNDER RDT&E RMSS CODE B344081466 Y99QAXSC00028 H2590D  
AND THE NATIONAL SCIENCE FOUNDATION UNDER NSF GRANT NO.  
CEE-81-05791.

**Prepared for  
Director  
DEFENSE NUCLEAR AGENCY  
Washington, DC 20305-1000**

**NATIONAL SCIENCE FOUNDATION  
Washington, DC 20550**

**DTIC FILE COPY**

**86 2 7 017**

Destroy this report when it is no longer needed. Do not return to sender.

PLEASE NOTIFY THE DEFENSE NUCLEAR AGENCY, ATTN: STTI, WASHINGTON, DC 20305-1000, IF YOUR ADDRESS IS INCORRECT, IF YOU WISH IT DELETED FROM THE DISTRIBUTION LIST, OR IF THE ADDRESSEE IS NO LONGER EMPLOYED BY YOUR ORGANIZATION.



UNCLASSIFIED

SECURITY CLASSIFICATION OF THIS PAGE

RDT&amp;E

## REPORT DOCUMENTATION PAGE

Form Approved  
OMB No. 0704-0188  
Exp. Date: Jun 30, 1986

1a. REPORT SECURITY CLASSIFICATION <b>UNCLASSIFIED</b>		1b. RESTRICTIVE MARKINGS	
2a. SECURITY CLASSIFICATION AUTHORITY		3. DISTRIBUTION/AVAILABILITY OF REPORT Approved for public release; distribution is unlimited.	
2b. DECLASSIFICATION/DOWNGRADING SCHEDULE N/A since UNCLASSIFIED		5. MONITORING ORGANIZATION REPORT NUMBER(S) DNA-TR-84-442	
4. PERFORMING ORGANIZATION REPORT NUMBER(S)		7a. NAME OF MONITORING ORGANIZATION Director Defense Nuclear Agency	
6a. NAME OF PERFORMING ORGANIZATION Merritt CASES, Inc.	6b. OFFICE SYMBOL (if applicable)	7b. ADDRESS (City, State, and ZIP Code) Washington, DC 20305-1000	
6c. ADDRESS (City, State, and ZIP Code) P.O. Box 1206 Redlands, CA 92373-0401		9. PROCUREMENT INSTRUMENT IDENTIFICATION NUMBER DNA 001-81-C-0242 NSF Grant CEE-81-05791	
8a. NAME OF FUNDING/SPONSORING ORGANIZATION	8b. OFFICE SYMBOL (if applicable)	10. SOURCE OF FUNDING NUMBERS	
8c. ADDRESS (City, State, and ZIP Code)		PROGRAM ELEMENT NO. 62715H	PROJECT NO. Y99QAXS
		TASK NO. C	WORK UNIT ACCESSION NO. DH005605
11. TITLE (Include Security Classification) TESTS OF BURIED LIFELINES AND INSTRUMENTATION/COMMUNICATION CONDUITS			
12. PERSONAL AUTHOR(S) H.C. Davis G.L. Wintergerst K.B. Morrill J.L. Merritt			
13a. TYPE OF REPORT Technical Report	13b. TIME COVERED FROM 810821 TO 830821	14. DATE OF REPORT (Year, Month, Day) 840101	15. PAGE COUNT 196
16. SUPPLEMENTARY NOTATION This work was sponsored by the Defense Nuclear Agency under RDT&E RMSS Code B344081466 Y99QAXSC00028 H2590D and the Natl Science Foundation under NSF Grant No. CEE-81-05791.			
17. COSATI CODES		18. SUBJECT TERMS (Continue on reverse if necessary and identify by block number)	
FIELD	GROUP	SUB-GROUP	
13	11		Instrumentation Conduits Pullout Tests
14	2		Communication Conduits Shear Tests
			Underground Lifelines Shear Offset
19. ABSTRACT (Continue on reverse if necessary and identify by block number) Over 100 laboratory tests were conducted to investigate the performance of buried life-line/instrumentation conduits. The tests were of two basic types: (1) axial pullout tests of 1 in. and 1/4 in. steel conduit in a pressurized sand backfill, and (2) shear offset tests of 4 in. ductile iron and vitrified clay pipe also in a pressurized sand backfill.  The pullout tests were performed to investigate conduit/backfill axial slip characteristics as a function of backfill confining pressure, conduit diameter and conduit length. A limited number of pullout tests were also performed to assess the effects of loading rate and moisture content in the backfill. The behavior was evaluated in terms of pullout force vs. slip displacement measured at the far end of the conduit. These results indicated a straight line relationship between pullout load and backfill confining pressures up to confining pressures of 4 MPa. Computed coefficients of sliding friction ranged between 0.17 and 0.20 for the 1 in. conduit and 0.07 to 0.13 for the 1/4 in. conduit. Above 4 MPa, the pullout			
20. DISTRIBUTION/AVAILABILITY OF ABSTRACT <input type="checkbox"/> UNCLASSIFIED/UNLIMITED <input checked="" type="checkbox"/> SAME AS RPT. <input type="checkbox"/> DTIC USERS		21. ABSTRACT SECURITY CLASSIFICATION UNCLASSIFIED	
22a. NAME OF RESPONSIBLE INDIVIDUAL Betty L. Fox		22b. TELEPHONE (Include Area Code) (202) 325-7042	22c. OFFICE SYMBOL DNA/STTI

DD FORM 1473, 84 MAR

83 APR edition may be used until exhausted  
All other editions are obsolete

SECURITY CLASSIFICATION OF THIS PAGE

UNCLASSIFIED

18. SUBJECT TERMS (Continued)

Sand Backfill  
Conduit Friction

Ductile Iron Pipe  
Vitrified Clay Pipe

19. ABSTRACT (Continued)

load-confining pressure relationship became concave upward reaching a coefficient of friction of about 0.29 at 8 MPa (1 in. conduit). The presence of moisture in the backfill caused a decrease in frictional resistance of nearly 13 percent for the 1 in. conduit.

The shear offset tests revealed the performance of relatively flexible conduit to be dramatically different from that of stiff conduit. Ductile iron pipe, partly due to the sand confining method, was able to resist the imposed shear offset by redistributing the shear-intensive loading into a primarily flexural deformation due to its strength and flexibility compared to the surrounding sand. Vitrified clay pipe showed very little tolerance to shearing deformations even in the presence of close, apparently quite flexible joints, and sustained complete transverse fractures at small shear offsets.

A ten page bibliography is included.

PREFACE

This program was sponsored jointly by the National Science Foundation (NSF) (Grant No. CEE-81-05791) and the Defense Nuclear Agency (DNA) (Contract No. DNA001-81-C-0242). Dr. S.C. Liu was the initial program manager at NSF until his leave of absence when he was replaced by Dr. K. Thirumalai. Dr. K.L. Goering was the Contracting Officer's Representative from the Strategic Structures Division at DNA. The organizational sponsorship and the participation of these personnel at NSF and DNA are greatly appreciated. The assistance and guidance of Dr. W.W. Hakala of NSF throughout the program is also gratefully acknowledged.

The authors would particularly like to acknowledge and thank the participants of the User's Panel, William Hall, Bruce Hartenbaum, Jeremy Isenberg, Toshio Mayeda, Irving Oppenheim, Michael O'Rourke and Richard Parmelee for their volunteered time and enthusiastic participation in the User's meetings which assisted in determining the emphasis of the work on this program. Their continued interest and involvement apart from the meetings and the several communications received with pertinent comments and data are also gratefully acknowledged.

Related technical publications and additional product information, not normally available, were generously supplied by Duane B. Ford of the Ductile Iron Pipe Research Association, Charles Calder, Pacific States Cast Iron Pipe Co., and William R. Veliquette, Mission Clay Products Corporation. Their interest and contributions were extremely helpful in planning and conducting the program.

Special thanks go to Richard B. Cason who surmounted a number of unusual requirements to produce an excellent design for the single-shear test fixture. Our gratitude is also expressed to the personnel of Rettig Machine Shop for the



Codes	
Dist	Avail and/or Special
A-1	

high quality of workmanship that was maintained in fabricating all of the test fixturing. The fine efforts of Joel Sweet in performing the finite element analyses of conduit pullout tests are also appreciated.

Any opinions, findings, conclusions or recommendations expressed in this report are those of the authors and do not necessarily reflect the views of the National Science Foundation or the Defense Nuclear Agency.

Conversion factors for U.S. customary  
to metric (SI) units of measurement.

To Convert From	To	Multiply By
angstrom	meters (m)	1.000 000 X E -10
atmosphere (normal)	kilo pascal (kPa)	1.013 25 X E +2
bar	kilo pascal (kPa)	1.000 000 X E +2
barn	meter <sup>2</sup> (m <sup>2</sup> )	1.000 000 X E -28
British thermal unit (thermochemical)	joule (J)	1.054 350 X E +3
cal (thermochemical)/cm <sup>2</sup> §	mega joule/m <sup>2</sup> (MJ/m <sup>2</sup> )	4.184 000 X E -2
calorie (thermochemical)§	joule (J)	4.184 000
calorie (thermochemical)/g§	joule per kilogram (J/kg)*	4.184 000 X E +3
curies	giga becquerel (GBq)†	3.700-000 X E +1
degree Celsius‡	degree kelvin (K)	$t_K = t_C + 273.15$
degree (angle)	radian (rad)	1.745 329 X E -2
degree Fahrenheit	degree kelvin (K)	$t_K = (t_F + 459.67)/1.8$
electron volts	joule (J)	1.602 19 X E -19
erg§	joule (J)	1.000 000 X E -7
erg/second	watt (W)	1.000 000 X E -7
foot	meter (m)	3.048 000 X E -1
foot-pound-force	joule (J)	1.355 818
gallon (U.S. liquid)	meter <sup>3</sup> (m <sup>3</sup> )	3.785 412 X E -3
inch	meter (m)	2.540 000 X E -2
jerk	joule (J)	1.000 000 X E +9
joule/kilogram (J/kg) (radiation dose absorbed)§	gray (Gy)*	1.000 000
kilotons§	terajoules	4.183
kip (1000 lbf)	newton (N)	4.448 222 X E +3
kip/inch <sup>2</sup> (ksi)	kilo pascal (kPa)	6.894 757 X E +3
ktap	newton-second/m <sup>2</sup> (N-s/m <sup>2</sup> )	1.000 000 X E +2
micron	meter (m)	1.000 000 X E -6
mil	meter (m)	2.540 000 X E -5
mile (international)	meter (m)	1.609 344 X E +3
ounce	kilogram (kg)	2.834 952 X E -2
pound-force (lbf avoirdupois)	newton (N)	4.448 222
pound-force inch	newton-meter (N·m)	1.129 848 X E -1
pound-force/inch	newton/meter (N/m)	1.751 268 X E +2
pound-force/foot <sup>2</sup>	kilo pascal (kPa)	4.788 026 X E -2
pound-force/inch <sup>2</sup> (psi)	kilo pascal (kPa)	6.894 757
pound-mass (lbm avoirdupois)	kilogram (kg)	4.535 924 X E -1
pound-mass-foot <sup>2</sup> (moment of inertia)	kilogram-meter <sup>2</sup> (kg·m <sup>2</sup> )	4.214 011 X E -2
pound-mass/foot <sup>3</sup>	kilogram-meter <sup>3</sup> (kg/m <sup>3</sup> )	1.601 846 X E +1
rad (radiation dose absorbed)§	gray (Gy)*	1.000 000 X E -2
roentgen§	coulomb/kilogram (C/kg)	2.579 760 X E -4
shake	second (s)	1.000 000 X E -8
slug	kilogram (kg)	1.459 390 X E +1
torr (mm Hg, 0° C)	kilo pascal (kPa)	1.333 22 X E -1

\*The gray (Gy) is the accepted SI unit equivalent to the energy imparted by ionizing radiation to a mass of energy corresponding to one joule/kilogram.

†The becquerel (Bq) is the SI unit of radioactivity; 1 Bq = 1 event/s.

‡Temperature may be reported in degree Celsius as well as degree kelvin.

§These units should not be converted in DNA technical reports; however, a parenthetical conversion is permitted at the author's discretion.

## TABLE OF CONTENTS

<u>Section</u>		<u>Page</u>
	Preface.....	1
	Conversion Table.....	3
	List of Illustrations.....	5
	List of Tables.....	9
1	Introduction.....	11
2	Background.....	13
3	Description of Test Apparatus and Procedures.....	19
4	Description of Tests .....	55
5	Discussion of Pullout Test Results.....	75
6	Discussion of Shear Test Results.....	115
7	Conclusions and Recommendations for Additional Research.....	125
8	List of References.....	129
<u>Appendices</u>		
A	Bibliography.....	131
B	List of Symbols.....	141
C	Conduit Radial Displacement.....	145
D	Finite Element Modeling of Conduit Pullout Tests.....	149
E	Summary of User's Panel Meetings.....	181

## LIST OF ILLUSTRATIONS

<u>Figure</u>		<u>Page</u>
3.1	CASES high pressure biaxial test cell.....	20
3.2	Biaxial pressure cell for 1-inch pullout tests.....	21
3.3	Typical pullout test apparatus.....	22
3.4	Biaxial pressure cell for 1/4-inch pullout tests.....	23
3.5	Pressure cell setup for variable length 1/4-inch pullout tests.....	25
3.6	Pullout test instrumentation schematic.....	26
3.7	Flexible tube subassembly and installation.....	27
3.8	150 cm pullout test setup.....	29
3.9	Single shear test concept.....	31
3.10	Single shear test fixture.....	32
3.11	Dual installation of attitude rams and load cells.....	33
3.12	Applied load and shearing forces for single shear test fixture.....	35
3.13	Bladder installation - West end.....	36
3.14	Bladder installation at stationary shear plane.....	37
3.15	Work platform.....	38
3.16	Shear test instrumentation schematic.....	39
3.17	Shear test instrument locations.....	42
3.18	Ductile iron specimen showing three top strain gages.....	43
3.19	Measurement bladder installed on sidewall.....	45
3.20	Ductile iron specimen - West end showing dumpy level, vertical dial gages, and closure gasket.....	46
3.21	Threaded stud for visual recording of inside displacement.....	47
3.22	Sand raining.....	49
3.23	Ductile iron specimen installed for testing.....	52
3.24	Full sand bin prior to bladder installation.....	53
4.1	Examples of pullout test load oscillation.....	66
4.2	Applied shear load versus end load.....	74

LIST OF ILLUSTRATIONS (Continued)

<u>Figure</u>	<u>Page</u>
5.1 Typical load/slip response for test series I.....	76
5.2 Test series I.....	77
5.3 Normalized load versus confining pressure for 1-inch and 1/4-inch conduit.....	78
5.4 Typical post test conduit surface condition.....	79
5.5 Conduit striation study.....	81
5.6 Finite element idealization.....	83
5.7 Calculated load/slip behavior (linear material).....	86
5.8 Slip development along conduit at pullout load of 1.8 kN.....	87
5.9 Slip development along conduit at pullout load of 20 kN.....	88
5.10 End displacement versus pullout load, $k = 0.20$ .....	90
5.11 End displacement versus pullout load, $k = 0.25$ .....	90
5.12 End displacement versus pullout load, $k = 0.30$ .....	91
5.13 End displacement versus pullout load, $k = 0.35$ .....	91
5.14 End displacement versus pullout load, $k = 0.40$ .....	92
5.15 Test 143, $P_c = 4$ MPa.....	93
5.16 Push/pull test comparison.....	95
5.17 Conduit peak axial pullout load as a function of test cycle (wet backfill).....	99
5.18 Scaled peak axial pullout load as a function of test cycle (dry backfill).....	101
5.19 Rubber confining bladder.....	102
5.20 Confining pressure mechanism: hydraulic oil versus air pressure....	103
5.21 Load/slip response: PVC versus rubber bladder.....	104
5.22 Test series II.....	107
5.23 Test series IV.....	108
5.24 Test series VI.....	109
5.25 Test series VII.....	110
5.26 Test series IX.....	111
5.27 Coefficients of friction for all pullout tests.....	112
5.28 Normalized pullout load versus confining pressure.....	114

LIST OF ILLUSTRATIONS (Continued)

<u>Figure</u>	<u>Page</u>
6.1 Ductile iron pipe shear test deformation.....	116
6.2 Load distribution models for DIP shear test.....	120
6.3 Beam functions for assumed load distribution.....	121
6.4 4-inch ductile iron pipe shear test.....	122
D.1 Finite element idealization.....	151
D.2 Calculated load/slip behavior (linear material).....	152
D.3 Slip development along conduit at pullout load of 1.8 kN.....	153
D.4 Slip development along conduit at pullout load of 3.6 kN.....	154
D.5 Slip development along conduit at pullout load of 5.5 kN.....	155
D.6 Slip development along conduit at pullout load of 7.3 kN.....	156
D.7 Slip development along conduit at pullout load of 9.1 kN.....	157
D.8 Slip development along conduit at pullout load of 10.9 kN.....	158
D.9 Slip development along conduit at pullout load of 12.8 kN.....	159
D.10 Slip development along conduit at pullout load of 14.6 kN.....	160
D.11 Slip development along conduit at pullout load of 16.4 kN.....	161
D.12 Slip development along conduit at pullout load of 18.2 kN.....	162
D.13 Slip development along conduit at pullout load of 20.0 kN.....	163
D.14 End displacement versus pullout load, Run A.....	164
D.15 End displacement versus pullout load, Run B.....	164
D.16 End displacement versus pullout load, Run C.....	165
D.17 End displacement versus pullout load, Run D.....	165
D.18 End displacement versus pullout load, Run E.....	166
D.19 End displacement versus pullout load, Run F.....	166
D.20 End displacement versus pullout load, Run G.....	167
D.21 End displacement versus pullout load, Run H.....	167
D.22 End displacement versus pullout load, Run I.....	168
D.23 End displacement versus pullout load, Run J.....	168
D.24 End displacement versus pullout load, Run K.....	169
D.25 End displacement versus pullout load, Run L.....	169
D.26 End displacement versus pullout load, Run M.....	170
D.27 End displacement versus pullout load, Run N.....	170

LIST OF ILLUSTRATIONS (Concluded)

<u>Figure</u>		<u>Page</u>
D.28	End displacement versus pullout load, Run O.....	171
D.29	End displacement versus pullout load, Run P.....	171
D.30	End displacement versus pullout load, Run Q.....	172
D.31	End displacement versus pullout load, Run R.....	172
D.32	End displacement versus pullout load, Run S.....	173
D.33	End displacement versus pullout load, Run T.....	173
D.34	End displacement versus pullout load, Run U.....	174
D.35	End displacement versus pullout load, Run V.....	174
D.36	End displacement versus pullout load, Run W.....	175
D.37	End displacement versus pullout load, Run X.....	175
D.38	End displacement versus pullout load, Run Y.....	176
D.39	End displacement versus pullout load, Run Z.....	176
D.40	End displacement versus pullout load, Run AE.....	177
D.41	End displacement versus pullout load, Run AF.....	177
D.42	End displacement versus pullout load, Run AK.....	178
D.43	Modified mesh used in Run AK.....	179
E.1	Double shear test apparatus.....	183

## LIST OF TABLES

<u>Table</u>		<u>Page</u>
2.1	User's panel participants.....	15
2.2	Test program summary.....	17
3.1	Shear test instrumentation plan.....	40
3.2	Sand density measurements.....	50
3.3	Sand density measurement summary.....	51
4.1	Summary of test series I.....	56
4.2	Lone star lapis lustre #1/20 kiln-dried monterey sand size distribution.....	58
4.3	Pre- and post-test grain size distribution.....	59
4.4	Summary of test series II.....	60
4.5	Summary of test series III.....	62
4.6	Summary of test series IV.....	63
4.7	Summary of test series V.....	64
4.8	Summary of test series VI.....	67
4.9	Summary of test series VII.....	69
4.10	Summary of test series VIII.....	70
4.11	Summary of test series IX.....	72
4.12	Summary of test series X.....	73
5.1	Summary of 'SATURN' runs.....	89
5.2	Values used for tangential strain computation.....	97
6.1	Selected shear test displacements and strains.....	118
C.1	Conduit deformation due to external radial pressure.....	146
D.1	Summary of 'SATURN' runs.....	150



## SECTION 1

### INTRODUCTION

The performance of lifeline conduits in earthquakes has been of concern to the National Science Foundation and others for some time. As a result, this performance has been the subject of many research programs, both analytical and experimental. A very similar problem of interest to the defense community in general and the Defense Nuclear Agency (DNA) in particular, is the performance of buried communication and instrumentation conduits under shock or blast loadings.

Merritt CASES, Inc. (CASES) has been intimately involved with the instrumentation conduit problem over a period of several years, and undertook this program to further that work while also considering the implications of the research on lifelines in earthquake situations. This effort was primarily experimental in nature, with some analytical efforts performed to improve understanding of the experiment results. One unique feature of the program was a "User's Panel" (explained in Section 2) to advise, direct, and generally assist in the development of the program plan.

The program plan, as it evolved, focused on two primary areas of research needs. These areas were: (1) axial pullout characteristics of conduits embedded in sand which were investigated using small diameter steel specimens, and (2) the shear performance of prototypical lifeline specimens in sand, in which ductile iron and vitrified clay pipe specimens were used.

Early results from the program were reported at and published in the proceedings of the 1983 International Symposium on Lifeline Earthquake Engineering

(Reference 1). This report contains further analyses of those results as well as describing and analyzing work completed in the latter portion of the program.

The second section of the report gives additional background information on the program. Special testing fixtures were developed or adapted for the program; these are described in Section 3. Details of the more than 100 individual tests performed are given in Section 4. Results of the two families of tests, pullout and single shear, are discussed at length in Sections 5 and 6, respectively. Section 7 presents the conclusions drawn from this program and the recommendations for additional research. Additionally, three appendices are included which detail analytical treatment of the conduit radial displacement and a finite element model of the conduit pullout phenomenon, and summarize the User's Panel meetings.

## SECTION 2

### BACKGROUND

#### Conduit Environment

Buried lifelines and instrumentation/communication conduits as studied in this program serve a variety of uses. These include fluid conveyances for domestic water, wastewater and natural gas, as well as cable raceways for electrical power, telecommunications, and other electrical signals. Also broadly included in the definition but less directly related to this program are large aqueducts and transcontinental pressure pipelines.

The external loads on these conduits vary somewhat, but generally exhibit quite similar effects. For "garden-variety" domestic pipelines, loads may range from vehicular wheel loads to severe earthquakes. Blastload performance of conduits is also of interest for defense purposes -- for their resistance to hostile attack as well as for their use as instrumentation conduits for nuclear or high explosive tests. Regardless of the load source, it can generally be characterized as a hydrostatic or near-hydrostatic lateral load in conjunction with an axial load, tensile or compressive, and/or a transverse shear load.

The conduit material composition may range from ductile material such as steel to brittle materials like clay and concrete. Combinations of materials are also used, as are plastics and composites. For this program, 1/4 in. and 1 in. steel conduit was selected for the axial load investigations, while 4 in. ductile iron pipe (DIP) and vitrified clay pipe (VCP) were used in the shear tests.

Performance of the conduit is also influenced by the medium in which it is placed. This medium is usually a soil mixture ranging from sand to clay. For some installations the backfill may be a grout mixture.

Sand was selected for use in this program (20/40 Lapis Lustre Monterey beach sand) as being representative of one limit of a real backfill material; it was also reasonably well characterized so that efforts could be concentrated on the conduit tests rather than sand characterization.

### Program Development

The selected bibliography illustrates that considerable research has been and continues to be done in this area. From CASES' past investigations of instrumentation/communication conduits (e.g., Reference 2), it was evident there were serious limitations on the available test data which tended to restrict further analytical efforts to better characterize conduit performance. This research program was developed in an effort to address some of those limitations.

In addition to the previous CASES work just referenced, some of the closely-related work by other organizations which influenced the program formulation, includes several of the Weidlinger Associates reports (References 3 through 9), work by Kennedy, et al. on buried oil pipelines (Reference 10), and other articles in the ASCE Technical Councils Journal (References 11, 12, and 13). As these sources demonstrate, a major task in formulating a meaningful test program is to select variables to examine from among the myriad of possibilities. The major factors considered for inclusion in this program were pipe size and type, loading conditions, backfill material and moisture content, static vs. dynamic environment, corrosion influence, joint performance, and straight vs. other pipe configurations.

Program direction and selection from the variables just listed were aided by an advisory group referred to as the User's Panel (see Table 2.1). The par-

Table 2.1. User's panel participants.

<u>Name</u>	<u>Affiliation</u>
Dr. W.J. Hall	Department of Civil Engineering University of Illinois
Dr. Bruce A. Hartenbaum	H-Tech Laboratories, Inc.
Dr. Jeremy Isenberg	Weidlinger Associates
Mr. Toshio Mayeda	Los Angeles Department of Water and Power
Dr. Irving J. Oppenheim	Department of Civil Engineering Carnegie-Mellon University
Dr. M.J. O'Rourke	Department of Civil Engineering Rensselaer Polytechnic Institute
Dr. R.A. Parmelee	Department of Civil Engineering Northwestern University

ticipants of this panel (who served on an essentially voluntary basis) represented the sponsoring agencies, lifeline/conduit operating agencies, pipe manufacturing companies, and other researchers, including academic institutions. It was largely through the assistance of this User's Panel that the program was finalized and came to emphasize axial pullout tests of steel conduit embedded in hydrostatically loaded sand, and single shear of DIP and VCP embedded in sand.

In addition to guiding overall program direction, the combined experience of the User's Panel participants also proved invaluable in resolving peculiar testing problems and in shedding light on the interpretation of certain test results.

The User's Panel was convened twice, at San Francisco in February 1982 and at Reno, Nevada in February 1983. Results of these meetings are summarized in Appendix E. Additional contacts with individual participants were made by telephone or in person as required or as opportunities arose.

The test plan as conducted is summarized in Table 2.2.

Table 2.2. Test program summary.

<u>Test Series</u>	<u>No. of Tests</u>	<u>Test Number(s)</u>	<u>Test Type</u>	<u>Conduit Type &amp; Size</u>	<u>Conditions</u>
I	10	141 - 146	Pullout	1"* x 23 cm steel	0-6 MPa Confinement
II	13	147 - 152	Pullout	1/4" x 23 cm steel	0-3.5 MPa Confinement
III	2	153, 154	Pullout	1" x 23 cm steel	1.0, 0.4 mm Displacement
IV	16	155 - 161	Pullout	1/4" steel 10 - 23 cm length	@ 6.0 MPa Confinement
V	25	162 - 172	Pullout	1" x 23 cm steel	Dry to fully saturated 0 - 6 MPa
VI	16	179 - 190	Pullout	1" x 150 cm steel	Dry, 0.5 - 2.0 MPa Confinement
VII	5	196 - 199	Pullout	1" x 150 cm steel	Dry, 0.5 - 2.0 MPa Polished bar
VIII	6	200 - 207	Pullout	1/4" x 150 cm steel	.5 - 2.0 MPa Confinement with air and rubber
IX	11	208 - 214	Pullout	1/4" x 150 cm steel	.25 - 1.0 MPa Confinement
X	4	221 - 224	Shear	4" Ductile Iron and Vitrified Clay	.07 MPa Confinement

\* Since the pipe was ordered using U.S. dimensions, these dimensions are used here.

## SECTION 3

### DESCRIPTION OF TEST APPARATUS AND PROCEDURES

Three CASES-developed test fixtures were used in this program: (1) the CASES high pressure biaxial test cell which was adapted for use on the program, (2) a 150 cm long, low pressure biaxial cell developed specifically for the program, and (3) the unique 5 m long, single shear tester which was designed and developed for the program. Each fixture is detailed separately below, with its corresponding instrumentation plan and test procedure.

#### High Pressure Biaxial Test Cell

The CASES high pressure biaxial test cell was developed, under a previous program, to study the deformation characteristics of 11 cm diameter conduit sections at static pressures up to 135 MPa. As shown in Figure 3.1, those specimens were surrounded by a thin, deep drawn brass sleeve against which the hydraulic pressure was exerted.

Figure 3.2 illustrates the modified end fittings used on the fixture to adapt it to perform 1 in. conduit pullout tests in sand. In that configuration, the specimen could slide in or out over a range of 30 mm with the full 23 cm length in contact with the pressurized sand. Figure 3.3 illustrates the overall test fixture and pullout assembly. The brass sleeve used previously was replaced by a very flexible, reinforced Polyvinyl Chloride (PVC) drainage hose for these tests. This hose separates the pressurizing fluid from the sand with negligible pressure attenuation. This configuration was used for test series I, III, and IV.

Figure 3.4 illustrates a further modification of the test fixture to allow 1/4 in. conduit to be tested. Since these specimens extend completely through

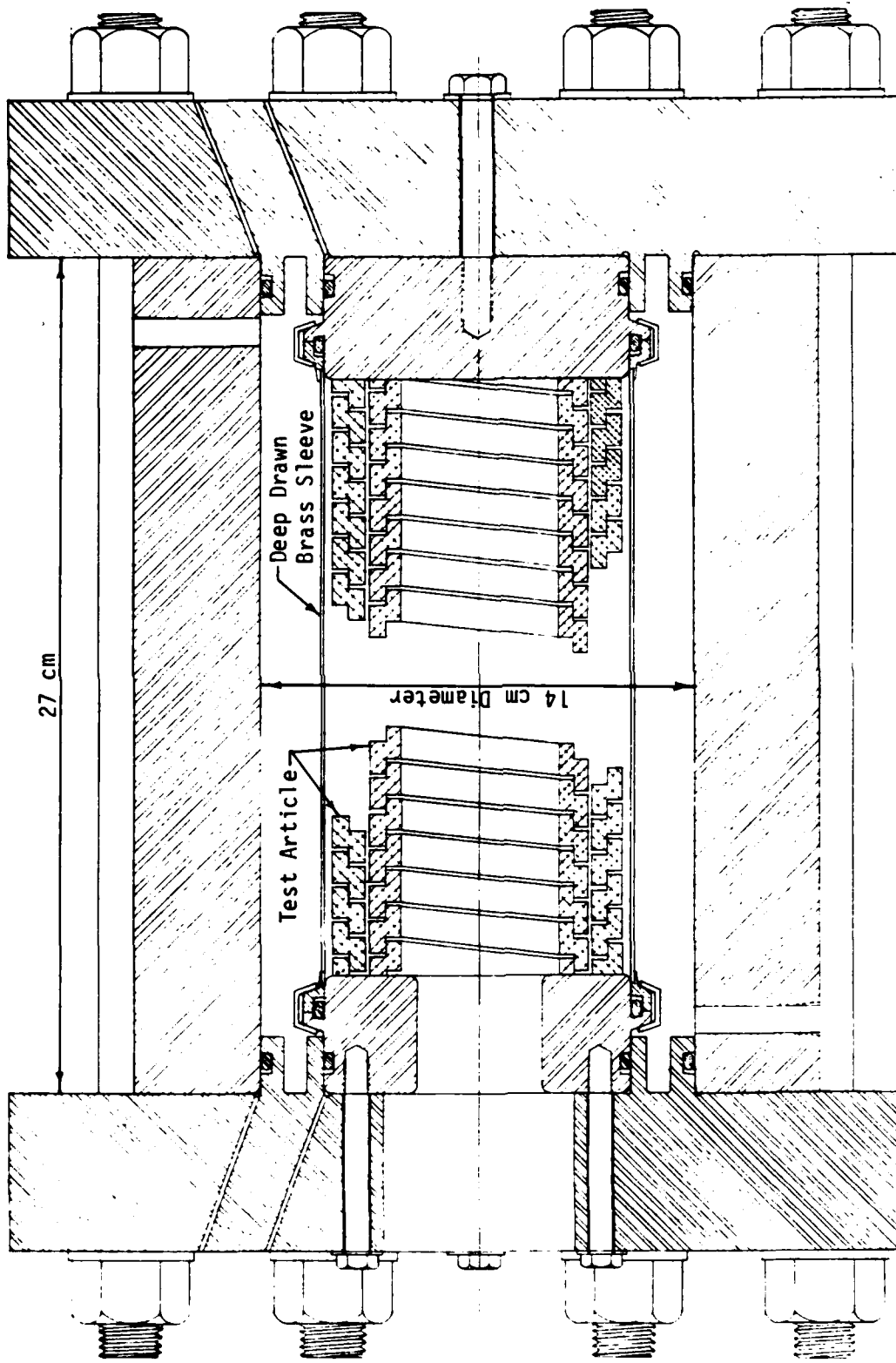


Figure 3.1. CASES high pressure biaxial test cell.

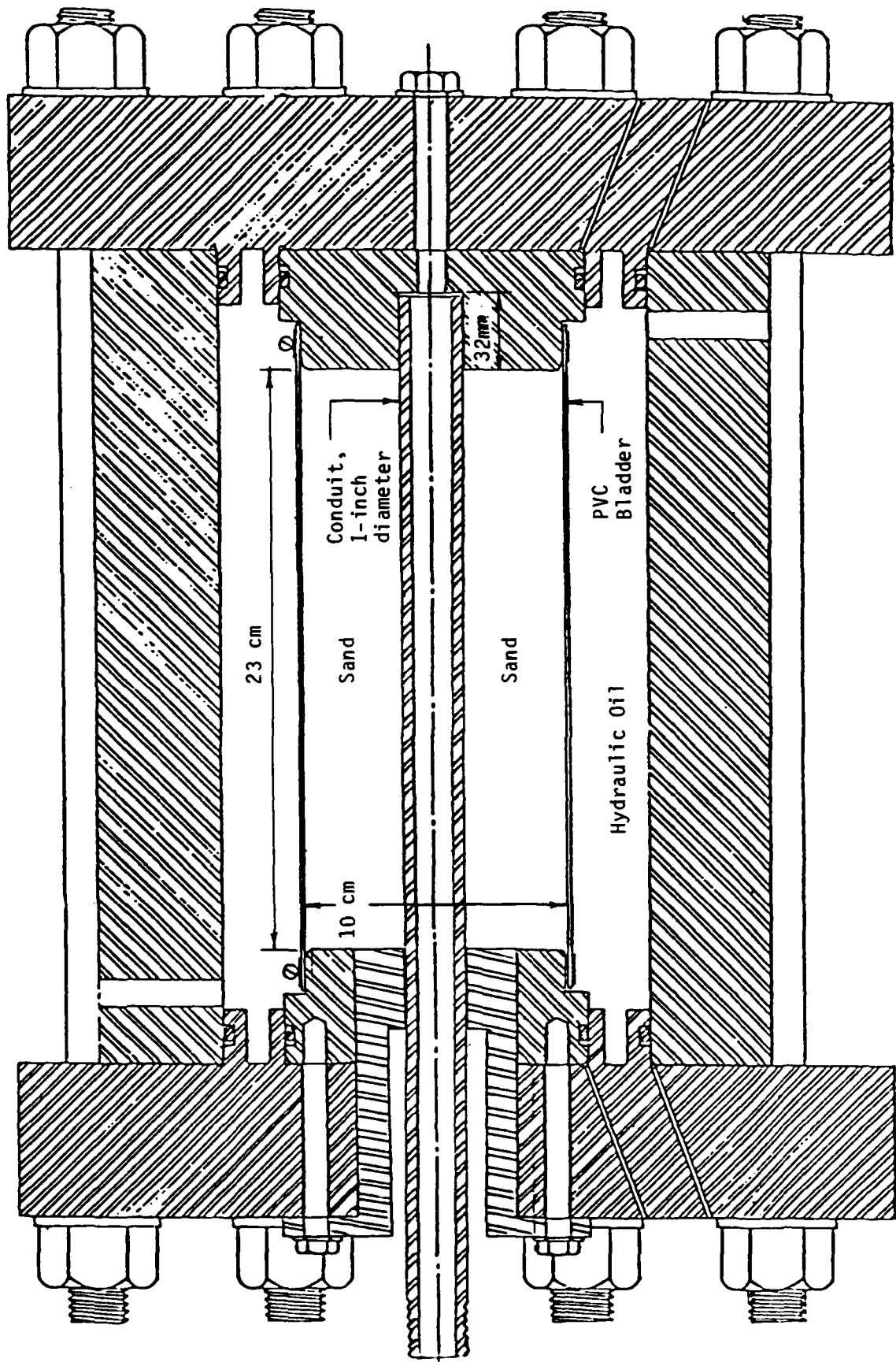


Figure 3.2. Biaxial pressure cell for 1-inch pullout tests.

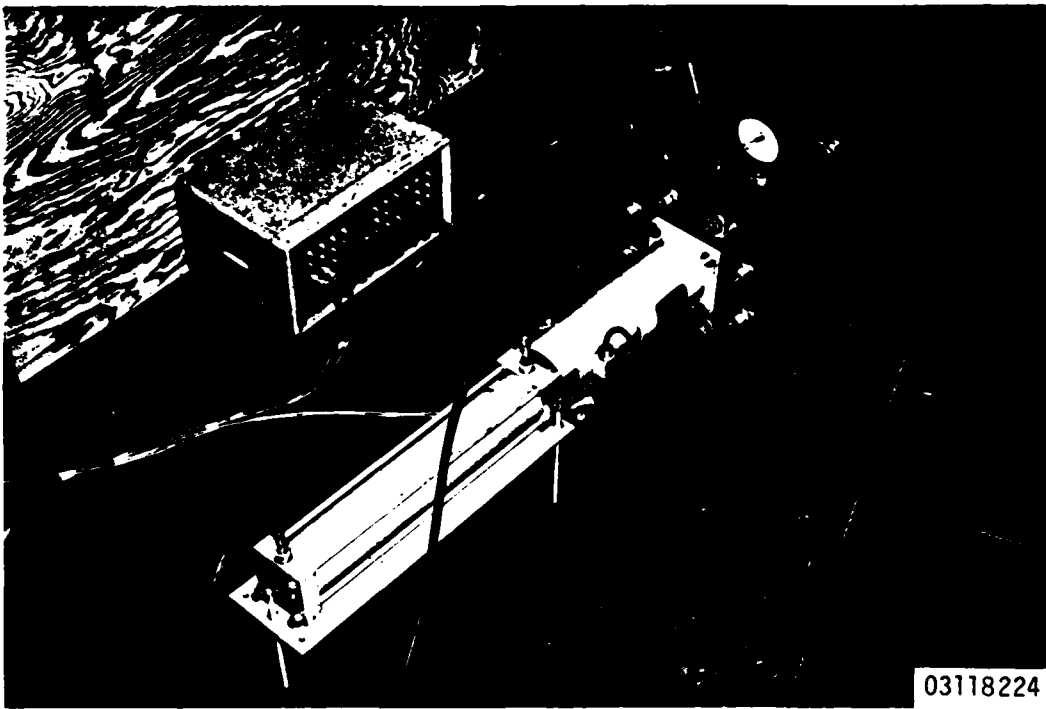


Figure 3.3. Typical pullout test apparatus.

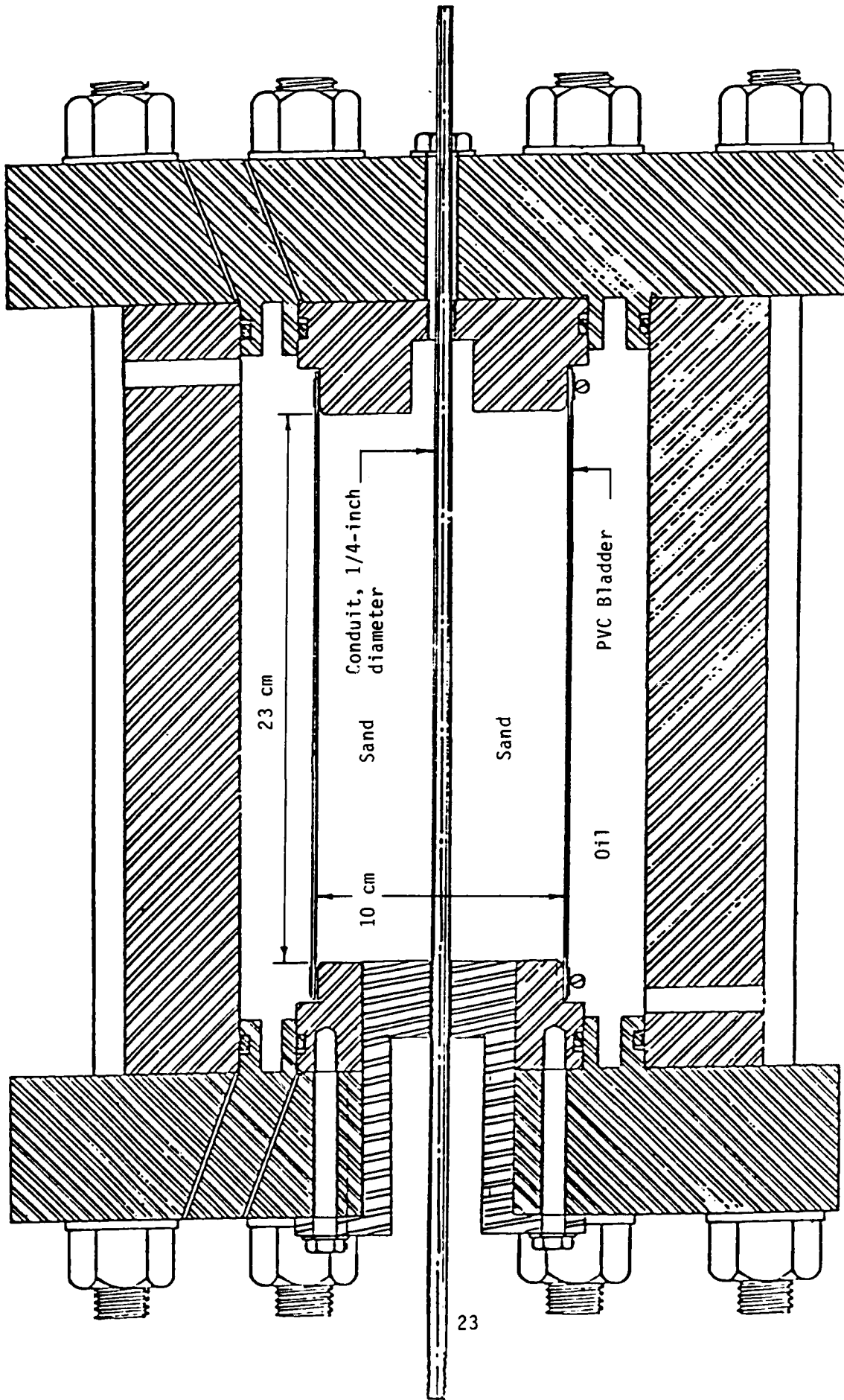


Figure 3.4. Biaxial pressure cell for 1/4-inch pullout tests.

the fixture, the 30 mm displacement limit is removed. A slight adaptation of this configuration used a longer hollow bolt at the right hand end (Figure 3.5) which allowed the portion of the conduit in contact with the sand to be varied between 10 cm and 23 cm. These configurations were used for test series II.

#### Pullout Instrumentation Plan

Three channels of active instrumentation were recorded on all pullout tests; Figure 3.6 depicts the instrumentation set up. The channels recorded were the axial pullout load on the specimen, the axial displacement measured at the opposite end, and the radial pressure on the outside of the sand cylinder. All channels were recorded on paper tape by a data logger at a rate of 2-1/2 samples per second. Simultaneously, the data were recorded on microcomputer floppy disks for postprocessing. Load and displacement were monitored continuously during the test on an x-y plotter, while a digital pressure display was updated at approximately two-second intervals.

#### Pullout Test Preparation and Procedure

The test apparatus was assembled with the specimen oriented vertically. The PVC tube was attached between the end fittings, and this subassembly was then installed in the pressure cell (Figure 3.7). The conduit specimen was placed in position without the upper end plug installed. This permitted careful "raining" of the confining medium, 20/40 Monterey Lapis Lustre sand, into the opening around the conduit. Some moderate tamping was employed to help expand the PVC cylinder to a fully circular section. After filling the tube completely with sand as determined by use of feeler gages, the upper end plug was installed and the assembly was placed horizontally for attachment to the pullout ram and load cell. The hydraulic pressure around the PVC sleeve was maintained with a two-

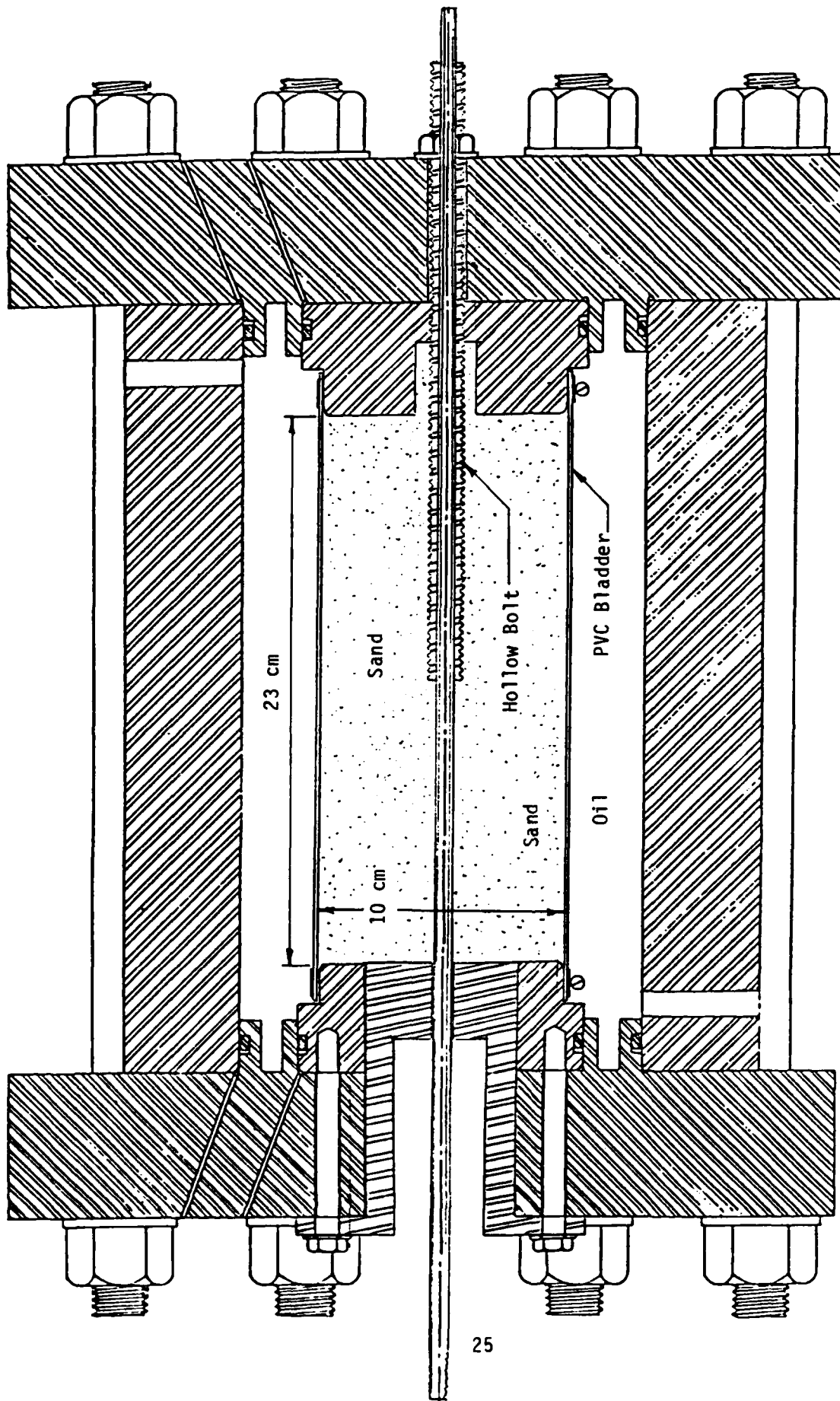


Figure 3.5. Pressure cell setup for variable length 1/4-inch pullout tests.

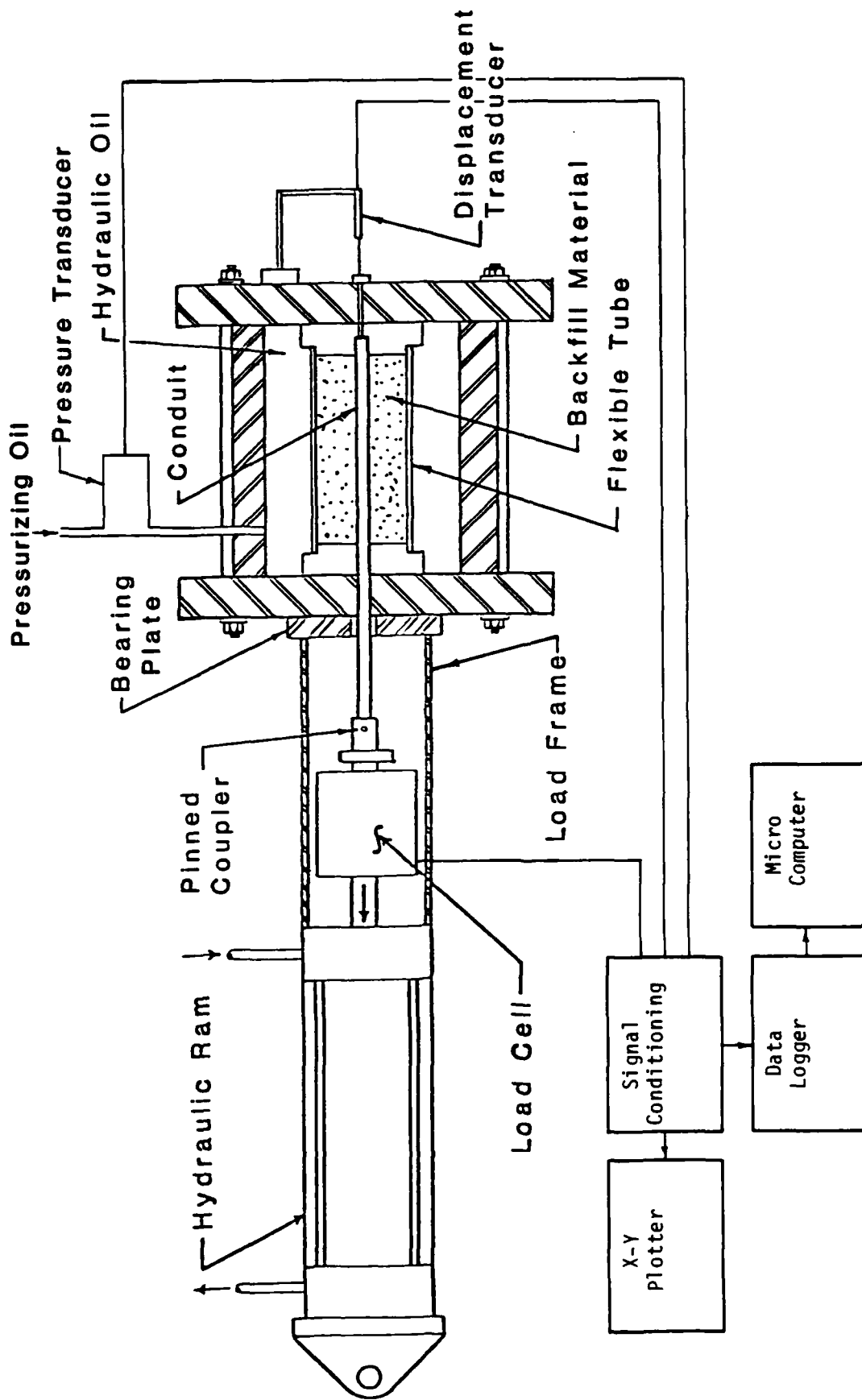


Figure 3.6. Pullout test instrumentation schematic.

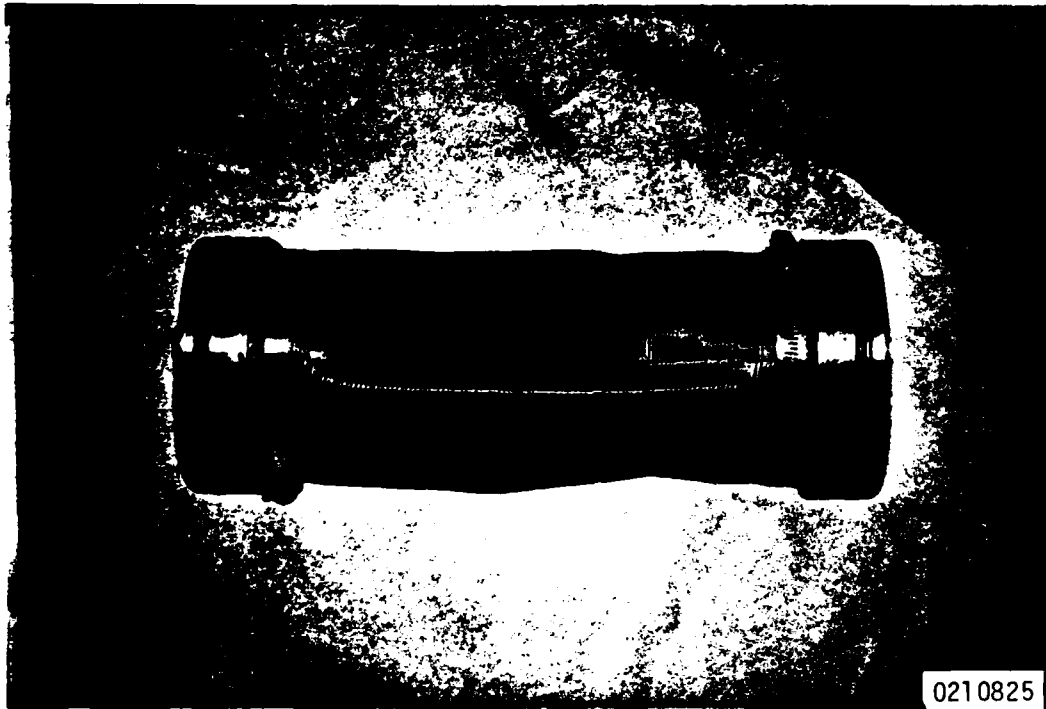


Figure 3.7a.

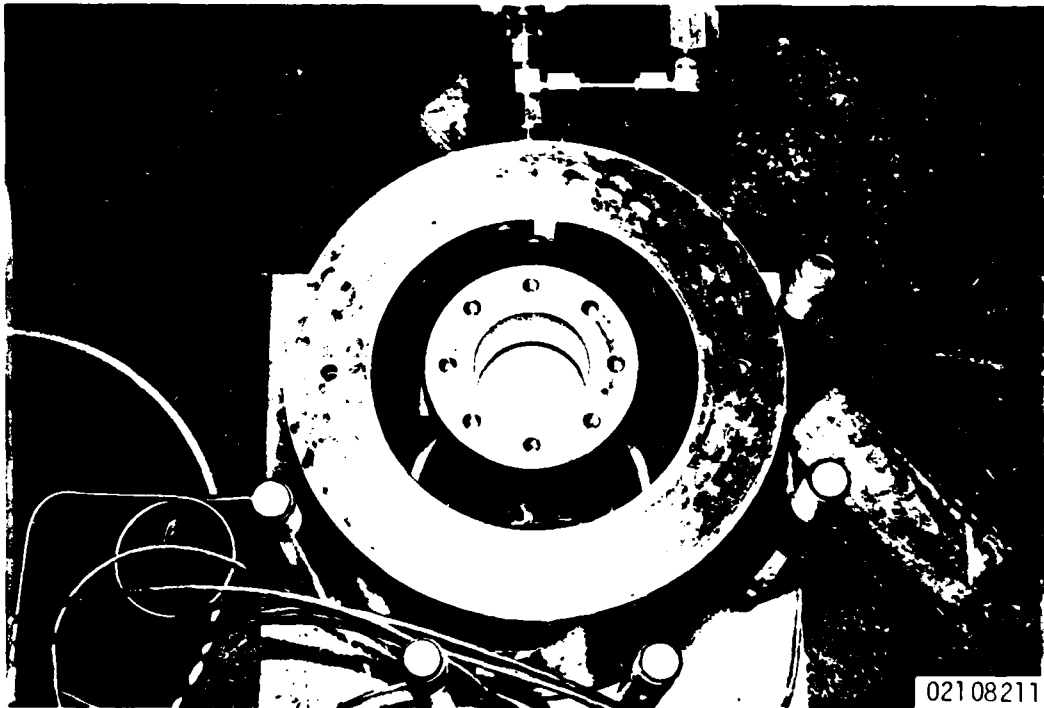


Figure 3.7b.

Figure 3.7. Flexible tube subassembly and installation.

stage hand pump and was manually controlled during each test by an operator reading the digital display of pressure. A stability of internal pressure of  $\pm .01$  MPa was readily achieved by experienced operators, with this control method.

#### 150 cm Low Pressure Test Cell

From the pullout test results of series I and II it became evident that the high pressure cell had considerably more pressure capacity than was required, and that accommodation of a much longer specimen would be desirable. Accordingly, a 150 cm long test fixture, shown in Figure 3.8, was designed and fabricated. The 6 MPa pressure capacity of this new fixture was wholly adequate, especially as its length provided over six times the sand/specimen contact area of the original fixture.

As with the original fixture, end fittings to accommodate either 1/4 in. or 1 in. conduit were fabricated. For this fixture, however, both sizes were allowed to extend completely through the device, a feature which could not be readily accommodated for larger conduit in the high pressure cell.

Instrumentation, test preparation, and test conduct were virtually identical to corresponding aspects of the high pressure cell tests.

#### Single Shear Tester

Shortly after the decision to include large scale shear tests in the final test plan, design work was begun on a shear test fixture. A single shear concept was chosen over a potentially simpler double shear apparatus based on two primary factors:

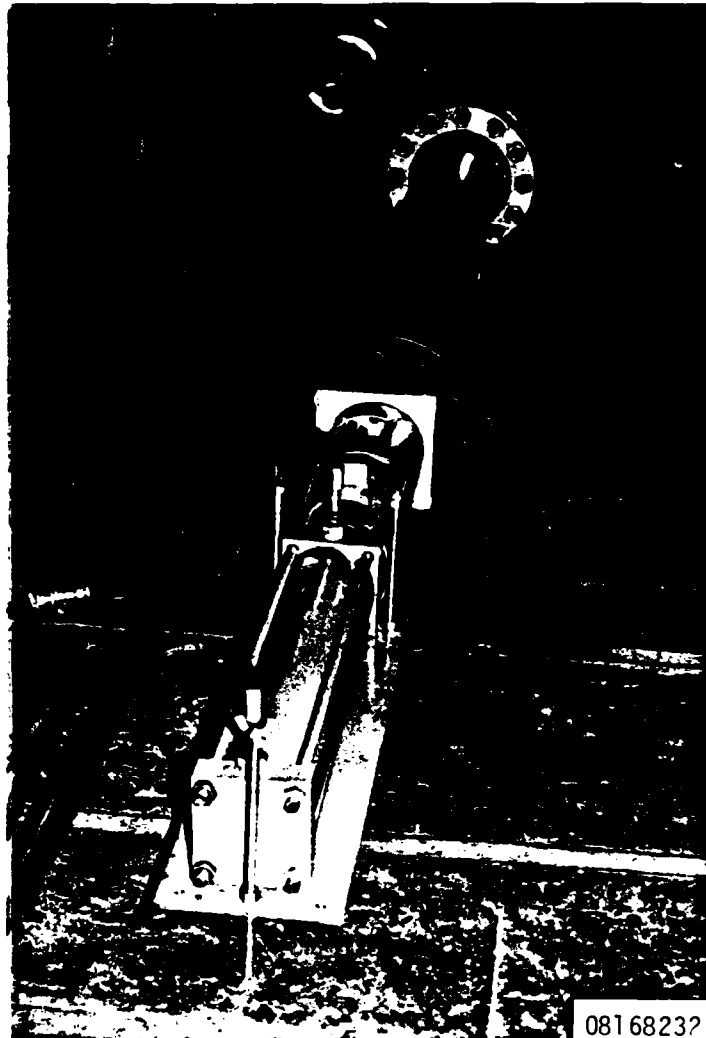


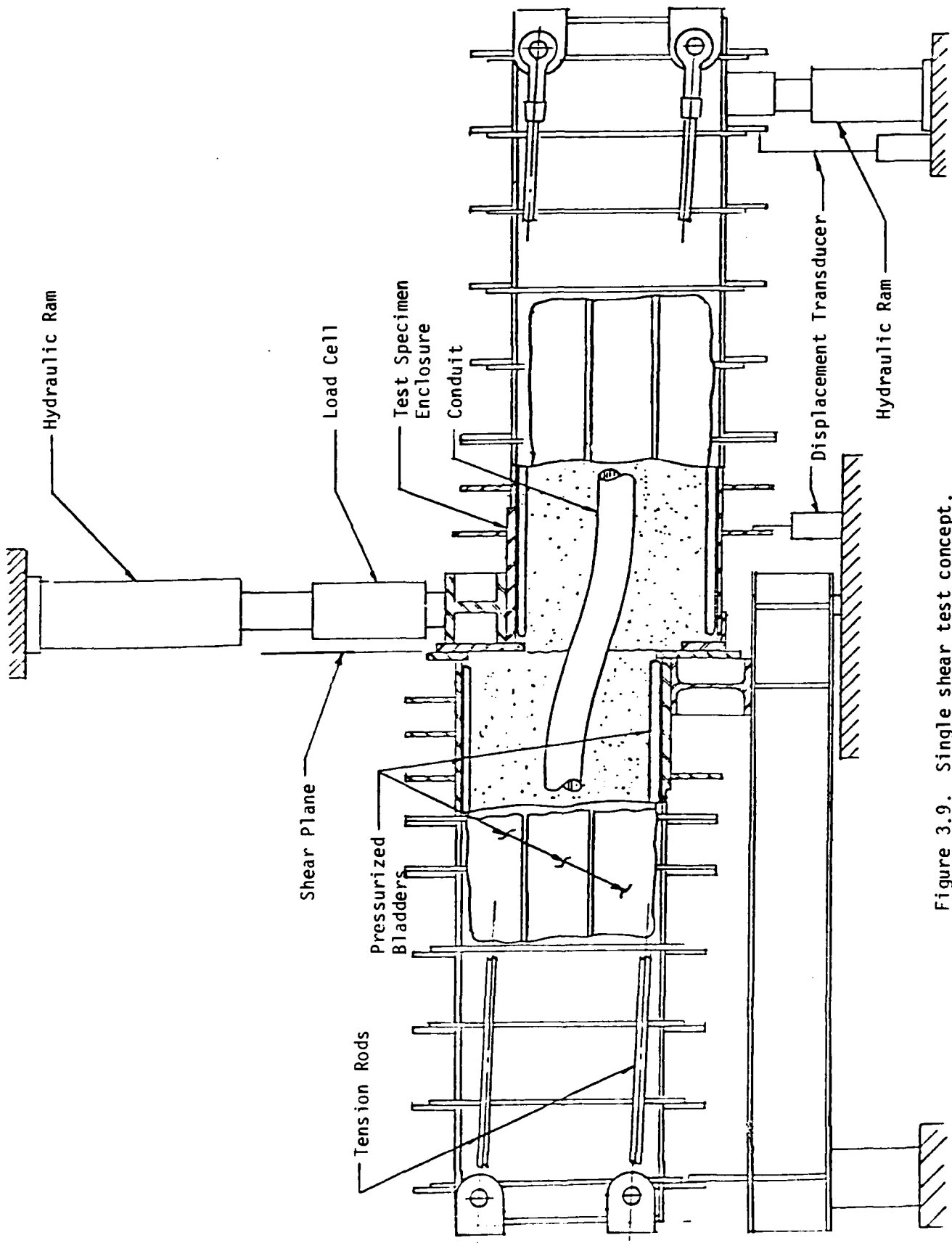
Figure 3.8. 150 cm pullout test setup.

- (1) Ability to simulate actual fault displacements which are associated with the movement along a single shear plane, and
- (2) Ability to provide geometric symmetry about the shear plane and to permit independent control of end conditions.

The single shear concept adopted is shown in Figure 3.9. The single shear tester consists of two soil bins, each 38 cm x 60 cm x 2.5 m placed end to end. Pressurized bladders in the top, bottom and/or sides permit overburden simulation of the backfill in which the specimen is embedded. A load of up to 1300 kN can be applied to the movable soil bin to effect the pipe shear condition. The design also incorporates provisions for conducting pullout tests of 4 in. pipe specimens embedded in the soil bin.

The single shear concept requires that the longitudinal axis of the moving box section of the apparatus remains perpendicular to the shear plane. This is accomplished by two features that have been incorporated into the device: axial tensioning and precise vertical displacement control. Figure 3.10 shows the tension rods running the length of the test fixture. Hydraulically actuated, the rods can apply a normal force preload on the steel surfaces of the shear plane to assist in maintaining alignment. Displacement control is maintained by the auxiliary hydraulic ram shown under the right end of the fixture (Figure 3.11). This system provides a fixture attitude control with end-to-end (auxiliary ram to main ram) displacement difference of less than 1 mm. To provide alternate support, a second attitude ram and load cell were installed under the movable section in order to allow further displacement of the section after the first ram had reached full extension.

The vertical load frame in which the fixture is mounted was a pre-existing CASES



Hydraulic Ram

Shear Plane

Load Cell

Test Specimen  
Enclosure

Conduit

Tension Rods

Pressurized  
Bladders

Displacement Transducer

Hydraulic Ram

Figure 3.9. Single shear test concept.



Figure 3.10. Single shear test fixture.



05258315

Figure 3.11. Dual installation of attitude rams and load cells.

fixture which was modified for this application. The soil bins, support beams, and loading blocks were fabricated for the program. To provide for installation of the device it was necessary to cast a base block using five cubic yards of concrete to counteract a potential upward force component of 100 kN which could be imposed at the maximum shear load of 1,300 kN (See Figure 3.12).

Flat flexible PVC drain pipe with nylon reinforcement was selected to provide confining pressure at the sand surface. Two nominal sizes were used: 4 in. diameter and 6 in. diameter, in their flat configuration, to cover the 38 cm span with a small overlap. Stainless steel bar stock, 1/4 in. by 1 in. was used to provide flat end closures for the bladder material. A bulkhead union was inserted through the bladder wall to provide a pressurization port. Air was used for pressurization up to 0.7 MPa. The end clamp and pressurization port are shown in Figure 3.13. The bladders were made longer than the soil bin to permit a foldback of the material at the shear plane and assure a close fit at the shearing surface (Figure 3.14).

A work platform was designed and constructed to run the full length of the test fixture at a convenient work height. All the handrails are removable to eliminate the possibility of interference with subsequent crane movements. The completed work platform is shown in Figure 3.15.

#### Shear Test Instrumentation Plan

Each shear test included a minimum of eight channels of automated instrumentation and nine channels of manual instrumentation, all of which were recorded at regular displacement intervals. A schematic of the instrumentation plan is presented in Figure 3.16. The individual data channels are listed in Table 3.1.

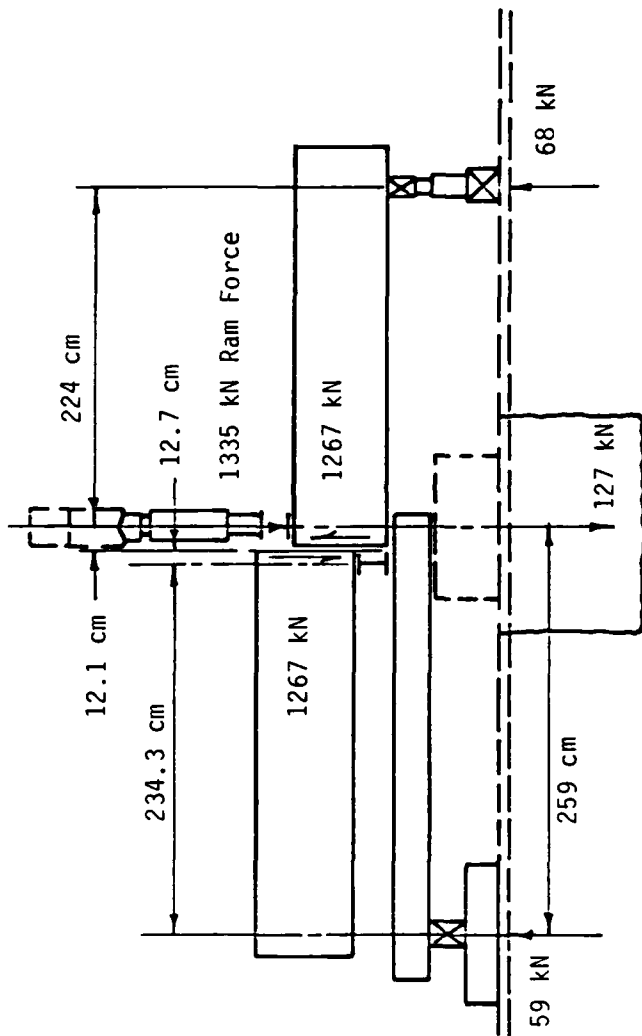


Figure 3.12. Applied load and shearing forces for single shear test fixture (neglecting weight of fixture).

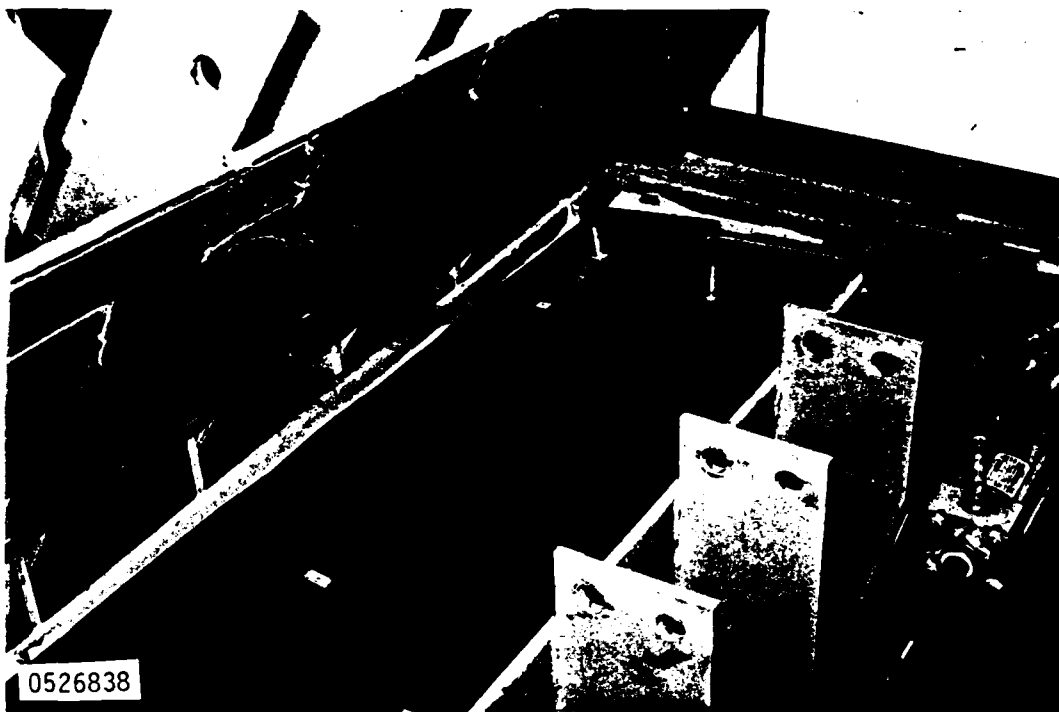


Figure 3.13. Bladder installation - West end.

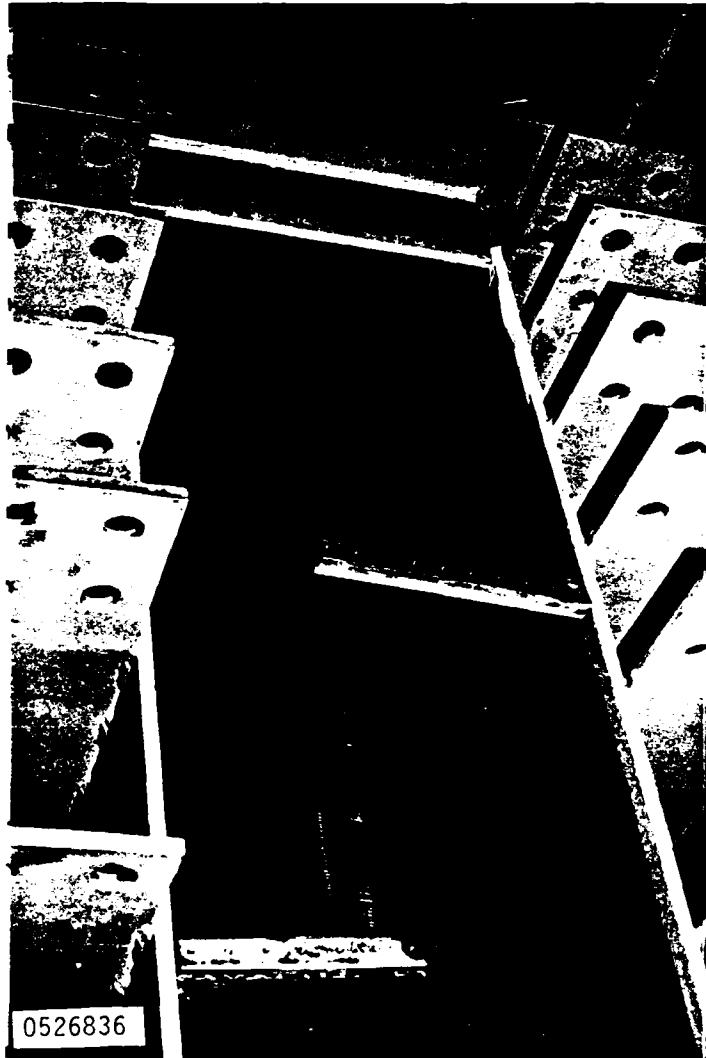


Figure 3.14. Bladder installation at stationary shear plane.

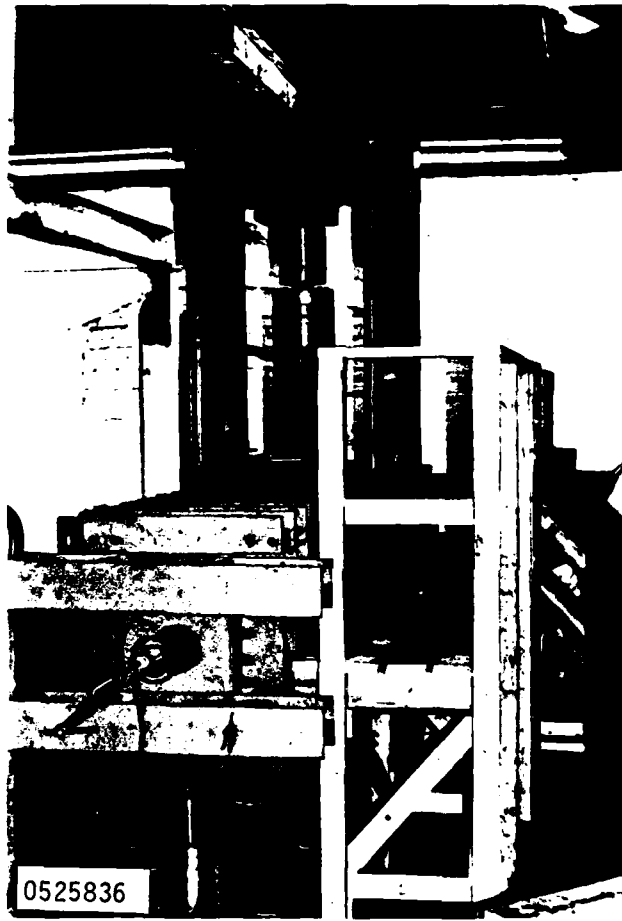


Figure 3.15. Work platform.

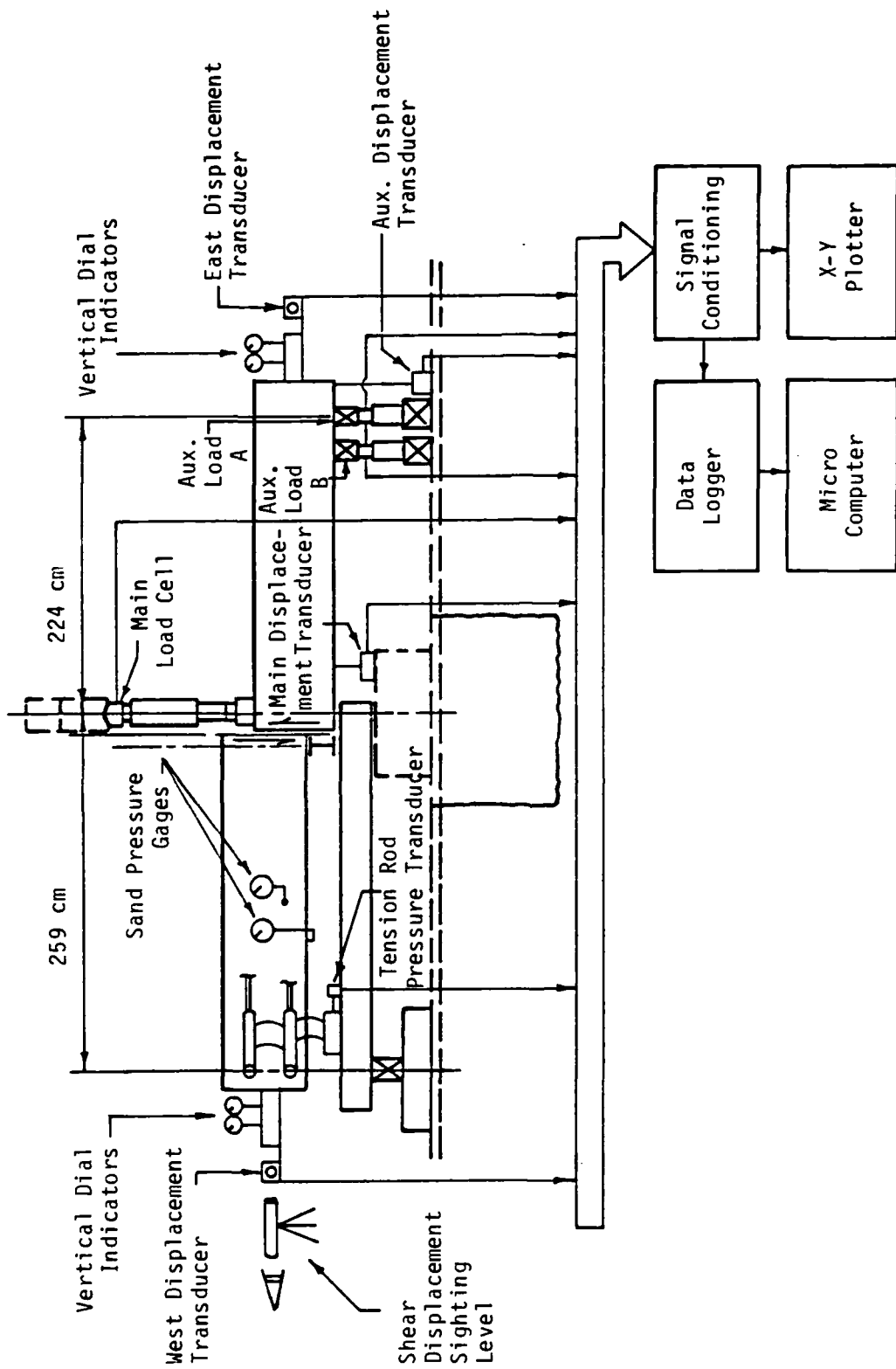


Figure 3.16. Shear test instrumentation schematic.

Table 3.1. Shear test instrumentation plan.

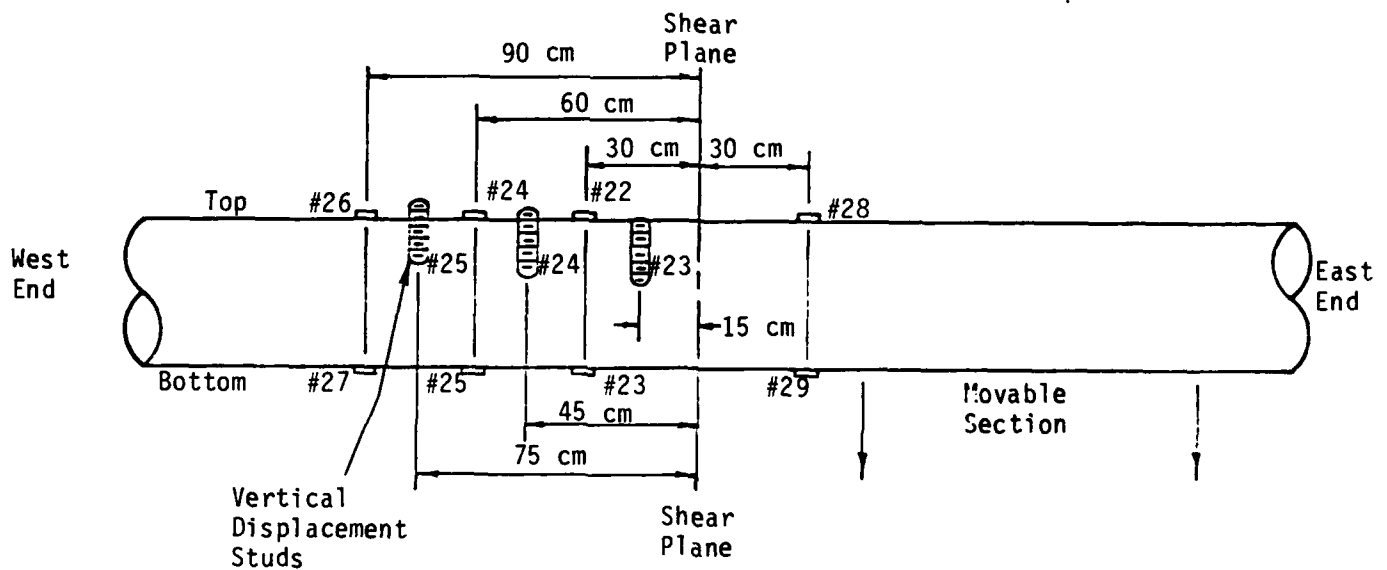
<u>Item</u>	<u>Channel</u>	<u>Description</u>	
1	10	Main Load	
2	11	Auxiliary Load 1	
3	12	Auxiliary Load 2	
4	13	Axial Rod Load (Pressure)	
5	14	Forward Displacement (Main)	
6	15	Rear Displacement	
7	16	Delta Displacement (Attitude Control)	
8	20	Inward Displacement - East	
9	21	Inward Displacement - West	
10	22	Strain - Top 30 cm West	} Ductile Iron Tests Only
11	23	Strain - Bottom 30 cm West	
12	24	Strain - Top 60 cm West	
13	25	Strain - Bottom 60 cm West	
14	26	Strain - Top 90 cm West	
15	27	Strain - Bottom 90 cm West	
16	28	Strain - Top 30 cm East	
17	29	Strain - Bottom 30 cm East	
18	X-Y Plotter	Main Load vs. Main Displacement	
19	Dial Gage	Outer Top Displacement - East	
20	Dial Gage	Inner Top Displacement - East	
21	Dial Gage	Outer Top Displacement - West	
22	Dial Gage	Inner Top Displacement - West	
23	Threaded Stud	Inside Displacement - 15 cm West	
24	Threaded Stud	Inside Displacement - 45 cm West	
25	Threaded Stud	Inside Displacement - 75 cm West	
26	Pressure Gage	Bladder Pressure	
27	Pressure Gage	Sidewall Pressure	
28	Pressure Gage	Bottom Pressure	

In addition to the channels listed, observations of the conduit condition after testing were noted. For the ductile iron pipe testing, eight strain gages were welded to the specimen and these channels were also monitored automatically. Figure 3.17 illustrates the positions of the strain gages. The gage locations were selected on the basis of the following considerations:

- (1) Initially, eight gages was deemed a reasonable compromise between the desire to profile strain along the pipe length and the uncertainty of the cost/benefit of any single strain measurement.
- (2) Top and bottom gage pairs were required in order to separate axial and flexural strain components.
- (3) Two pairs of gages should be symmetrically located about the shear plane in order to evaluate symmetry/asymmetry of the strain pattern.
- (4) Two additional pairs of gages on one side of the shear plane were felt to be the minimum required to provide a meaningful indication of longitudinal strain distribution.

As depicted in Figure 3.18, the strain gage wires were routed from each gage into the pipe through a 5 mm hole. This routing allowed the wires to exit through the pipe ends for easy connection and minimized the influence of the wires at the pipe/sand interface.

Two short bladders were assembled, each approximately 30 cm in length, to provide a means for measuring the pressure imposed by the sand at the bottom and side surfaces. These were carefully and completely filled with water and hooked to Bourdon tube pressure gages for monitoring the pressure. Holes were drilled at the center of the bottom and the center of the side wall for the water lines



Note: All Strain Gages are Longitudinal

Figure 3.17. Shear test instrument locations.

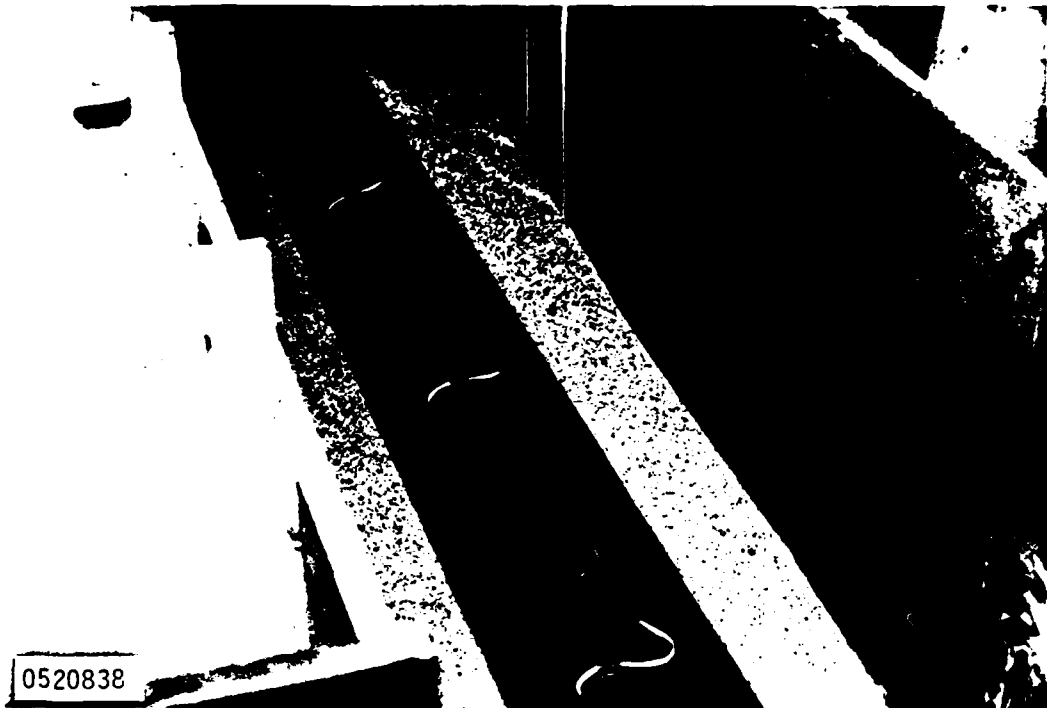


Figure 3.18. Ductile iron specimen showing three top strain gages.

to pass through, and both units were bonded in place on a firm bed of gypsum casting cement (Ultracal 30); see Figure 3.19.

Displacement transducers were installed to record the downward motion of the movable section and the horizontal displacement of the specimen ends. In addition to these four displacements, two dial indicators were used at each end to measure vertical displacement and rotation of the specimen relative to the test fixture end piece (Figure 3.20).

One further element of the instrumentation plan was the use of graduated vertical studs (Figure 3.21) to measure vertical displacement inside the pipe. These were sighted at regular increments of the main displacement (typically 0.5 cm) using a dumpy level which was fixed with respect to the test fixture (see Figure 3.20). Locations of the studs (used in both DIP and VCP tests) are shown in Figure 3.17.

#### Shear Test Preparation and Procedure

Prior to each shear test, the soil bin tops were removed, the bins emptied or cleaned as required, and the movable section raised to its highest elevation. The bins were then ready for the backfill sand to be rained in.

A sand raining apparatus was set up using a 55 gallon drum with a funnel fitting installed in the bottom for attachment to a flexible hose. The sand-filled barrel was raised with a fork-lift to a height sufficient for a continuous flow of sand through the 2 in. hose. Several raining techniques were tried, and in-place density measurements provided evaluation of each method. Best results were obtained using a large distribution screen of 1/8 inch mesh over the end of the sand tube and maintaining a drop height of not less than 30 cm. The sand



Figure 3.19. Measurement bladder installed on sidewall.

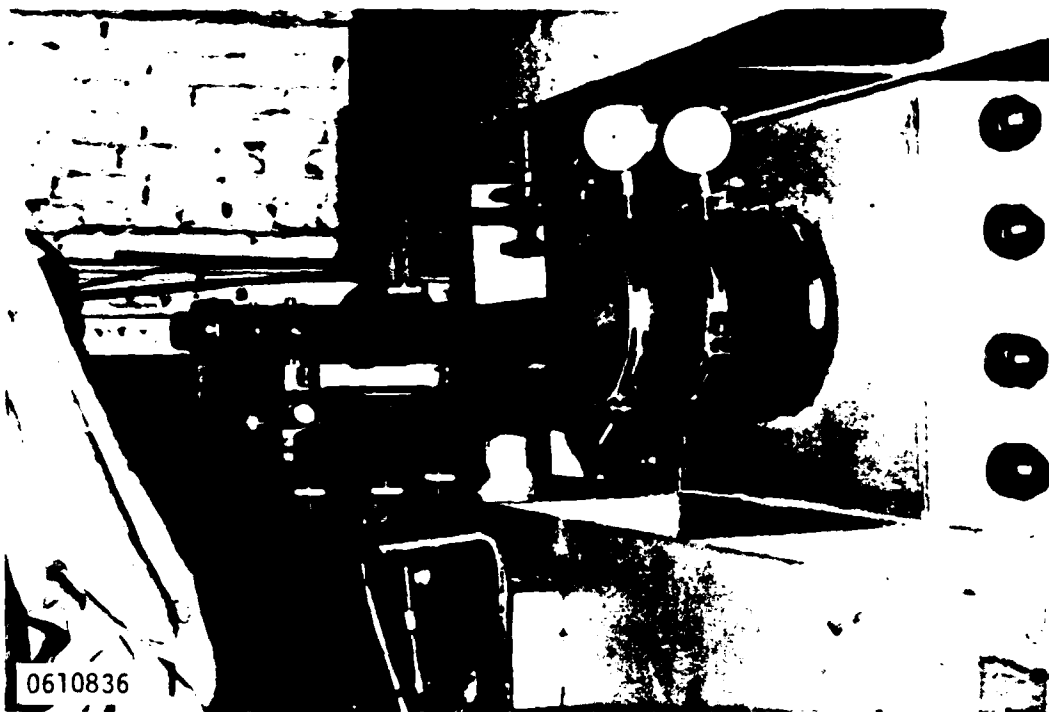
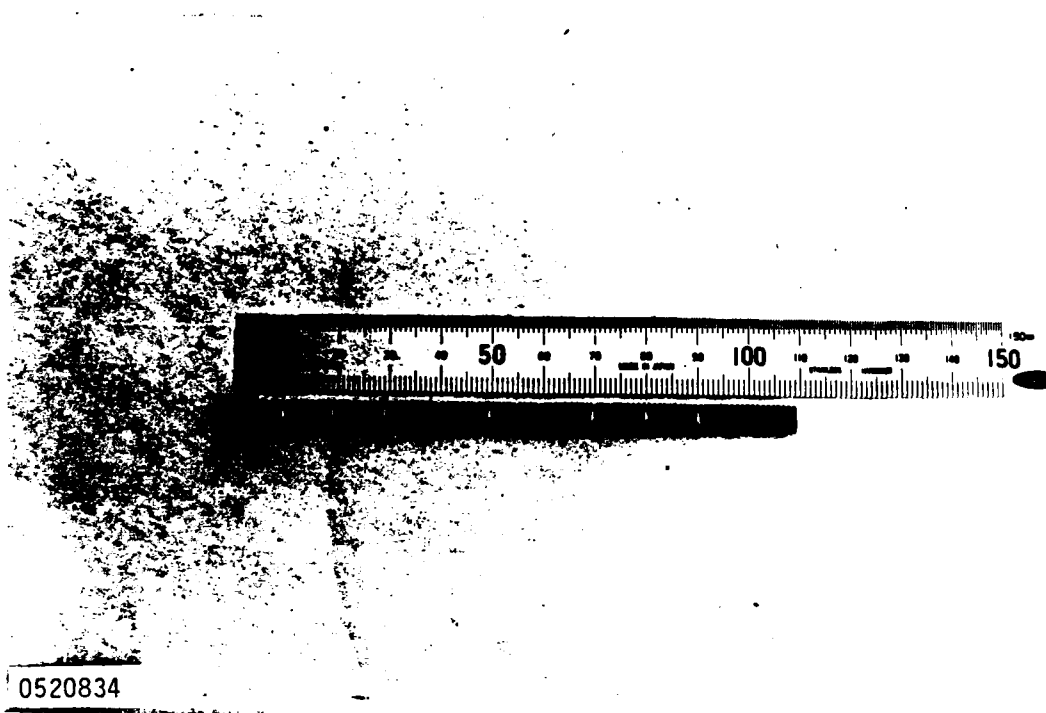


Figure 3.20. Ductile iron specimen - west end showing dumpy level, vertical dial gages, and closure gasket.



0520834

Figure 3.21. Threaded stud for visual recording of inside displacement.

raining operation is shown in Figure 3.22. A number of density measurements were made to find the raining method which produced the most consistent densities. This series of measurements, using standard 6 x 12 in. sample cylinders, is shown in Table 3.2. Table 3.3 summarizes the sand density measurements.

After sand had been rained into the fixture to a level slightly below the bottom of the specimen, the specimen itself was placed in position by sliding it through the fixture from one end (Figure 3.23). After carefully centering the specimen with respect to the shear plane ( $\pm 1$  mm), the end holes were plugged by placing rubber gaskets around the pipe (Figure 3.20). These gaskets sealed the sand against outward leakage while permitting essentially unrestricted movement of the specimen longitudinally and vertically in the ends of the fixture.

Next the vertical displacement measuring rods were inserted in threaded holes in the top of the specimen and set to their final adjustments. Sand raining then continued as previously described to complete filling of the chamber. As the raining resumed, special care was taken to insure complete and uniform distribution of sand in the region beneath the pipe.

After completing the sand raining to fill the test fixture, the surface was screeded off, providing 2.5 cm of space at the top for the bladder installation (Figure 3.24). Figures 3.13 and 3.14 showed the overlapping bladders in place just prior to installing the top covers. After the bladders were placed, the bin tops and load beam were bolted in place to complete the preparation phase.

Testing began by loading the four axial tension rods to the prescribed load. After that, the retaining bolts securing the two bins together during preparation could be removed. The pressurizing bladders were then inflated to their prescribed pressure as the final step before imposing the main shear load.



Figure 3.22. Sand raining.

Table 3.2. Sand density measurements. Shear test #1 - lapis lustre #1/20 backfill, 15.24 cm diameter x 30.48 cm long cylinder (in place).

<u>Sample No.</u>	<u>Raining Condition</u>	<u>Drop Height (cm)</u>	<u>Net Weight (grams)</u>	<u>Density (kN/m<sup>3</sup>)</u>
1	Open Tube	60-30	8629	15.22
2	Open Tube	60-30	8657	15.27
3	Open Tube	75-45	8612	15.19
4	Open Tube	75-45	8460	14.92
5	1/4 Inch Mesh Flat	60-30	8890	15.68
6	1/4 Inch Mesh Flat	60-30	9163	16.16
7	1/4 Inch Mesh Flat	60-30	8978	15.84
8	1/4 Inch Mesh Flat	60-30	8918	15.73
9	1/8 Inch Mesh Flat	60-30	8995	15.87
10	1/8 Inch Mesh Flat	60-30	9019	15.91
11	1/8 Inch Mesh Flat	60-30	8953	15.79
12	1/8 Inch Mesh Flat	60-30	8945	15.78
13	1/8 Inch Mesh Flat	60-30	8908	15.71
14	1/8 Inch Mesh Flat	60-30	8726	15.39
15	1/8 Inch Mesh Formed	60-30	9068	15.99
16	1/8 Inch Mesh Formed	60-30	9166	16.17
17	1/8 Inch Mesh Formed	60-30	9237	16.29
18	1/8 Inch Mesh Formed	60-30	9129	16.10
Average, 15-18		60-30	9150	16.14

Table 3.3. Sand density measurement summary  
 lone star lapis lustre 1/20 sand.

	<u>lb/ft<sup>3</sup></u>	<u>kN/M<sup>3</sup></u>
Loose Sand Density (Quoted by supplier)	97.00	15.24
First Raining Density (Open 2" Pipe)	96.51	15.16
Final Raining Density (1/8" Mesh)	102.75	16.14
Vibration (tapping) of the test fixture after sand raining followed by additional loading caused density to increase an average of 1.1%.	103.89	16.32
Maximum Density Obtained by Repeated Vibrations of a Dry Sample	105.48	16.57



Figure 3.23. Ductile iron specimen installed for testing.



05208313

Figure 3.24. Full sand bin prior to bladder installation.

The main load was increased to achieve the desired displacement rate and the auxiliary attitude ram was operated to keep the moving bin level. Loading pauses for data recording at regular displacement steps were made by briefly closing the hydraulic control valves. This procedure was continued until the desired final displacement was reached.

## SECTION 4

### DESCRIPTION OF TESTS

Early in the test program, the emphasis was placed on the axial slip characteristics between conduit and backfill. These pullout tests were a logical continuation of previous testing of buried instrumentation/communication conduits (Reference 2). These tests were a necessary precursor to the shear testing in that they define the necessary axial resistance of the conduit which in turn has a direct effect on conduit response to large amplitude shear offsets. The information gained from these pullout tests also serves to establish the end conditions that should be imposed in the shear test fixture to simulate the axial forces developed under actual field conditions where the length of the conduit is quite long in comparison to the test specimens. This is particularly important for ductile iron pipe with welded joints.

Test series I, II, III, and IV consisted of 1 in. and 1/4 in. conduit pullout tests conducted in the CASES high pressure biaxial test cell. Series V, VI, VII, and VIII were also pullout tests but these were conducted in the 150 cm long, low pressure cell. Each test series is described below.

#### Test Series I

Test series I included tests numbered 141 through 146A, a total of 10 tests listed in Table 4.1. All tests were on 1 in. conduit with a 23 cm length embedded in dry 20/40 Monterey Lapis Lustre sand. The principal variable in these tests was the confining pressure which varied between 2.0 and 8.0 MPa. Actually, test 141 was conducted at 20.0 MPa but the conduit failed at the pull linkage so that the results served only to indicate an upper limit of useful

Table 4.1. Summary of test series I.

<u>Test I.D.</u>	<u>Conduit Diameter</u>	<u>Test Date</u>	<u>Confining Pressure (MPa)</u>	<u>Peak Load (kN)</u>	<u>Residual Load (kN)</u>	<u>Remarks</u>
141	1-inch	2/5/82	20.0	83.5	81.5	Conduit failed
142	1-inch	2/10/82	2.0	11.1	10.4	Displacement transducer stuck
143-A	1-inch	2/10/82	4.0	25.0	19.7	
143-B	1-inch	2/10/82	4.0	25.0	18.5	
143-C	1-inch	2/10/82	4.0	27.4	19.5	Fast load rate
144-A	1-inch	2/10/82	5.0	28.8	25.2	Moderate load rate
144-B	1-inch	2/10/82	5.0	36.0	25.3	
145-A	1-inch	2/10/82	6.0	44.9	34.2	
145-B	1-inch	2/10/82	6.0	-	44.0	Fast load rate
146-A	1-inch	2/10/82	8.0	75.8	65.8	

confining pressure. Some observations of loading rate effects were also made in this series.

The sand used for this and all test series was #1/20 Lapis Lustre Kiln-Dried Monterey Sand which has been used on prior test programs at CASES and is well characterized. The granular form is coarse sand, subrounded to rounded, and well sorted. Size distribution, crystalline structure, and chemical composition are shown in Table 4.2.

Passive data obtained included pre- and post-test sand grain distribution sieve analysis for test series I. Results are given in Table 4.3. These analyses were performed locally by Pioneer Consultants, Inc. Additional information was obtained by careful observation of the specimen surface post-test and the sand condition adjacent to the specimen.

The tubing used in this series was 1 in., welded, drawn over mandrel (DOM) steel with 3 mm wall thickness. The minimum yield strength is specified as 414 MPa. ASTM designation for this material is A513 Type 5 ERW 1020 Mechanical Tubing. This tubing was selected over more common varieties due to its closer dimensional tolerances as compared to standard tubing.

#### Test Series II

Test series II, consisting of 13 tests numbered 147A through 152B, was similar to series I in that all were pullout tests of sand embedded steel tubing conducted in the high pressure test cell. The conduit for this series was 1/4 in. size with a 0.7 mm wall thickness and 483 MPa minimum yield. Other properties, including the ASTM designation, were the same as for the larger steel conduit. The ratio of inside diameters for the two sizes was 3.9. Tests in this series are listed in Table 4.4.

Table 4.2. Lone star lapis lustre #1/20 kiln-dried monterey sand size distribution.

Nominal Sieve Size: 20 x 40

<u>U.S. Sieve Number</u>	<u>Cumulative % Passing</u>
16	100
20	90 - 100
30	14 - 40
40	0 - 5

Crystalline Composition

Approximate Content

Quartz	65%
Feldspar	30%
Dark Minerals and Dark Lithic Fragments	5%

Chemical Analysis

Percent by Weight

Silicon Dioxide (SiO <sub>2</sub> )	81.08
Iron Oxide (Fe <sub>2</sub> O <sub>3</sub> )	.64
Aluminum Oxide (Al <sub>2</sub> O <sub>3</sub> )	10.36
Calcium Oxide (CaO)	1.40
Magnesium Oxide (MgO)	.41
Potassium Oxide (K <sub>2</sub> O)	2.80
Sodium Oxide (Na <sub>2</sub> O)	3.53
Chloride	0.006

Table 4.3. Pre- and post-test grain size distribution.

<u>Sample Ref.</u>	<u>Percent Passing Individual Sieves</u>				
	<u>#10</u>	<u>20</u>	<u>40</u>	<u>100</u>	<u>200</u>
141 Pre-Test, As-Received Moisture	100	89	3	1	.1
141 Pre-Test, Oven Dry	100	81	3	.4	.2
146 Pre-Test, As-Received Moisture	100	85	5	1	.4
146 Post-Test, Oven Dry	100	89	5	1	.4

Table 4.4. Summary of test series II.

<u>Test I.D.</u>	<u>Conduit Diameter</u>	<u>Test Date</u>	<u>Confining Pressure (MPa)</u>	<u>Peak Load (kN)</u>	<u>Residual Load (kN)</u>	<u>Remarks</u>
147-A	1/4-inch	2/18/82	1.0	0.85	0.58	
147-B	1/4-inch	2/18/82	1.0	0.87	0.51	
147-C	1/4-inch	2/18/82	1.0	0.97	0.62	Fast load rate
148-A	1/4-inch	2/18/82	2.0	2.14	1.38	
148-B	1/4-inch	2/18/82	2.0	2.24	1.40	
149-A	1/4-inch	2/18/82	2.5	2.65	1.94	
149-B	1/4-inch	2/18/82	2.5	2.70	1.88	Moderate load rate
150-A	1/4-inch	2/18/82	3.0	3.41	2.36	
150-B	1/4-inch	2/18/82	3.0	2.88	2.38	Fast load rate
151-A	1/4-inch	2/18/82	3.5	4.21	3.05	Slow load rate
151-B	1/4-inch	2/18/82	3.5	3.69	2.81	
152-A	1/4-inch	2/18/82	0.0	-	0.03	Loading
152-B	1/4-inch	2/18/82	0.0	-	-	Unloading

### Test Series III

Test series III consisted of only two tests, numbers 153 and 154, which were conducted to investigate specifically the incipient slip and immediate postslip condition of conduit in sand. Both tests used polished 1 in. conduits in the 23 cm high pressure cell. The tests were identical to test 145 of series I except for the longitudinal displacement imposed. In test 154, displacement was limited to 0.75 mm which corresponded to a lower than peak load condition. The 2.0 mm displacement imposed in test 153 corresponded, in turn, to a condition slightly beyond peak load. These tests are listed in Table 4.5.

### Test Series IV

Sixteen tests numbered 155A through 161C were included in series IV. These were tests of 1/4 in. conduit conducted in the high pressure tester. These tests differed from series II in that the effective length of conduit was varied between 10 cm and 23 cm by the device described in Section 3. Prior to conducting seven of these tests, as noted in Table 4.6, a pressure of 13 MPa was imposed on the sand to investigate the effect, if any, of such a preload. In all cases, this preload was removed prior to conducting the test at 3 MPa confining pressure. Test 160 was a push-pull test conducted with no confining pressure.

### Test Series V

Test series V was the last group conducted in the high pressure cell and included 25 tests numbered 162 to 172. These tests are listed in Table 4.7. The primary variable in these tests was the moisture content of the sand. The tests included dry, 1/8, 1/4, 1/2, and fully saturated conditions. The water required to achieve saturation was determined by carefully adding water to a

Table 4.5. Summary of test series III.

<u>Test I.D.</u>	<u>Conduit Diameter</u>	<u>Test Date</u>	<u>Confining Pressure (MPa)</u>	<u>Peak Load (kN)</u>	<u>Residual Load (kN)</u>	<u>Remarks</u>
153	1-inch	3/3/82	6.0	35.6	-	1.0 mm displacement
154	1-inch	3/5/82	6.0	34.3	-	0.4 mm displacement

Table 4.6. Summary of test series IV.

Test I.D.	Conduit Diameter	Test Date	Confining Pressure (MPa)	Peak Load (kN)	Residual Load (kN)	Remarks
155-A	1/4-inch	3/18/82	3.0	1.70	1.24	L=10 cm } L=10 cm } L=15 cm } Loading Sequence: L=15 cm } 0, 3, 0 MPa L=20 cm } L=20 cm }
155-B	1/4-inch	3/18/82	3.0	1.50	1.14	
156-A	1/4-inch	3/18/82	3.0	1.47	0.86	
156-B	1/4-inch	3/18/82	3.0	1.23	0.80	
157-A	1/4-inch	3/18/82	3.0	2.00	1.24	
157-B	1/4-inch	3/18/82	3.0	1.85	1.33	
158-A	1/4-inch	3/18/82	3.0	3.10	1.95	Loading Sequence: 0, 13, 3, 0 MPa
158-B	1/4-inch	3/18/82	3.0	2.72	1.57	
158-C	1/4-inch	3/18/82	3.0	3.38	2.00	
159-A	1/4-inch	3/18/82	3.0	2.62	1.32	P=0, 13, 0, 3, 0 } P=0, 3, 0 } L=15 cm P=0, 13, 3, 0 }
159-B	1/4-inch	3/18/82	3.0	1.89	1.18	
159-C	1/4-inch	3/18/82	3.0	2.59	1.50	
160	1/4-inch	3/18/82	0.0	0.85	0.08	in and out } L=10 cm
161-A	1/4-inch	3/18/82	3.0	2.02	0.76	P=0, 13, 0, 3, 0 } P=0, 3, 0 } L=10 cm P=0, 13, 3, 0 }
161-B	1/4-inch	3/18/82	3.0	1.16	0.60	
161-C	1/4-inch	3/18/82	3.0	1.60	0.85	

Table 4.7. Summary of test series V.

Test I.D.	Conduit Diameter	Test Date	Confining Pressure (MPa)	Peak Load (kN)	Residual Load (kN)	Remarks
162	1-inch	3/26/82	6.0	34.00	31.70	Stopped after 10 mm
163-A	1-inch	3/26/82	6.0	33.80	31.00	Dry sand
163-B	1-inch	3/26/82	6.0	41.00	32.00	Dry sand
164-A	1-inch	3/29/82	6.0	39.00	27.50	1/8 sat. (70 g. H <sub>2</sub> O) sand
164-B	1-inch	3/29/82	6.0	38.20	24.80	1/8 sat. (70 g. H <sub>2</sub> O) sand
165-A	1-inch	3/31/82	6.0	38.70	24.00	1/4 sat. (140 g. H <sub>2</sub> O) sand
165-B	1-inch	3/31/82	6.0	41.50	27.00	
165-C	1-inch	3/31/82	6.0	45.00	32.00	
165-D	1-inch	3/31/82	6.0	53.00	36.00	
165-E	1-inch	3/11/82	6.0	56.00	39.40	
166	1-inch	3/11/82	0.0	-	-	No pressure - push/pull after 165D
167-A	1-inch	4/2/82	6.0	57.6	43.2	Half-saturated
167-B	1-inch	4/2/82	6.0	62.0	49.9	
167-C	1-inch	4/2/82	6.0	62.5	53.6	
167-D	1-inch	4/2/82	6.0	67.4	56.6	
168-A	1-inch	4/2/82	4.0	42.7	36.8	
168-B	1-inch	4/2/82	4.0	44.1	38.1	
168-C	1-inch	4/2/82	4.0	45.0	39.3	
168-D	1-inch	4/2/82	4.0	45.5	39.7	
169	1-inch	4/5/82	6.0	74.8	57.9	Fully saturated; initial seepage of water from specimen after attitude adjustment. Also 96.5 g. H <sub>2</sub> O in cup.
170-A	1-inch	4/5/82	1.0-1.5	15.2	7.5	Fully saturated; pressurized in steps.
170-B	1-inch	4/5/82	0.5-5.0	63.7	4.0	
170-C	1-inch	4/5/82	4.9-4.5	58.5	48.8	
171	1-inch	4/6/82	2.0-3.0	59.6	45.7	Hand-pump operating ram; drop in pressure during testing -- fully saturated. Fully saturated; hand pump - plot only.
172	1-inch	4/6/82	2.0-3.0	57.3	42.3	Pulled conduit out completely - hole open - plot only.

sample sand volume until saturation was first barely noticeable. Proportionate amounts were added to the actual sample to achieve each desired saturation percentage.

A load oscillation effect was observed in these tests which was initially attributed to the moisture. Due to this unusual behavior, tests 170 - 172 varied the confining pressure application method in an effort to define better the situation observed. No effect of the test apparatus was apparent and further investigation of the phenomenon was deferred to later test series. Figure 4.1 is included to illustrate the effect described.

#### Test Series VI

Test series VI included tests 179 through 190, the first 16 tests conducted in the 150 cm long test cell. These were all pullout tests of the larger steel conduit similar to series I except for the longer test cell. Due to the increased conduit contact surface areas, confining pressures used in the 150 cm cell were lower than those in the high pressure cell in order to avoid tensile failure of the conduit. These tests are listed in Table 4.8. Test 179 is included in the list but was unsuccessful due to a problem with the fixture. The problem was corrected prior to test 180.

Tests 180 to 184 were tests with varying confining pressures - nominally 2.0, 1.5, 1.4, 1.0 and 0.5 MPa. Tests 185, 186A, B, C and 187A were all tests at nominally 1.5 MPa to investigate repeatability, "conditioning" effects and loading perturbations. In most of the tests, confining pressure was maintained within 0.5 percent of the desired level, although in a few instances greater variations occurred. Tests 187B and 188 addressed this by eliminating the pressure regulation mechanism. That is, the confining pressure was applied

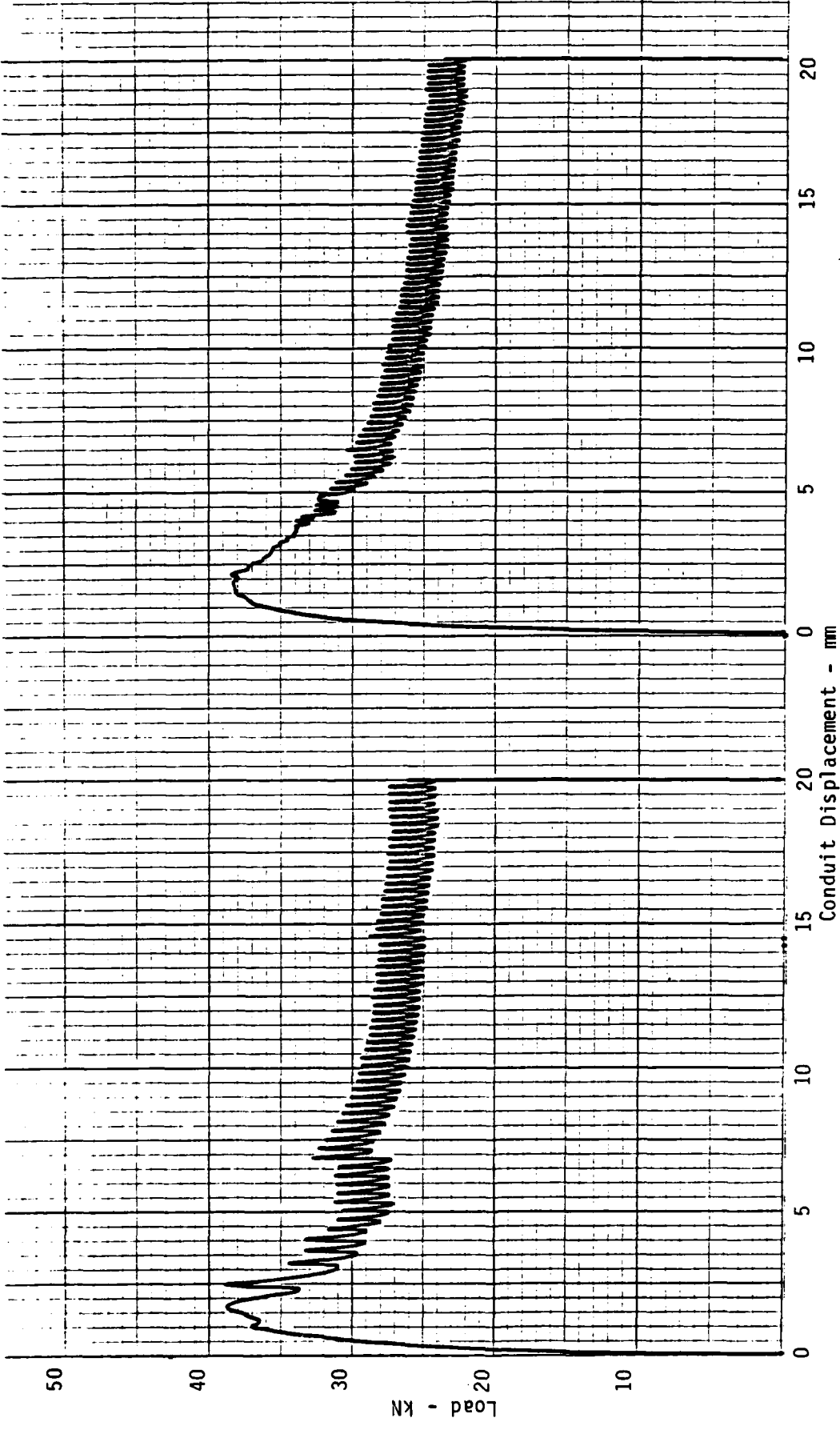


Figure 4.1. Examples of pullout test load oscillation.

Table 4.8. Summary of test series VI.

Test I.D.	Test Date	Conduit Diameter (in.)	Conduit Length (cm)	Area (cm <sup>2</sup> )	Confining Pressure (MPa)	Peak Load (kN)	Peak F/A (KPa)	Residual Load (kN)	Residual F/A (KPa)	F/PA	Remarks
179	8/18/82	1-inch	150	1197	1.00	26.20	219	-	-	-	Fixture problem
180	8/23/82	1-inch	150	1197	2.05	81.00	677	76.00	635	.309	
181	8/23/82	1-inch	150	1197	1.55	59.40	496	57.00	476	.307	
182	8/23/82	1-inch	150	1197	1.39	52.40	438	51.00	426	.306	
183	8/23/82	1-inch	150	1197	1.00	37.90	317	37.00	309	.300	
184	8/23/82	1-inch	150	1197	.51	20.80	174	19.50	163	.310	
185	8/23/82	1-inch	150	1197	1.50	59.90	500	54.00	451	.300	
186-A	8/24/82	1-inch	150	1197	1.57	56.80	475	55.50	464	.295	
186-B	8/24/82	1-inch	150	1197	1.53	56.10	469	53.00	443	.289	
186-C	8/24/82	1-inch	150	1197	1.55	56.80	475	53.00	443	.285	
187-A	8/24/82	1-inch	150	1197	1.50	53.10	444	53.00	443	.295	
187-B	8/24/82	1-inch	150	1197	1.80	41.90	350	40.00	334	.180	Pressure
188	8/24/82	1-inch	150	1197	1.80	43.10	360	43.00	359	.199	unregulated
189	8/24/82	1-inch	150	1197	1.51	55.10	460	56.00	468	.309	
190-A	8/24/82	1-inch	150	1197	.79	-29.80	-249	-28.50	-238	-.301	Push Test
190-B	8/24/82	1-inch	150	1197	.52	18.50	155	19.00	159	.305	

before the test and allowed to decay naturally during the test. This resulted in a generally exponential pressure decay to about 65% of the initial value. For test 189, slightly less sand was installed in the fixture to determine if any effect on performance or loading perturbation was observable as a function of the sand "density."

Tests 190A and B were a test pair to determine if an initial push test performed significantly different from an initial pull test upon fixture assembly.

#### Test Series VII

Test series VII included five tests numbered 196A through 199. These tests, listed in Table 4.9, were similar to tests 180 to 184 except that the conduit was polished prior to testing. One push test without confinement plus pull tests at 2.0, 1.5, 1.0 and 0.5 MPa confinement were performed.

#### Test Series VIII

Test series VIII, test numbers 200A through 207, were primarily investigations of the test fixture itself. In 200A and 200B a pull and push test were done with air pressure substituted for the hydraulic fluid to provide confinement. In tests 202, 203, 206 and 207 the thin bladder containing the sand was replaced by a heavy (approximately 8 mm thick) rubber hose. Those results were somewhat inconsistent and indicated the alternate material was probably not suitable for the application. The tests are tabulated in Table 4.10.

#### Test Series IX

Test series IX was the last set of tests performed in the 150 cm cell, and were the last pullout tests conducted. The series included eleven tests numbered 208

Table 4.9. Summary of test series VII.

Test I.D.	Test Date	Conduit Diameter (in.)	Conduit Length (cm)	Area (cm <sup>2</sup> )	Confining Pressure (MPa)	Peak Load (kN)	Peak F/A (KPa)	Residual Load (kN)	Residual F/A (KPa)	F/PA	Remarks
196-A	10/21/82	1-inch	150	1197	.00	-1.70	-14	-1.60	-13	-	Push Test, Polished Bar
196-B	10/21/82	1-inch	150	1197	2.00	69.50	581	60.00	501	.250	Polished Bar
197	10/21/82	1-inch	150	1197	1.50	47.90	400	45.00	376	.250	Polished Bar
198	10/21/82	1-inch	150	1197	1.00	32.70	273	30.00	251	.250	Polished Bar
199	10/21/82	1-inch	150	1197	.50	16.80	140	15.50	129	.258	Polished Bar

Table 4.10. Summary of test series VIII.

Test I.D.	Test Date	Conduit Diameter (in.)	Conduit Length (cm)	Area (cm <sup>2</sup> )	Confining Pressure (MPa)		Peak Load (kN)		Peak F/A (KPa)		Residual Load (kN)		Residual F/A (KPa)		Remarks
200-A	10/26/82	1-inch	150	1197	.51	18.20	152	16.00	.262	134	16.00	134	.262	Air Pressure	
200-B	10/26/82	1-inch	150	1197	.51	-17.50	-146	-16.00	-.262	-134	-16.00	-134	-.262	Air Pressure, Push Test	
202	10/29/82	1-inch	150	1197	1.00	21.80	182	17.50	.146	146	17.50	146	.146	Rubber Bladder	
203	10/29/82	1-inch	150	1197	2.00	43.80	366	43.00	.179	359	43.00	359	.179	Rubber Bladder	
206	11/4/82	1-inch	150	1197	2.00	55.70	465	51.00	.213	426	51.00	426	.213	Rubber Bladder	
207	11/4/82	1-inch	150	1197	1.00	27.50	230	23.50	.190	196	23.50	196	.190	Rubber Bladder	

through 214 as listed in Table 4.11. These tests were all done on 1/4 in. conduit with confining pressures of 0.25, 0.38, 0.50, 0.63, 0.75 and 1.0 MPa confinement (though at 1.0 MPa the conduit failed). This provided comparisons with earlier smaller diameter, shorter samples as well as with the larger diameter samples. Fast and slow loadings were also performed at several confinement levels.

#### Test Series X

Test series X (see Table 4.12) consisted of the four single shear tests conducted in the single shear test fixture. Test number 219 was a checkout and calibration of the fixture to indicate the vertical main load required to overcome the shear plane friction imposed on the empty fixture at various axial tension loads. The results of that test are presented in Figure 4.2.

Test number 222 was a shear test of a nominal 4 in. unjointed ductile iron pipe specimen. Test 223 was conducted on vitrified clay pipe consisting of three 6 foot long sections with BAND-SEAL® joints symmetrically located about the shear plane. Test 224 was a repeat of the VCP test in number 223.

Table 4.11. Summary of test series IX.

Test I.D.	Test Date	Conduit Diameter (in.)	Conduit Length (cm)	Area (cm <sup>2</sup> )	Confining Pressure (MPa)	Peak Load (kN)	Peak F/A (KPa)	Residual Load (kN)	Residual F/A (KPa)	F/PA	Remarks
208	11/10/82	1/4-inch	150	299	.50	3.46	116	3.07	103	.205	
209-A	11/11/82	1/4-inch	150	299	.50	3.28	110	2.92	98	.195	Rapid Loading
209-B	11/11/82	1/4-inch	150	299	.50	3.50	117	3.06	102	.204	Slow Loading
210	11/11/82	1/4-inch	150	299	.25	1.79	60	1.64	55	.219	Slow Loading
211-A	11/11/82	1/4-inch	150	299	.38	2.46	82	2.14	72	.190	
211-B	11/11/82	1/4-inch	150	299	.38	-	-	2.24	75	.199	Fast Loading
211-C	11/11/82	1/4-inch	150	299	.38	-	-	2.26	76	.201	Fast Loading
212-A	11/11/82	1/4-inch	150	299	.63	3.85	361	3.53	118	.188	
212-B	11/11/82	1/4-inch	150	299	.63	3.98	133	3.76	126	.201	
213	11/11/82	1/4-inch	150	299	.75	4.78	160	4.56	152	.203	
214	11/11/82	1/4-inch	150	299	1.00	5.08	170	-	-	-	Conduit Failed

Table 4.12. Summary of test series X.

<u>Test I.D.</u>	<u>Test Date</u>	<u>Conduit Type</u>	<u>Rod Load (kN)</u>	<u>Peak Shear Load (kN)</u>	<u>Maximum Displacement (cm)</u>	<u>Remarks</u>
219	2/23/83	-	0-100	52.3	-	Fixture Calibration
222	5/18/83	4-inch DIP	150	53.8	15.1	
223	6/10/83	4-inch VCP	150	10.8	1.4	
224	6/23/83	4-inch VCP	150	16.8	2.0	

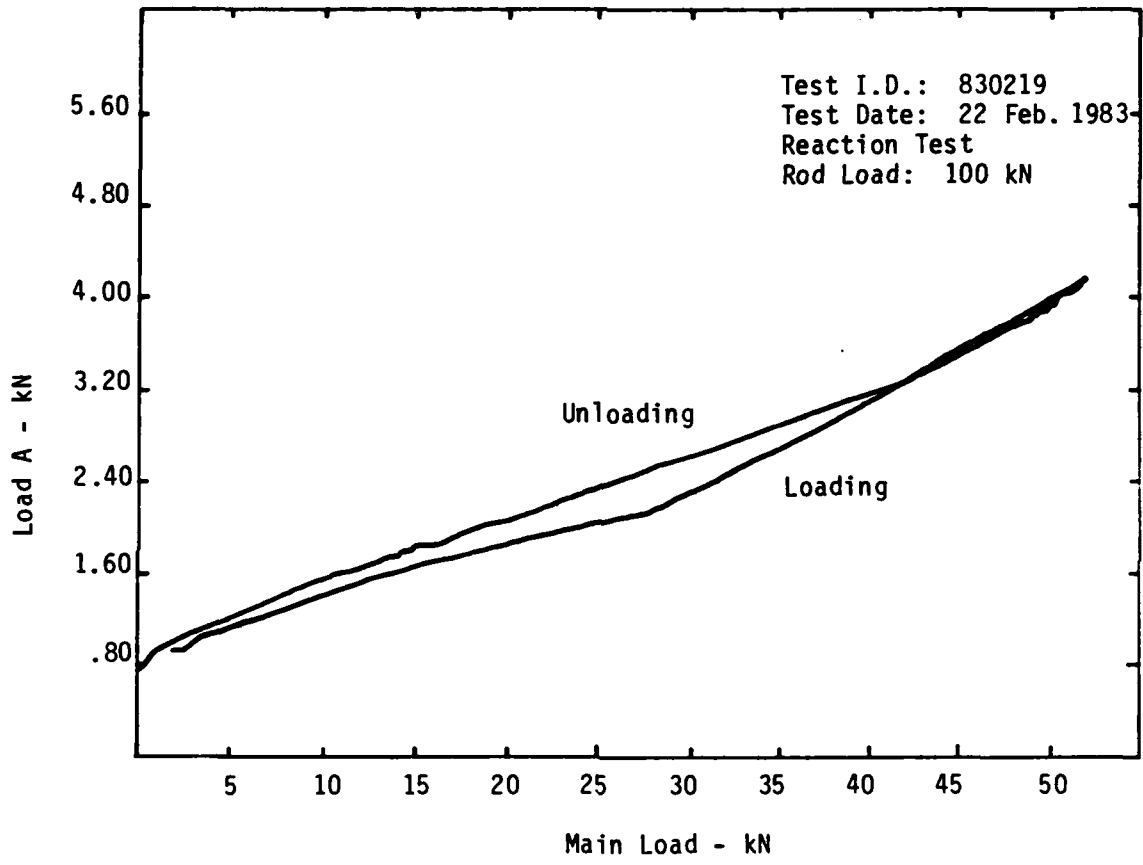


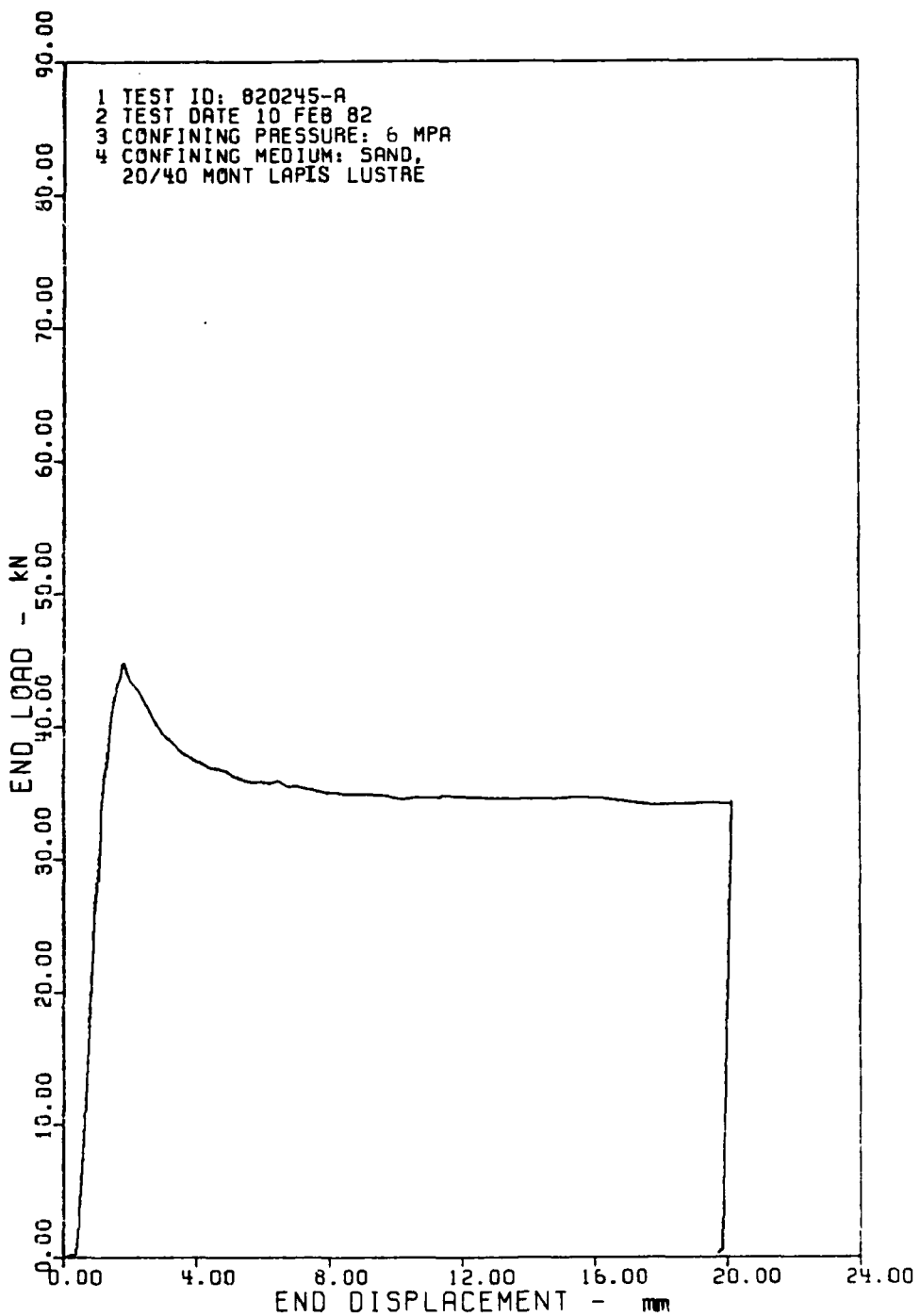
Figure 4.2. Applied shear load versus end load.

## SECTION 5

### DISCUSSION OF PULLOUT TEST RESULTS

The principal variable studied throughout the pullout tests was the sand confining pressure. Over various conduit lengths and two conduit diameters, pressures from 0 to 8 MPa were tested. In the early tests using 1 in. conduit in the high pressure cell, several important aspects of slip behavior were observed. Referring to the pullout load conduit slip response shown in Figure 5.1, it is seen that a characteristic initial peak resistance is achieved followed by a gradual decrease in resistance to a nearly constant value. The second key aspect of behavior was the pullout load increasing at a faster rate than the corresponding confining pressure, at pressures above about 4 MPa. At lower pressures the increase is linear. This behavior is illustrated in Figure 5.2. The difference between high and low confining pressure is more clearly shown in Figure 5.3. The linear trend for low pressures is especially evident for the 1/4 in. conduit. In addition, post test visual inspections of the conduit surface conditions indicated surface striations (Figure 5.4) caused by individual sand grains scratching the surface. These observations taken collectively indicated that the coefficient of sliding friction between the conduit and sand was effectively increased by the sand grains embedding themselves into the conduit surface.

From test series I, a hypothesis of the pullout bond failure slip mechanism was developed. This hypothesis was developed as a means of explaining the load deflection curves observed; that is, a steep initial rise curving over slightly as the peak is reached, followed by a rather symmetric initial decline which levels out quite quickly to a reasonably steady load as full slip proceeds.



LIFELINES TEST #5-A - 1" CONDUIT

Figure 5.1. Typical load/slip response for test series I.

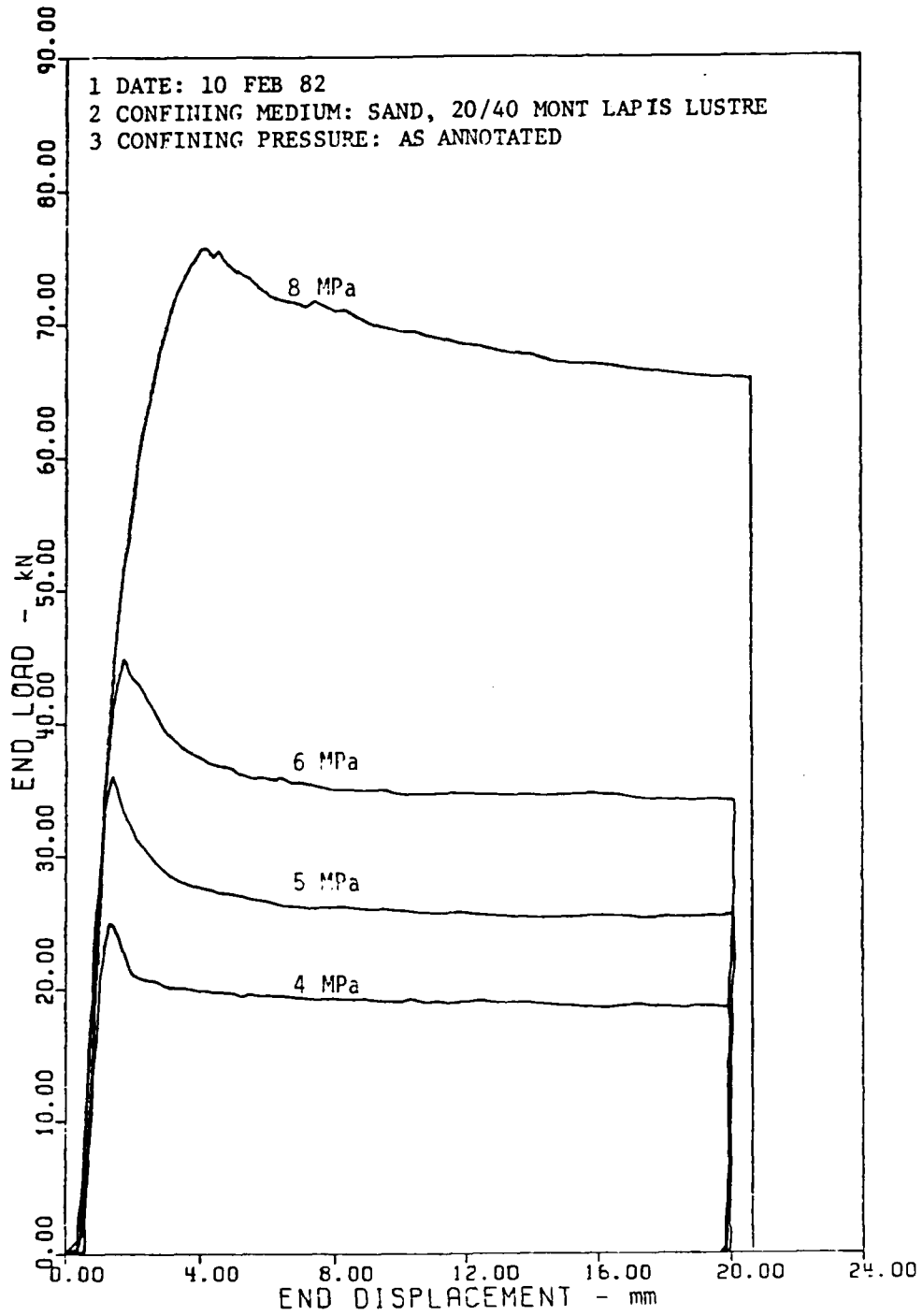


Figure 5.2. Test series I.

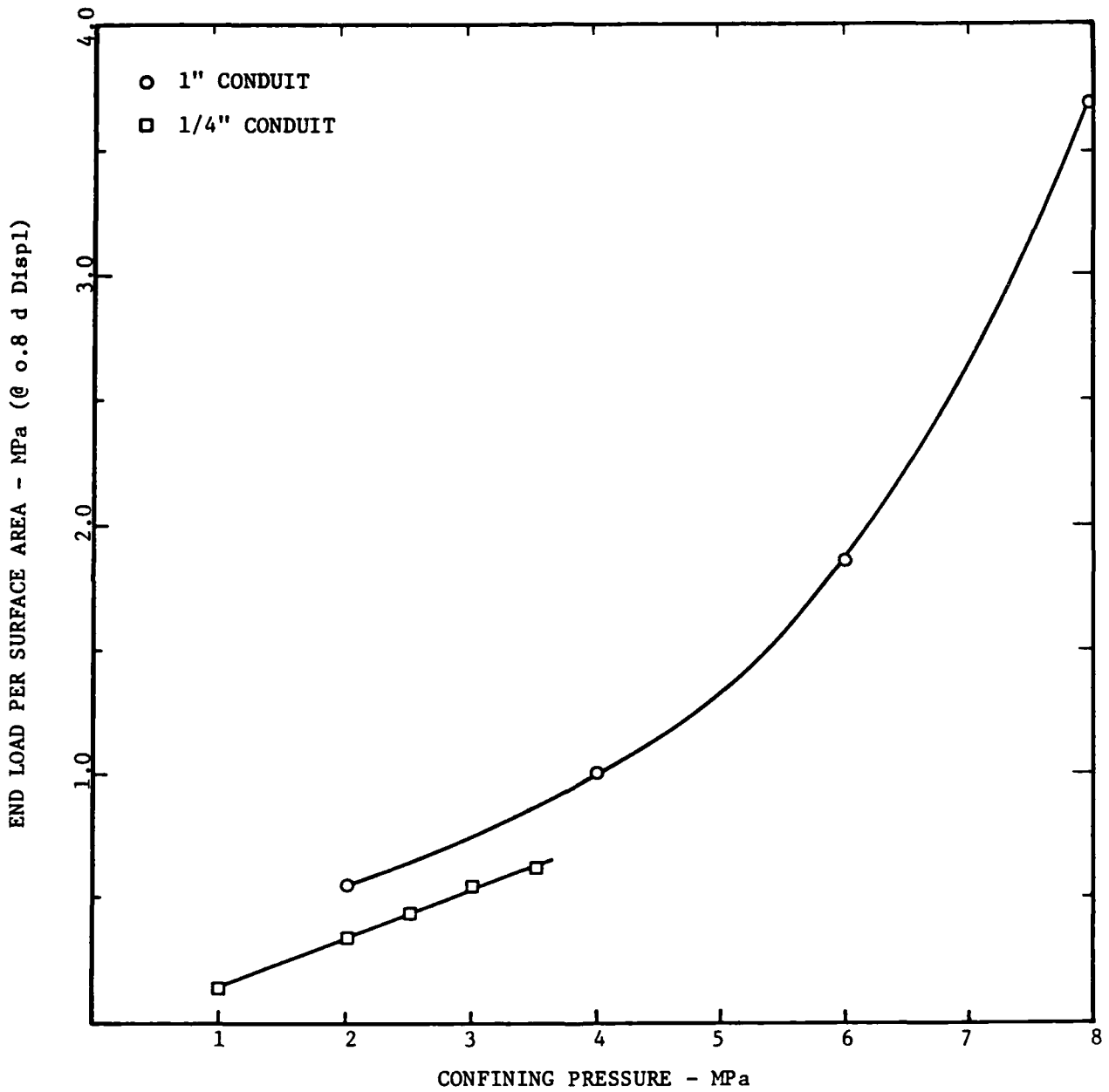
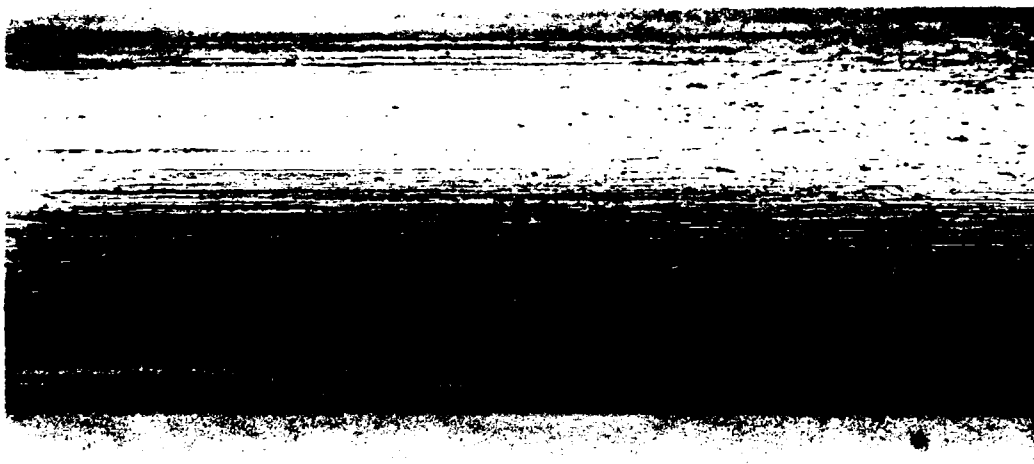


Figure 5.3. Normalized load versus confining pressure for 1-inch and 1/4-inch conduit.



02108215

Figure 5.4. Typical post test conduit surface condition.

As the confining pressure is applied to the sand, individual sand grains begin to embed in the conduit along its entire length. The subsequent pullout load is initially transferred by the static friction at the sand conduit interface to the sand column. This creates a triaxial state of stress in the sand whose axial component is reacted by the test fixture at the pulled end. This stress causes the sand to migrate toward the pulled end and at the same time causes the radial pressure on the conduit near the pulled end to increase as a result of the axial component of stress. This sand "bunching" allows the pullout load to rapidly increase as the sand grains at the pulled end embed themselves further into the conduit increasing the static frictional force. This behavior continues until a critical load is reached at which time the static friction force is exceeded and sliding of the sand grains along the conduit begins at the pulled end. The load then begins to decrease as this sand grain sliding propagates along the conduit toward the far end of the conduit. The pullout load then reaches a constant value as slip occurs along the entire conduit length.

To test this hypothesis, the two tests of series III were conducted. In test 153, a displacement of 2.0 mm was imposed on a fresh, polished, 1 in. conduit. This corresponds to a point on the downward sloped portion of the load-displacement curve as shown in Figure 5.5b. In test 154, a displacement of 0.75 mm was imposed on an identical specimen corresponding to a point on the initial upward sloped portion of the response curve shown in Figure 5.5c. Both tests had a confining pressure of 6.0 MPa as used in test 145 (Figure 5.5a). Careful examination of the post test conduit surfaces revealed:

- (1) For the 0.75 mm displacement, pits approximately 0.05 mm diameter were observed over the pulled end region while very few pits were even discernable at the opposite end. No evidence of sand/conduit slip was detected.

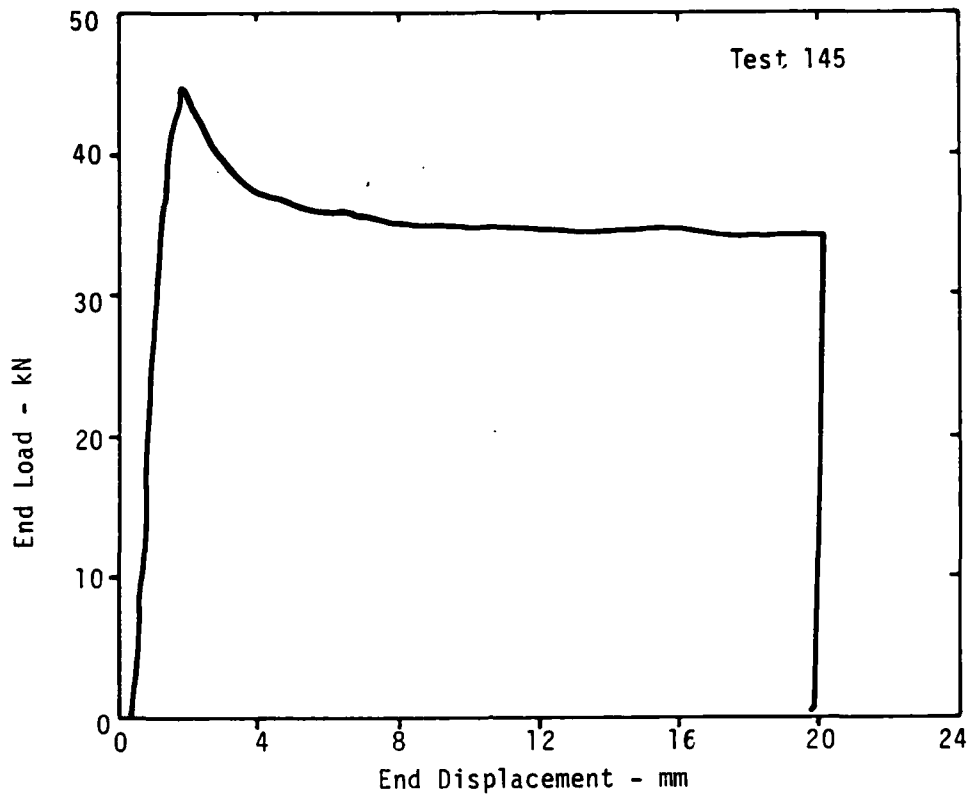


FIGURE 5.5a.

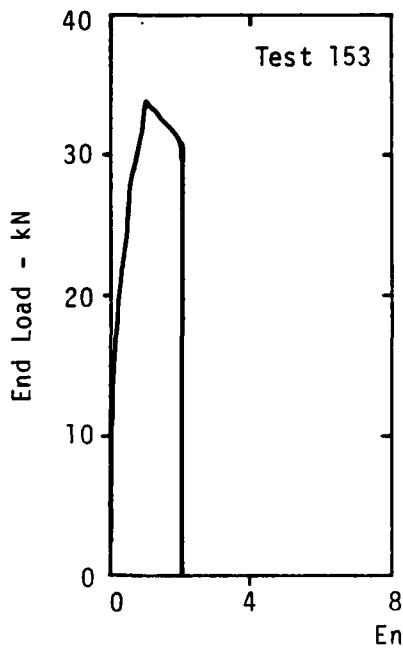


FIGURE 5.5b.

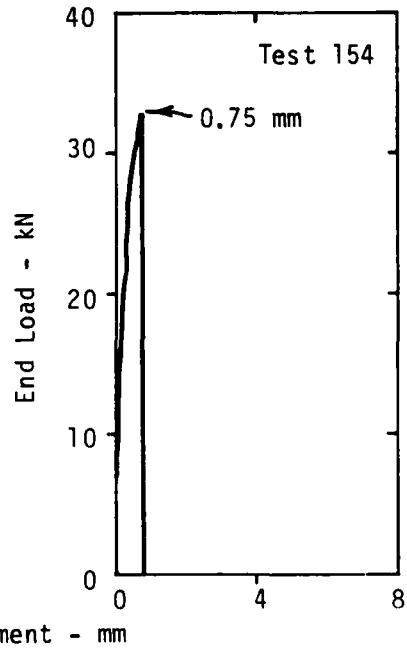


FIGURE 5.5c.

Figure 5.5. Conduit striation study.

- (2) For the 2.0 mm displacement case, striation lengths decreased from 1.0 mm at the pulled end to 0.8 mm at the far end. The 1.0 mm striation length with 2.0 mm displacement and the fact that peak load occurred at approximately 1.0 mm (Figure 5.5b) indicate no slip occurs until after peak pullout load is achieved.

While these tests do not constitute a rigorous proof of the hypothesis, we considered them to be sufficient evidence that the mechanism was reasonably well understood.

This postulate suggests that the initial peak in the load displacement curve was an artifact of the test device resulting from the rigid end plate and that the full slip or residual pullout load should be used for determining the effective slip friction coefficients for the sand/conduit interface.

It is also felt that the postulate applies to the lower pressure, linear region of Figure 5.3. It is believed that at the higher pressures, the sand grains dig into the conduit surface much more severely, thereby altering the sand/conduit interaction and resulting in the non-linear frictional characteristics shown.

As a result of this behavior, a limited analytical program was initiated to investigate the slip response in a more quantitative manner. Using the finite element program SATURN (Reference 14) the pullout test configuration was modeled as shown in Figure 5.6. The case considered here is the 1 in. diameter (2.54 cm outside diameter) conduit with a length of 23 cm. The outside diameter of the soil is 10.54 cm.

The SATURN runs are performed with the axisymmetric assumption. The lateral confining stress  $P_c$  is first applied and then the axial conduit force,  $F$ , is

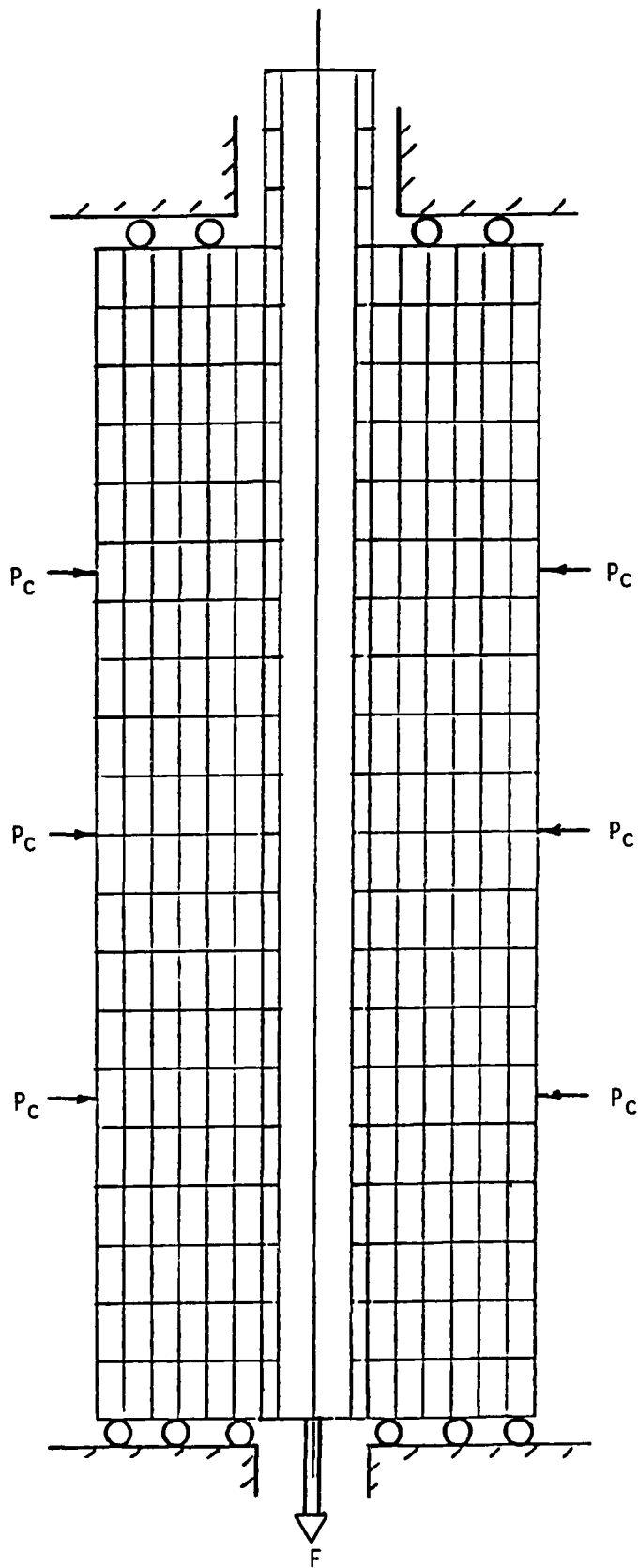


Figure 5.6. Finite element idealization.

incremented until the conduit is slipping at all node locations in contact with the soil. The sand is modeled as an elasto-plastic material with a Drucker-Prager failure law. The elastic moduli were determined from the following empirical relations suggested by Seed and Idriss (Reference 15):

$$G = 330 (1 + 4 D_Y) \left( \frac{\sigma_{kk}^o}{3} \right)^{1/2} \quad (5-1)$$

where  $D_Y$  is the relative density and  $G$  and  $\sigma_{kk}^o$  are in bars. Assuming a confining pressure of 3.0 MPa and a relative density of 0.8 yields:

$$G = 5660 \text{ bars} = 566 \text{ MPa}$$

$$\text{Using } K = \frac{2}{3} \frac{1 + \nu}{1 - 2\nu} G \text{ and assuming that } \nu = 1/4 \text{ yields:} \quad (5-2)$$

$$K = 9430 \text{ bars} = 943 \text{ MPa}$$

Assuming that the conduit is steel ( $E = 200,000 \text{ MPa}$ ,  $\nu = 0.29$ ) completes the material model.

### Slip Failure

Shear failure at the conduit-sand interface (i.e., slipping) is modeled by assuming zero cohesion and a constant friction coefficient ( $k$ ) which also determines failure. Thus:

$$\begin{aligned} \text{slip failure if: } & |F_t| > k F_n \\ \text{during slip: } & |F_t| = k F_n \\ \text{zero cohesion: } & F_n \geq 0 \end{aligned} \quad (5-3)$$

where  $F_t$  and  $F_n$  are the tangential and normal forces acting at the contact between the conduit and sand nodes.

The displacement of the end of the conduit as a function of the axial force,  $F$ , appears in Figure 5.7 for a linear material. The development of the slip along the conduit as a function of axial load appears in Figures 5.8 and 5.9, again for a linear material model. The displacements in these figures are magnified by a factor of 100 in the longitudinal direction.

A total of 29 runs were performed to parametrically assess the effects of the key variables. Failure model parameters were varied as well as slip friction coefficient and confining pressure. These runs are summarized in Table 5.1. Results of all the runs are given in Appendix D.

Plots of the end displacement versus pullout load for five selected runs are presented in Figures 5.10 through 5.14 (runs K through O in Table 5.1) for a confining stress of 4 MPa. These runs can be directly compared with test 143 (Figure 5.15). The variable in these five runs is slip friction coefficient which is varied between 0.2 and 0.4. In test 143 peak load is 25 kN while load at full slip is 19.7 kN.

Since the calculations are force controlled, the solution becomes unstable after slip occurs along the total length of conduit. Peak load and end displacement in the calculations thus correspond to the residual load in test 143 (19.7 kN). Run "O" with a full slip load of 21.4 kN most closely matches the test. However, in the calculations, the end slip is much less than the actual test value.

In order to produce results such as those of test 143, a more sophisticated friction failure law must be utilized -- perhaps one that has a friction coef-

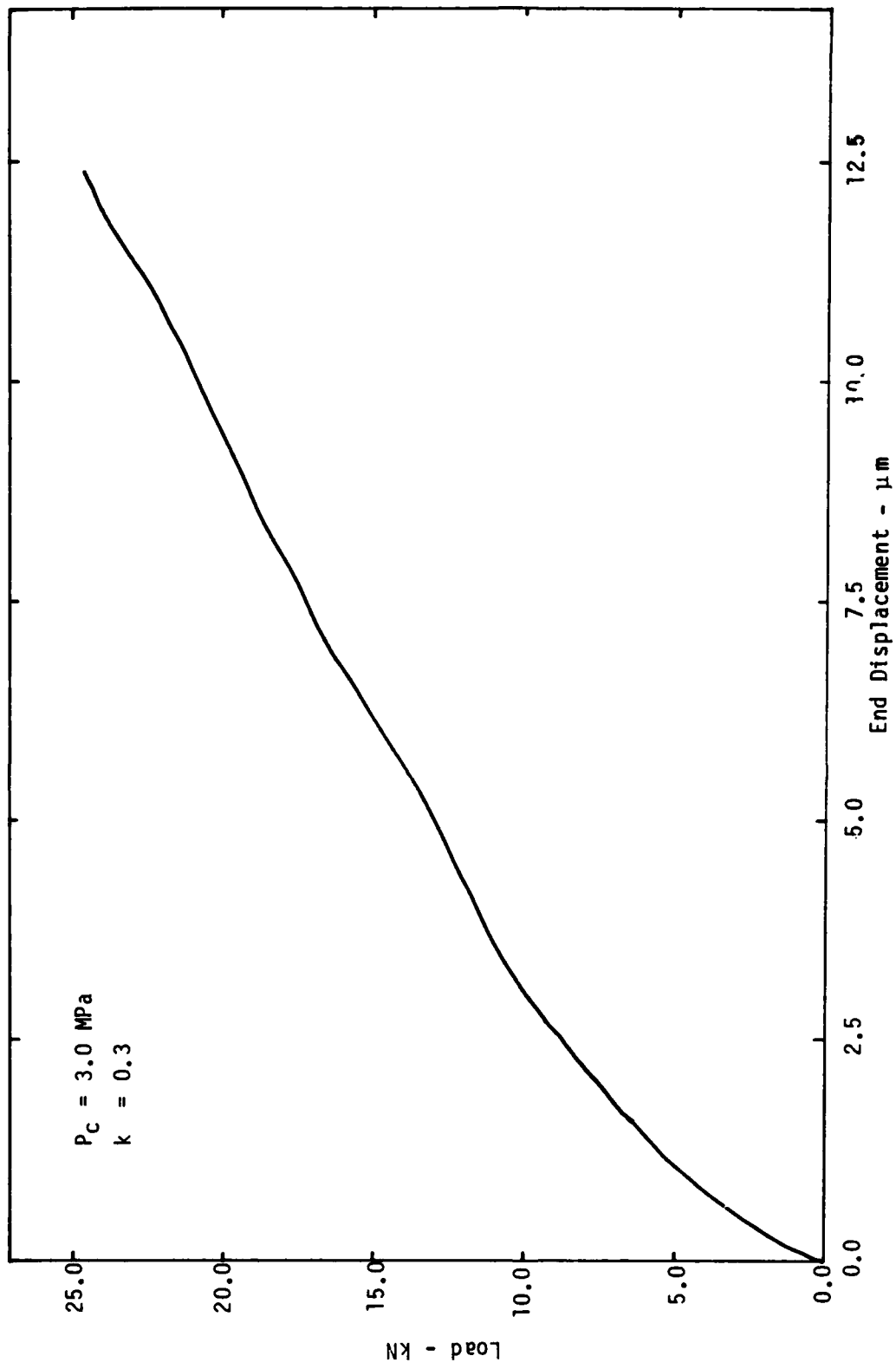


Figure 5.7. Calculated load/slip behavior (linear material).

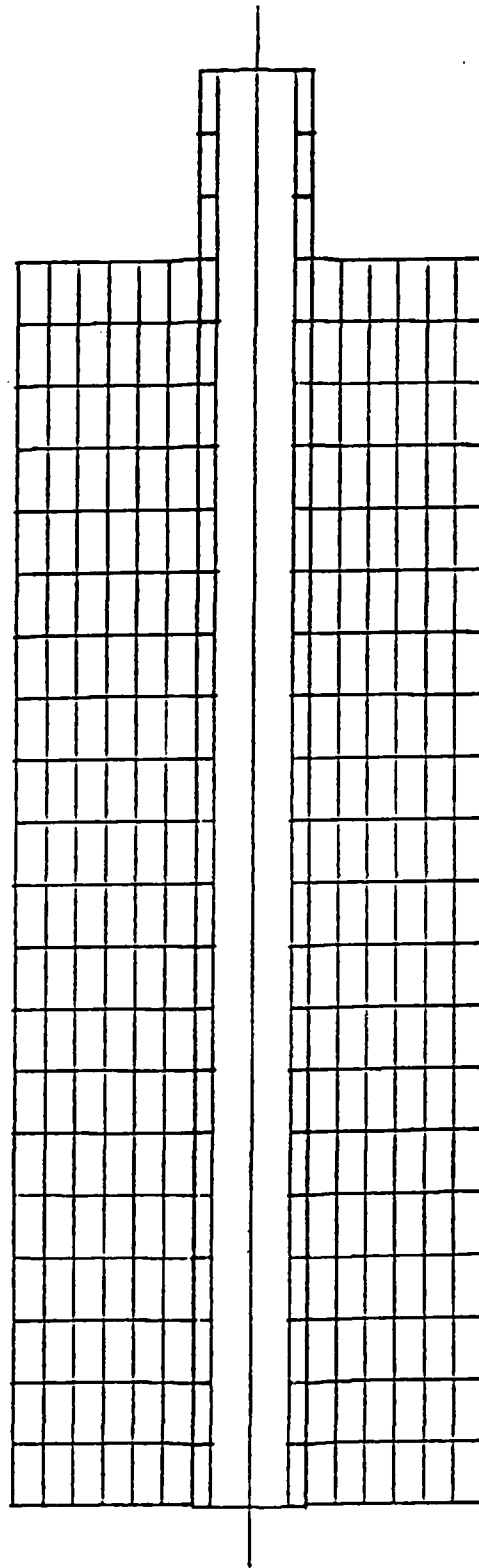


Figure 5.8. Slip development along conduit  
at pullout load of 1.8 kN  
 $P_c = 3 \text{ MPa}$ ;  $k = 0.3$ .

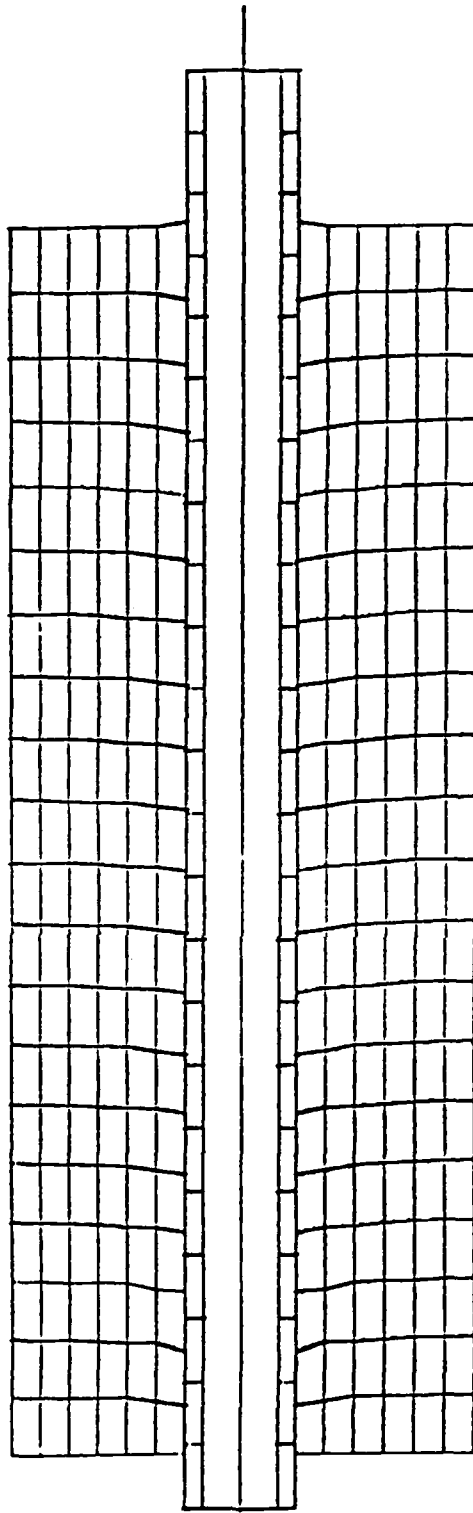


Figure 5.9. Slip development along conduit  
at pullout load of 20 kN  
 $P_c = 3 \text{ MPa}$ ;  $k = 0.3$ .

Table 5.1. Summary of 'SATURN' runs.

Run	Sand * Failure Model	Friction Coef., k	Conf. Press., P <sub>c</sub> , MPa	Max. End Displ., mm	Max. End Force, kN	No. of Plastic Elements	Remarks
A	1	.30	3.0	.0124	24.6	0	
B	2	.30	3.0	.0131	23.9	16	
C	3	.30	3.0	.0142	24.5	35	
D	4	.30	3.0	.0206	23.5	52	
E	5	.30	3.0	.0375	25.3	76	
F	6	.30	3.0	.151	30.7	114	
G	3	.25	3.0	.0102	19.2	11	
H	3	.35	3.0	.0218	29.8	33	
I	3	.40	3.0	.0207	31.3	33	
J	3	.20	3.0	.0091	16.9	7	
K	3	.30	4.0	.0180	31.6	28	
L	3	.25	4.0	.0133	25.4	9	
M	3	.35	4.0	.0312	37.8	35	
N	3	.40	4.0	.0263	38.5	32	
O	3	.20	4.0	.0120	21.4	3	
P	3	.30	2.0	.0095	17.1	16	
Q	3	.25	2.0	.0068	13.6	8	
R	3	.35	2.0	.0106	18.7	33	
S	3	.40	2.0	.0168	23.6	31	
T	3	.20	2.0	.0050	11.4	6	
U	5	.25	3.0	.0154	19.0	60	
V	5	.35	3.0	.049	27.7	80	
W	5	.40	3.0	.0801	32.0	90	
X	5	.20	3.0	.0114	16.4	60	
Y	3	.40	3.0	.093	40.0	85	
Z	7	.30	3.0	.0137	24.5	15	
AE	8	.30	3.0	.043	25.1	83	
AF	9	.30	3.0	.033	24.5	14	
AK	3	.30	3.0	.014	24.3	32	New mesh

1. Linear
2. Drucker-Prager,  $\phi = 32^\circ$
3. Drucker-Prager,  $\phi = 30^\circ$
4. Von Mises,  $\tau_{\max} = 1 \text{ MPa}$
5. Von Mises,  $\tau_{\max} = 0.6 \text{ MPa}$
6. Von Mises,  $\tau_{\max} = 0.2 \text{ MPa}$
7. Drucker-Prager,  $\phi = 30^\circ$  with Associated Flow Rule
8. Drucker-Prager,  $\phi = 8^\circ$
9. Drucker-Prager,  $\phi = 30^\circ$ ,  $K = 236 \text{ MPa}$ ,  $G = 142 \text{ MPa}$

\* Unless noted otherwise all sand models have elastic constants of:  
 $K = 943 \text{ MPa}$ ,  $G = 566 \text{ MPa}$ ,  $\nu = 0.25$

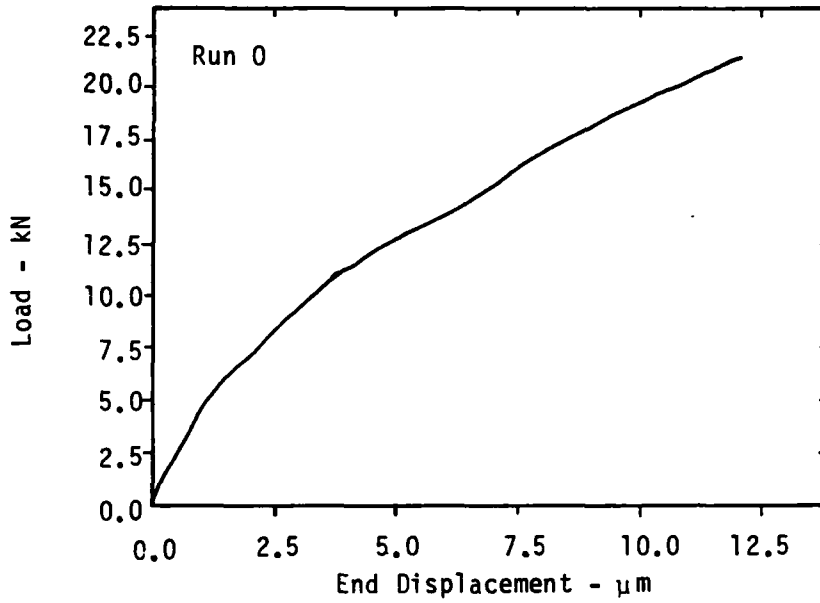


Figure 5.10. End displacement versus pullout load,  $k = 0.20$ .

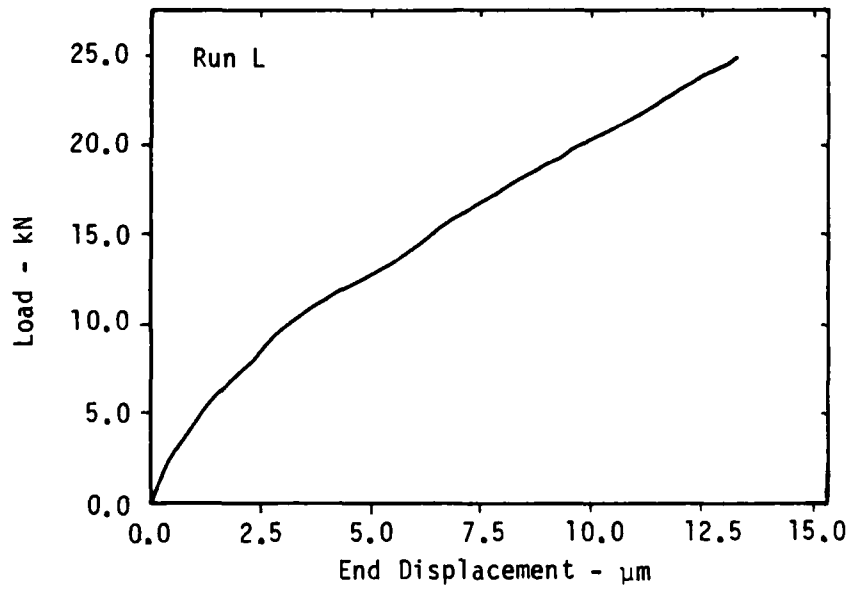


Figure 5.11. End displacement versus pullout load,  $k = 0.25$ .

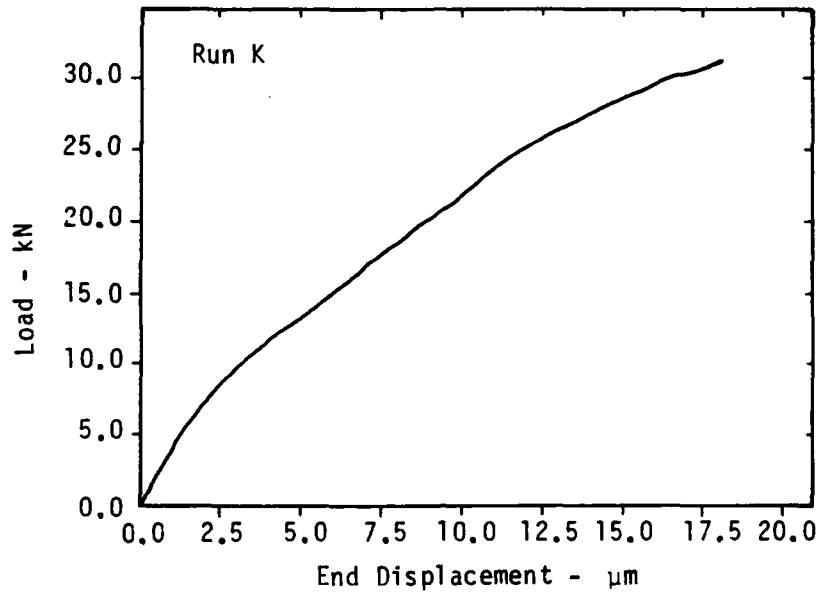


Figure 5.12. End displacement versus pullout load,  $k = 0.30$ .

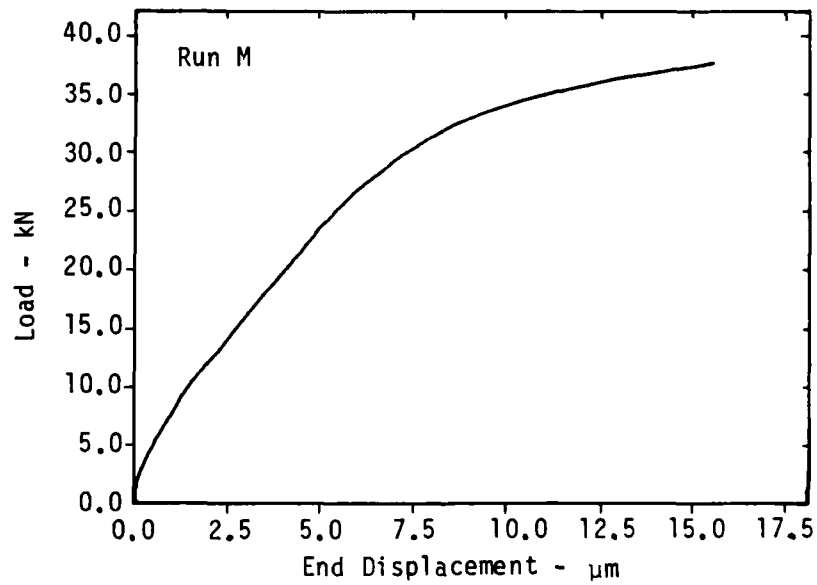


Figure 5.13. End displacement versus pullout load,  $k = 0.35$ .

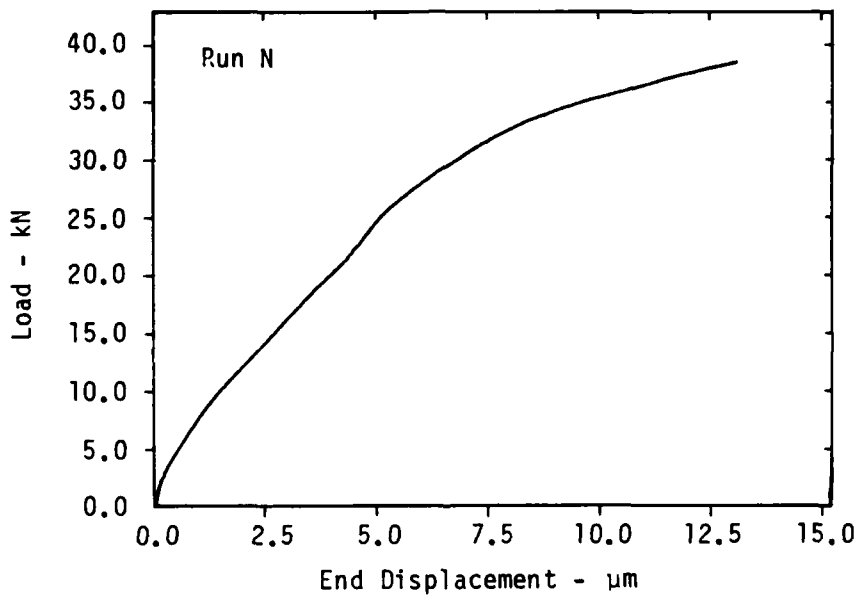
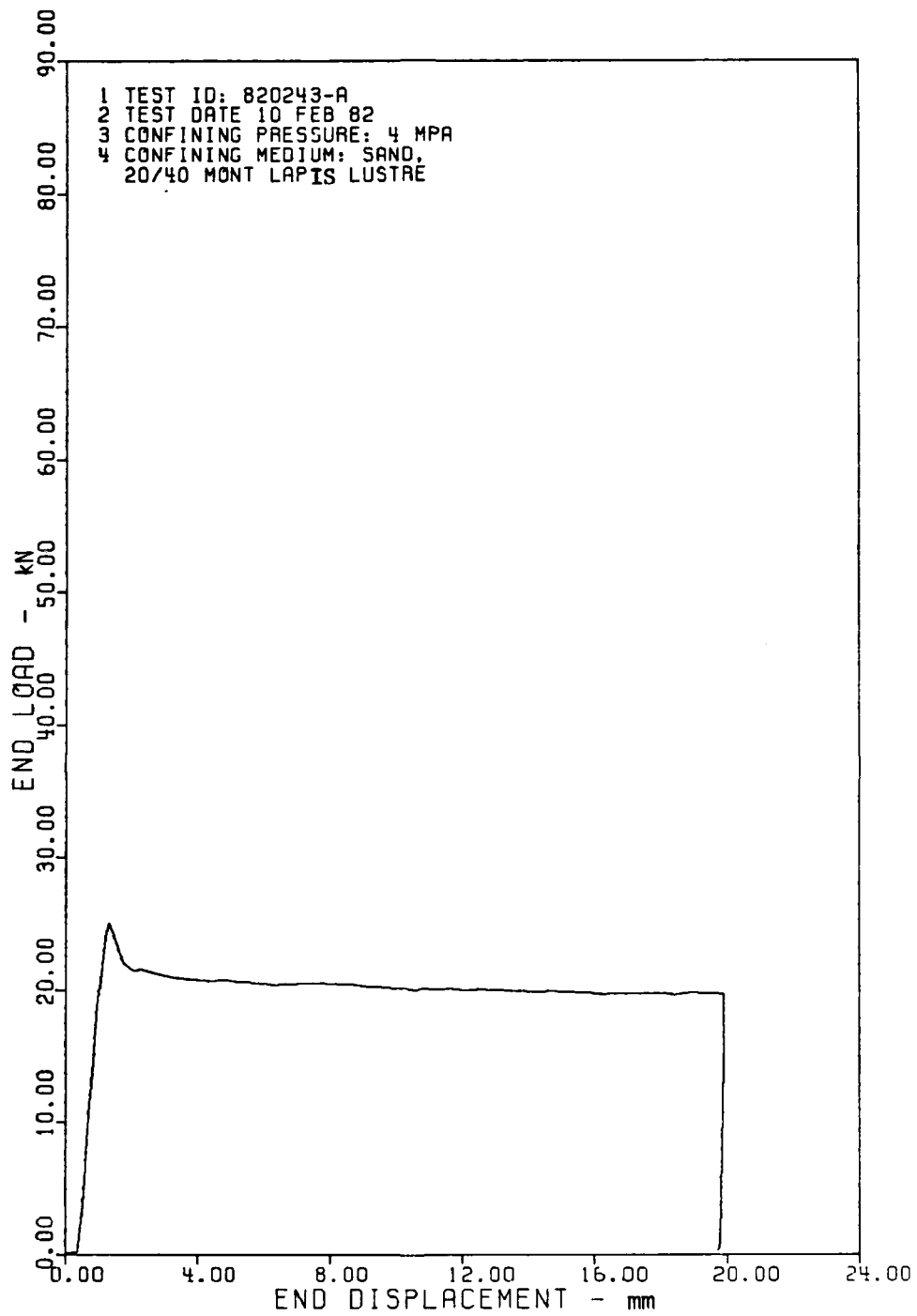


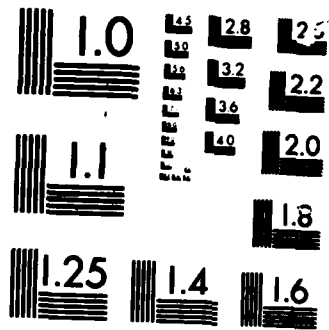
Figure 5.14. End displacement versus pullout load,  $k = 0.40$ .



LIFELINES TEST #3-A - 1" CONDUIT

Figure 5.15. Test 143,  $P_c = 4$  MPa.





MICROCOPY RESOLUTION TEST CHART

ficient that reduces with relative slip. Also the computation of elastic moduli may need to be modified to produce larger displacements in the sand prior to slip.

Several early tests (especially 145B and 145C) were conducted at a faster loading rate to assess the importance of that factor. These tests showed little effect on either the peak load or the residual load except that there seems to be a time constraint on development of the residual load. Thus if the total test duration is sufficient, the peak and residual loads are virtually independent of the loading rate.

The axial stress in the conduit, either tension (pull test) or compression (push test) was studied in tests 190A and B. A comparison of the two tests is presented in Figure 5.16.

A direct comparison is difficult since the confining pressures are different. However, the shapes of the curves are quite similar. If the residual load is scaled in proportion to the confining pressure, then the pull test load should be increased by about 52 percent (0.52 MPa vs. 0.79 MPa). Figure 5.16 indicates that for conduit slip greater than 1.00 cm, the push test is actually about 52 percent greater than the pull test. On the basis of this test, then, the push and pull tests are virtually identical. A few simple calculations will affirm that this should indeed be the case since the effect of Poisson's ratio should be negligible for the stresses induced in the conduit.

The tangential conduit strains can be computed from

$$\epsilon_{\theta} = \frac{u}{r_0} = -\frac{\nu\sigma_z}{E} + \frac{1}{E}(\sigma_{\theta} - \nu\sigma_r) \quad (5-4)$$

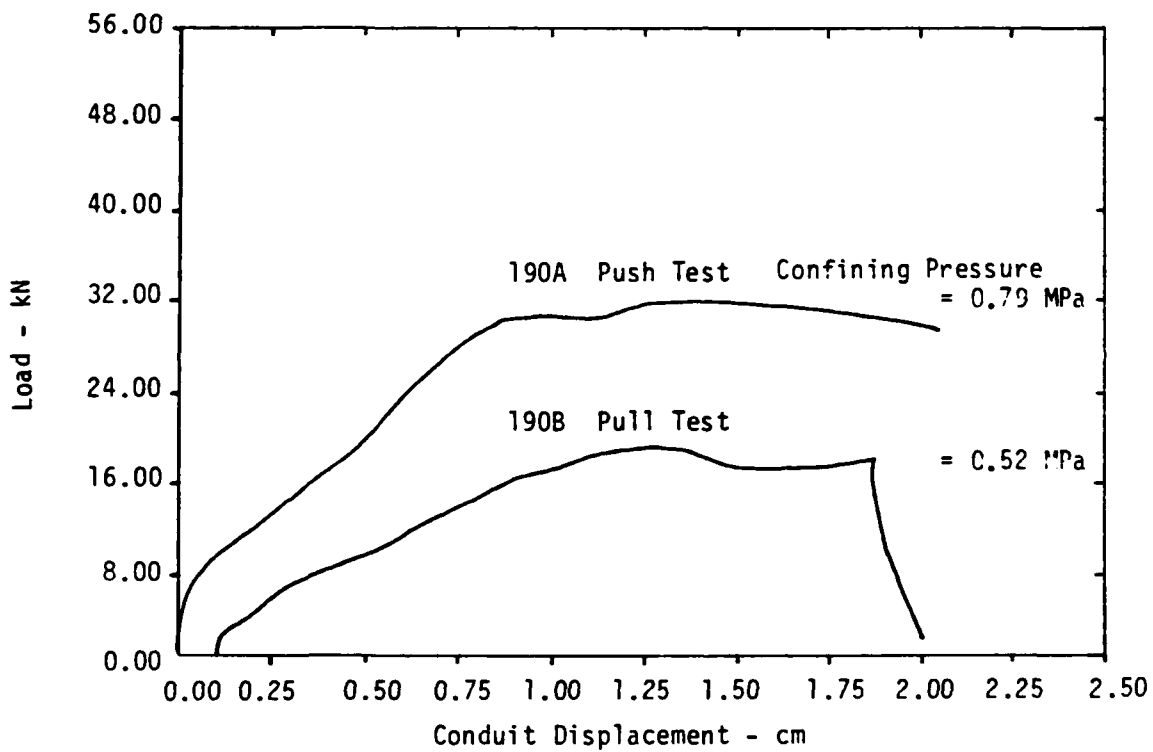


Figure 5.16. Push/pull test comparison.

or

$$\epsilon_{\theta} = -\frac{\nu \sigma_z}{E} - \frac{P}{E} \left( \frac{r_o^2 + r_i^2}{r_o^2 - r_i^2} - \nu \right) \quad (5-5)$$

in which  $r_i$  and  $r_o$  are the internal and external conduit radii,  $u$  is radial displacement,  $E$  and  $\nu$  are modulus of elasticity and Poisson's ratio, respectively,  $P$  is the external normal pressure on the conduit, and  $\sigma_z$  is the axial stress (+ tension, - compression).

For this purpose,  $P$  is taken as 1.5 times the oil confining pressure  $P_o$ . This is derived in Appendix C from an assumed Poisson's ratio in the sand of 0.25 which translates to an effective 0.333 for a plane strain condition.  $P$  is obtained from

$$P = \frac{2P_o}{1 + \nu'} \quad (5-6)$$

where  $\nu'$  is the plane strain Poisson's ratio for sand.

For the values tabulated in Table 5.2 the axial load and external pressure components of tangential strain can be computed from (1b).

$$\begin{aligned} \epsilon_{\theta} &= -\frac{0.29 (140 \text{ MPa})}{200,000 \text{ MPa}} - \frac{1.2 \text{ MPa}}{200,000 \text{ MPa}} \left[ \frac{(1.27 \text{ cm})^2 + (.965 \text{ cm})^2}{(1.27 \text{ cm})^2 - (.965 \text{ cm})^2} - 0.29 \right] \quad (5-7) \\ &= \pm 203 - 21 \text{ } \mu\text{m/m.} \end{aligned}$$

This shows that the first term, "maximum axially induced tangential strain," is an order of magnitude larger than the component resulting from confining pressure. However, the radius change is miniscule in either case:

$$u = \Delta r = r \epsilon_{\theta} = (1.27 \text{ cm}) (\pm 200 \text{ } \mu \text{ strain}) = \pm 0.00025 \text{ cm} \quad (5-8)$$

Table 5.2. Values used for tangential strain computation.

Outside radius of conduit	$r_o = 1.27 \text{ cm}$
Inside radius of conduit	$r_i = 0.965 \text{ cm}$
Cross sectional area of conduit	$A = 2.14 \text{ cm}^2$
Modulus of elasticity of conduit	$E = 200,000 \text{ MPa}$
Poisson's ratio of conduit	$\nu = 0.29$
Axial force in conduit	$F = +30 \text{ kN}$
Axial stress in conduit	$\sigma_z = F/A = \underline{+} 140 \text{ MPa}$
Conduit normal force	$P = 1.5 (0.8 \text{ MPa}) = 1.2 \text{ MPa}$

or  $\pm 2.5 \mu\text{m}$ . This change is so small compared to the dimensional variations of the specimen, test fixture, and sand that it would come as a surprise if any difference between tension and compression was evident.

Another primary variable addressed was the amount of water in the sand backfill. This series of tests was the result of interest expressed by some participants of the User's Panel at the first meeting in the effect of moisture on the slip characteristics of the conduit. These initial tests were performed using a single conduit specimen. The confining pressure was fixed at 6 MPa throughout this test series. The conduit was first tested with dry sand. Confining pressure was then released and the conduit pushed back to its initial position. A predetermined amount of water was then added to the sand and the procedure repeated. This sequence continued until the sand was fully saturated. The results show an initial increase followed by a marked increase in the pullout peak load with increasing quantity of water. However in reviewing the manner in which the tests were performed, it became apparent that the repeated cycling of a single conduit specimen had a greater influence on response than the degree of saturation of the sand. This is illustrated in Figure 5.17 where the peak load is plotted as a function of cycle number. Cycle eighteen shows a two-fold increase in load. Careful inspection of the conduit surface after completion of the series of tests showed evidence of the water mixing with the surface scale on the conduit, creating a distinctly different surface condition. The surface striations were very fine indicating a greater surface contact area between the sand grains and the steel.

This would explain the increase in pullout load due to the increasing contact area resulting from an increased number of sand grain/steel contact points. Earlier tests were examined where a conduit was tested repeatedly with dry sand.

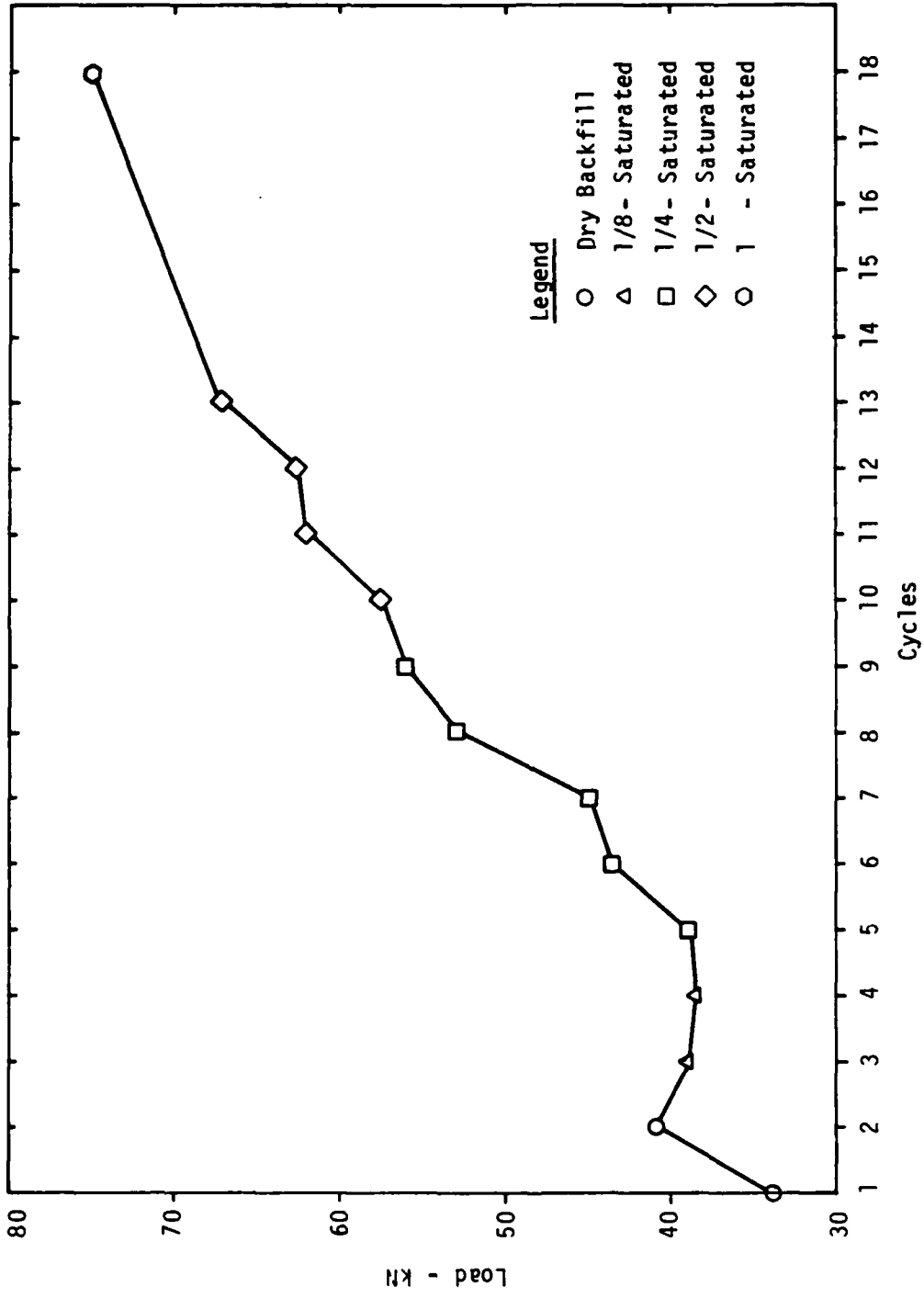


Figure 5.17. Conduit peak axial pullout load as a function of test cycle (wet backfill).

Although the number of cycles was limited the same trend can be seen in Figure 5.18. Pullout load was scaled to a 6 MPa confining pressure assuming the load is proportional to confining pressure. Note that fast loading clips the peak load resulting in the lower values shown in Figure 5.18. Additional testing would be required to determine to what extent this effect occurs at lower confining pressures.

Although the results of the saturated tests were generally masked by the recycling effect, the potential influence of moisture in the backfill can be seen in Figure 5.17 at cycles 3, 4, and 5. At these low cycles the increase in resistance due to surface preconditioning is not as great. As a result the effective functional resistance between the conduit and sand is reduced nearly 13% compared to the second cycle which was dry. Additional tests are indicated to determine the influence of the quantity of water in the backfill using a different conduit specimen for each quantity of water.

Two secondary variables studied dealt with operational characteristics of the test fixture itself. One set of tests changed the confining pressure medium from hydraulic oil (relatively incompressible) to air (compressible). The second set of tests changed the confining bladder from thin PVC to a thick rubber (see Figure 5.19). Both the changes were aimed at altering the stiffness of the confining pressure mechanism. It was postulated that this may have influenced the failure point of the sand, thereby influencing the load/displacement response. The hydraulic oil versus air is shown in Figure 5.20 at a confining pressure of 0.5 MPa. The PVC versus rubber comparison is presented in Figure 5.21 for confining pressures of 1.0 and 2.0 MPa.

The air pressure confinement made a difference in the initial portion of the curve in Figure 5.20. The hydraulic oil test (test 184) indicated effects of

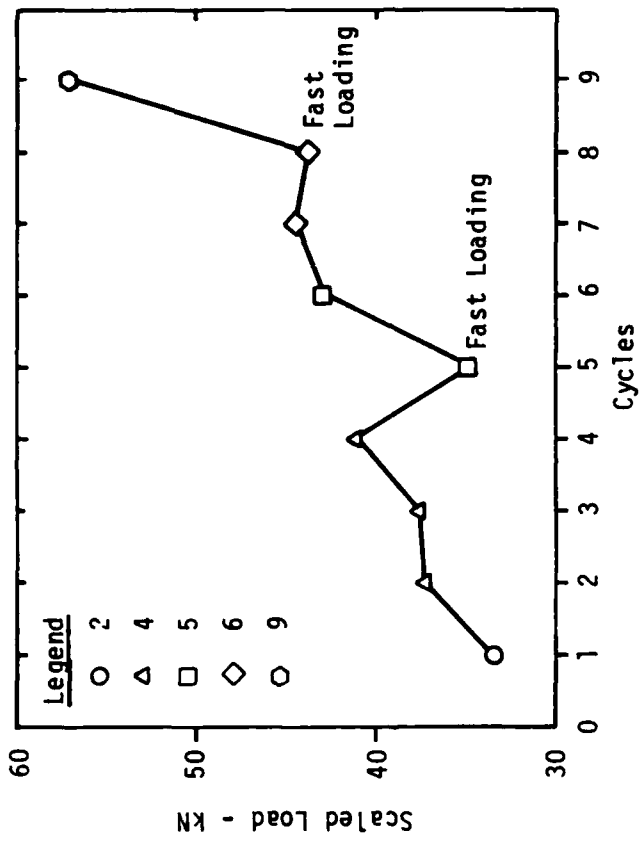


Figure 5.18. Scaled peak axial pullout load as a function of test cycle (dry backfill).



Figure 5.19. Rubber confining bladder.

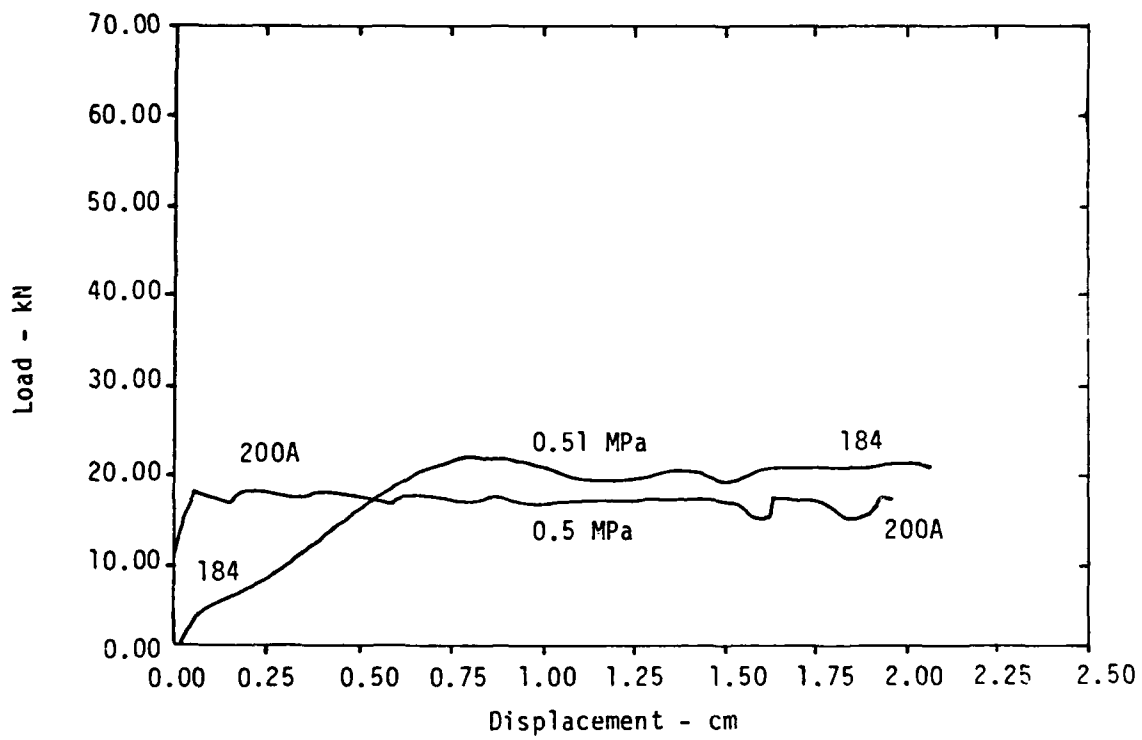


Figure 5.20. Confining pressure mechanism: hydraulic oil versus air pressure.

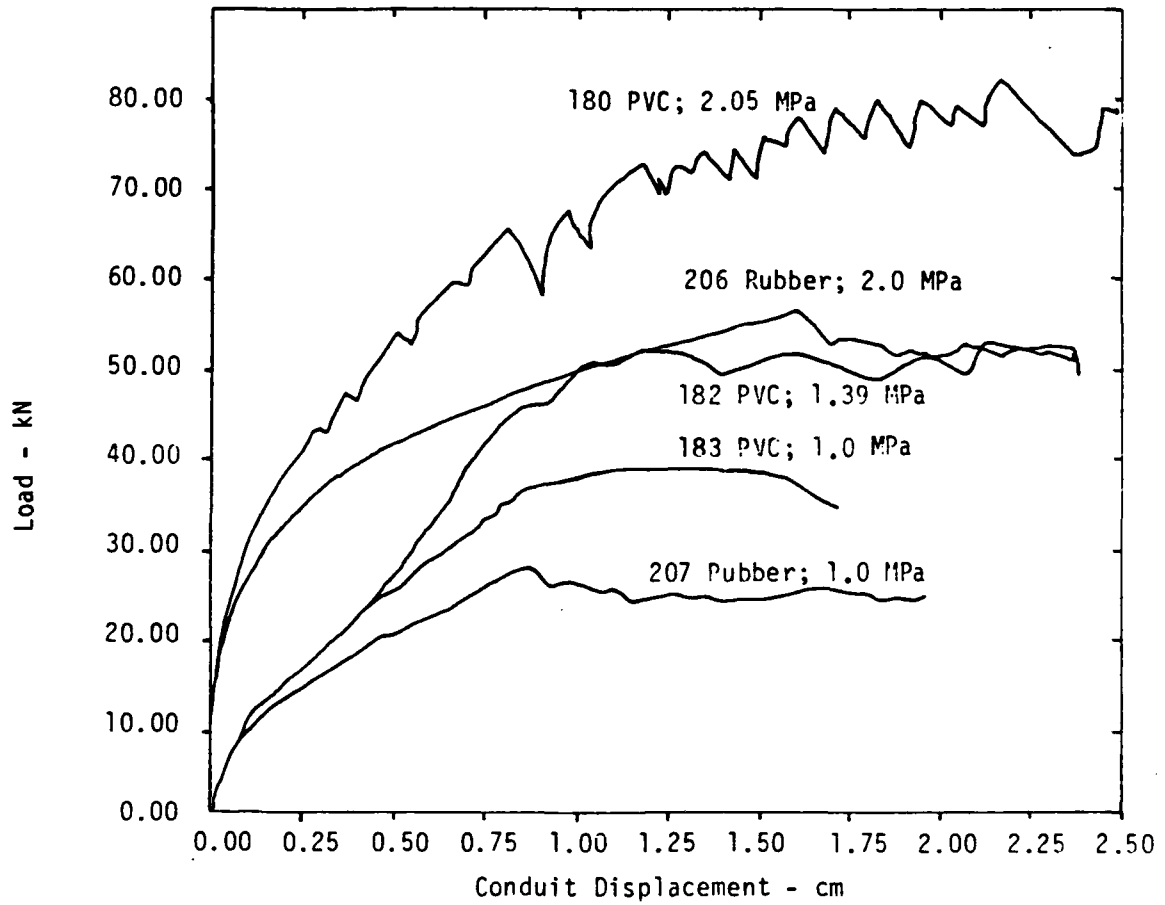


Figure 5.21. Load/slip response: PVC versus rubber bladder (2.0 MPa confining pressure).

preconditioning as discussed earlier. However, if one compares the peak load values, the difference is small.

The PVC versus rubber comparison shows a marked difference in response. The loads achieved with the rubber bladder are lower for both confining pressures. The presence of the thick-walled rubber tube (Figure 5.21) results in less confining pressure being transmitted to the sand backfill. In fact, the residual load for test 206 at a confining pressure of 2.0 (Figure 5.21) has an effective value which compares to a confining pressure of only 1.39 based on the PVC (test 182) results.

The intent of these latter test series was to eliminate the test fixture as a source of the load oscillations observed in test series V, VI, and VII. As no single cause could be found, it was finally assumed that the effect was not due to the test fixture or procedures. It is apparently characteristic of the load-resistance properties of the confined sand and conduit in the tests under some combinations of the test variables. It also does not seem to be limited to this type of test; subsequent discussions with Dr. S.L. Paul of the University of Illinois reveal that he has observed similar loading characteristics on quite different types of tests (Reference 16) involving model tunnel linings.

Both length and diameter were varied in the laboratory tests. The initial length variations were conducted primarily to determine whether or not end effects were affecting results in the high pressure tester. In fact, from these results and the User's Panel recommendations, the decision to construct the 150 cm long tester was made. The longer device increased confidence in the resulting data (especially for the larger steel conduit) and provided a further basis for using the full slip or residual pullout load to determine friction

coefficients. Results of the dry sand pullout tests are summarized in Figures 5.22, 5.23, 5.24, 5.25, and 5.26 for test series II, IV, VI, VII and IX, respectively.

Diameter also proved to be deserving of investigation as indicated by the difference in results obtained for the two sizes considered. The difference can be attributed to the difference in relative grain size of the sand to the conduit. It is felt that the larger conduit is close to the lower limit of diameters at which grain size would be significant for this type of sand. This combination of sand and diameter might prove directly scalable though to a larger pipe size in a gravel backfill. In any event, the two diameters tested should prove useful in extending limited data for other grain/pipe size combinations when such data become available.

Conduit surface condition exhibited a significant effect on the frictional pullout characteristics. Use of a polished 1 in. by 150 cm conduit specimen resulted in a 17% lower coefficient of sliding friction than an otherwise similar and reasonably smooth unpolished specimen. This may be particularly significant in that the conduits used were considerably smoother than many lifeline pipelines would be; in particular, the ductile iron pipe used in the shear tester had quite a rough surface finish. Actual conduits would also be subject to surface smoothness modification as a result of corrosion, erosion, and related environmental effects.

A graphical summary of all pullout tests is presented in Figure 5.27 in the form of coefficient of sliding friction as a function of conduit/sand contact length both for the 1/4 in. diameter and the 1 in. diameter conduit. To compute the conduit surface pressure, the oil-imposed confining pressure was multiplied by

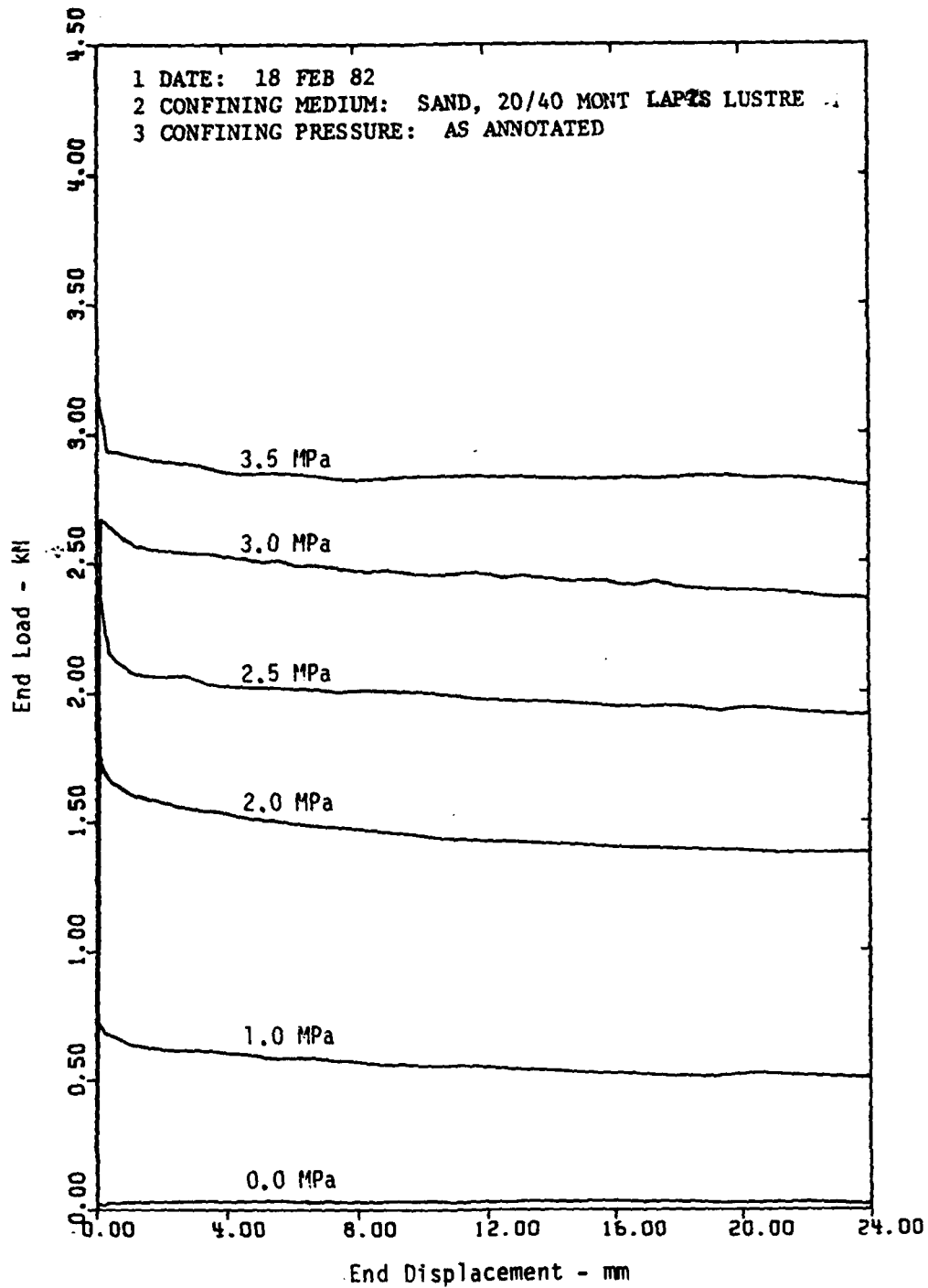


Figure 5.22. Test series II.

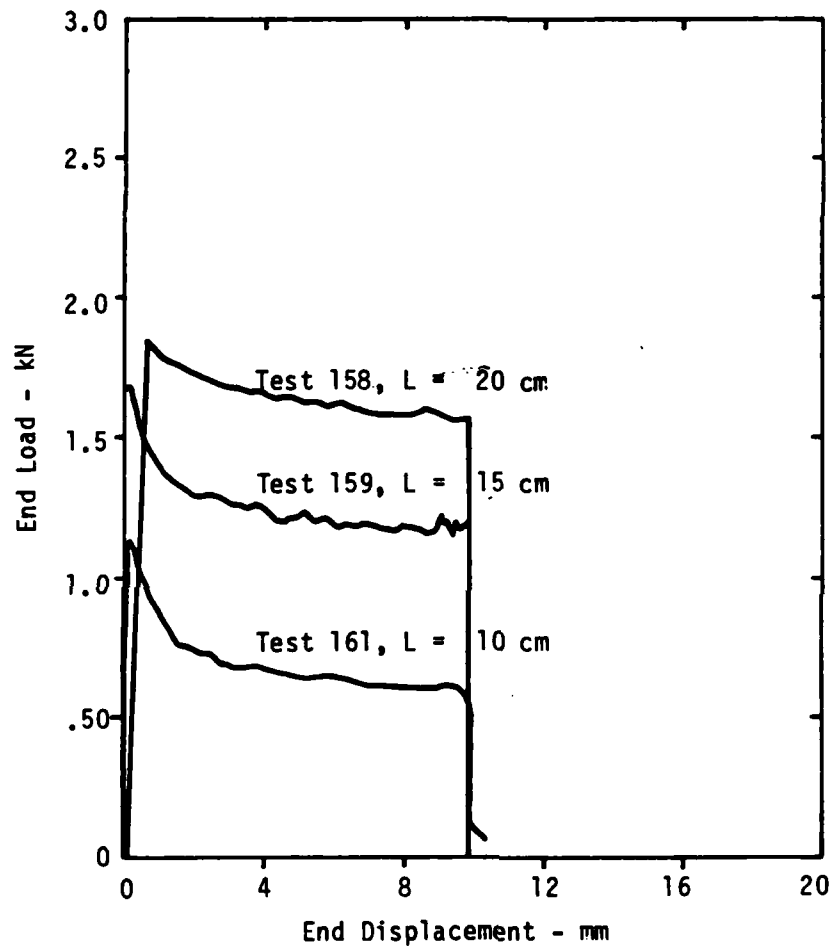


Figure 5.23. Test series IV.

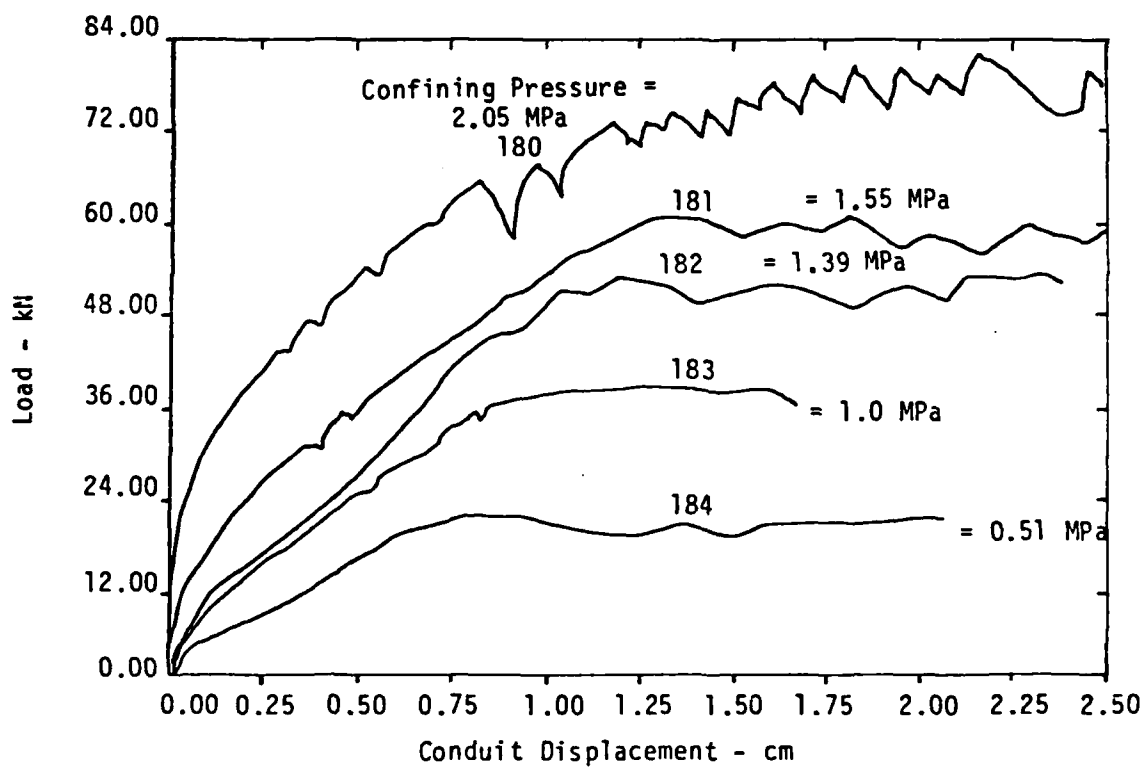


Figure 5.24. Test series VI.

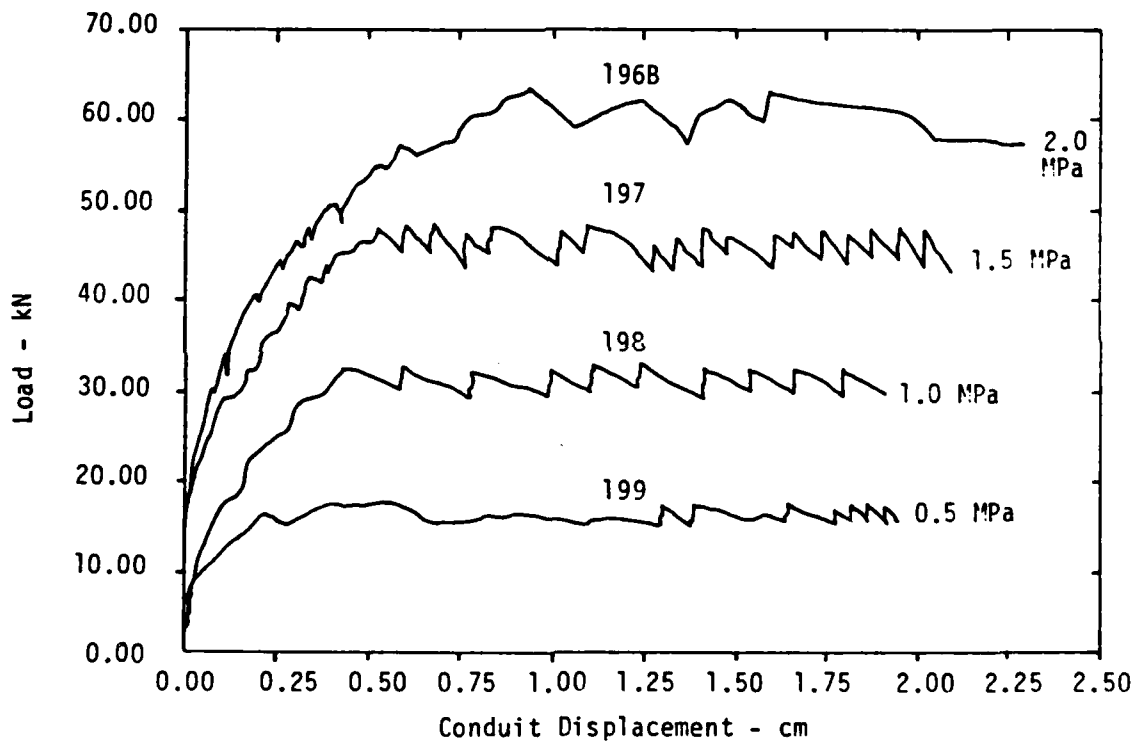


Figure 5.25. Test series VII.

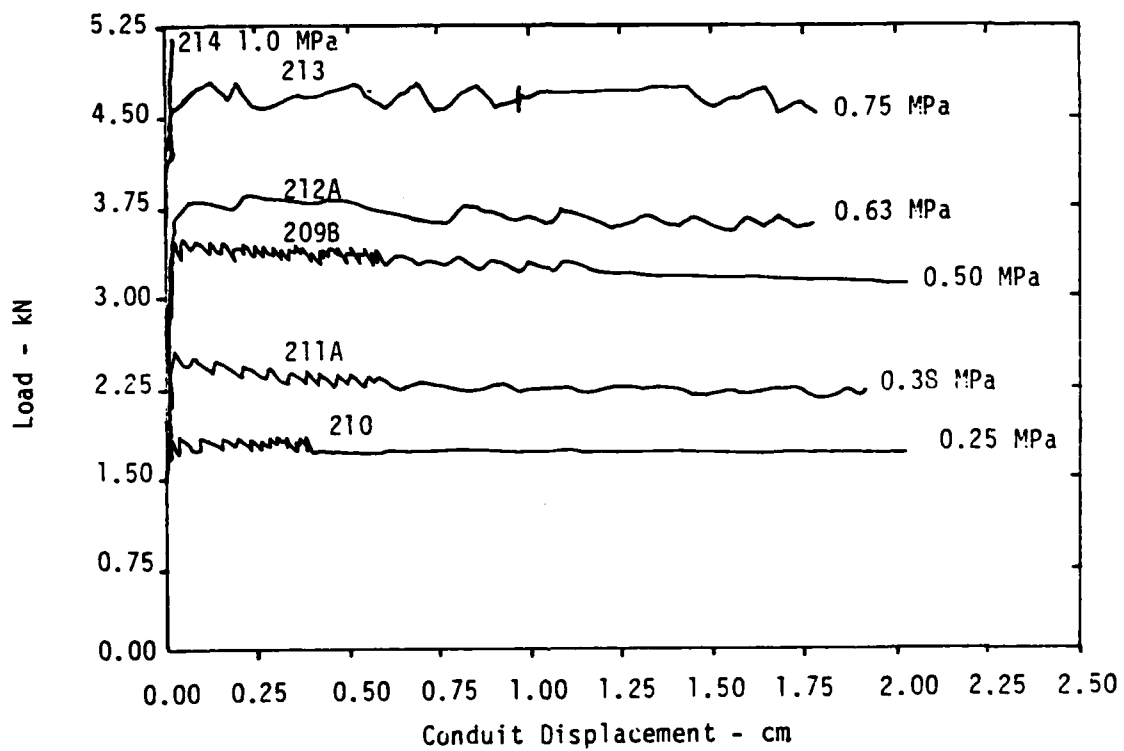


Figure 5.26. Test series IX.

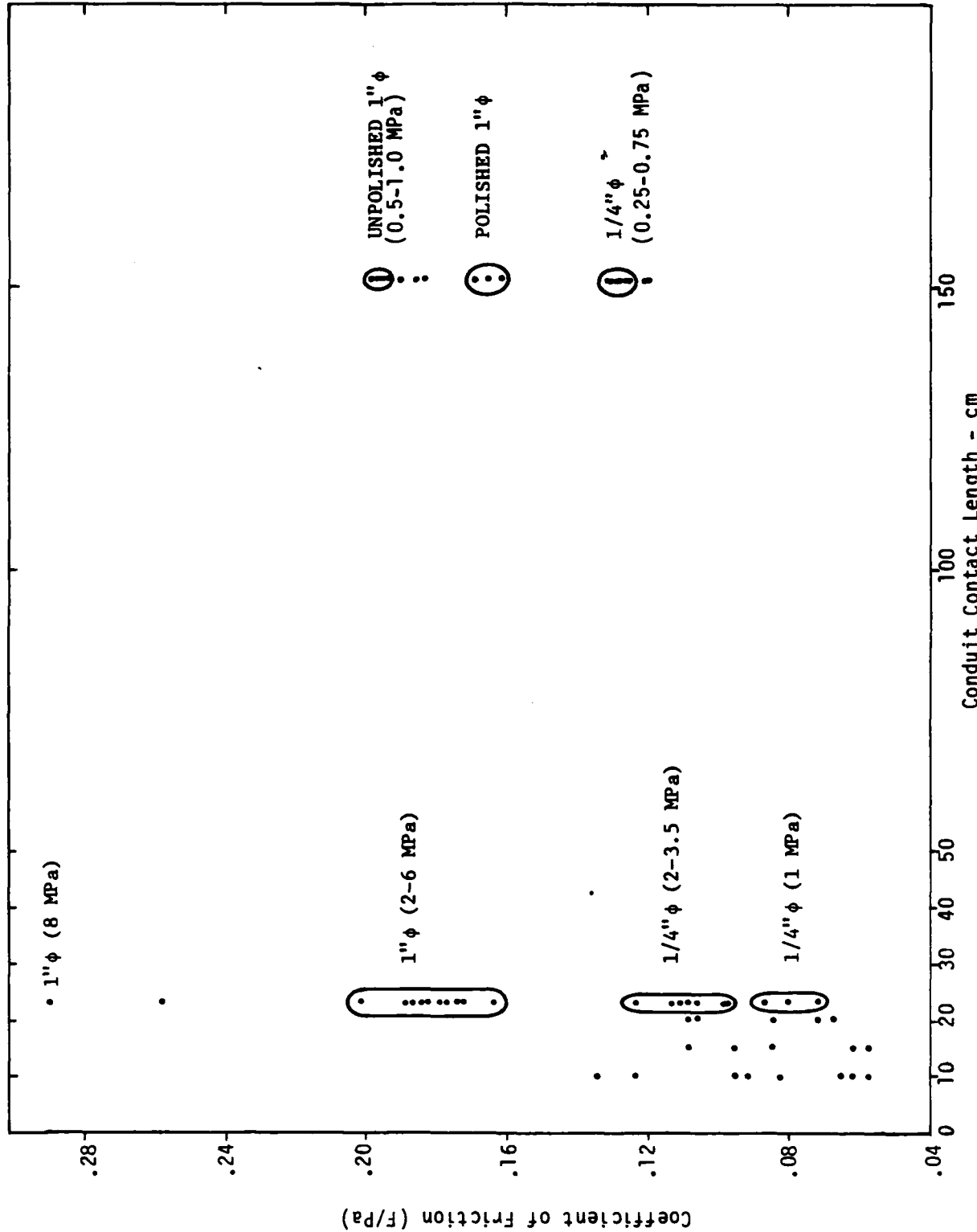


Figure 5.27. Coefficients of friction for all pullout tests.

1.5 as obtained from equation (5-6) earlier. The major point, illustrated by the ovals on the plot, is that both the short (23 cm) and the long (150 cm) test fixtures exhibit the same trends, showing a slight coefficient of friction dependence on confining pressure and relatively less influence of conduit length on slip friction characteristics. An exception is the shorter lengths ( $\leq 23$  cm), smaller diameter tests with confining pressures less than 2.0 MPa. These tests have slightly greater scatter and show a length effect when compared to the 150 cm smaller diameter results, assumed to be due to end effects of the test set up as noted earlier. Another form of graphical summary for the lower confining pressure tests are presented in Figure 5.28 in terms of normalized pullout load vs. confining pressure.

To summarize the frictional characteristics observed in the pullout tests, the coefficient of sliding friction for medium sand on 1 in. steel conduit is approximately 0.2. For a 1/4 in. conduit the value is 0.15. For a polished surface in the 1 in. size the value decreases approximately 20%. There are indications of decreasing friction with increasing sand moisture content though more tests are needed to confirm and better quantify this effect.

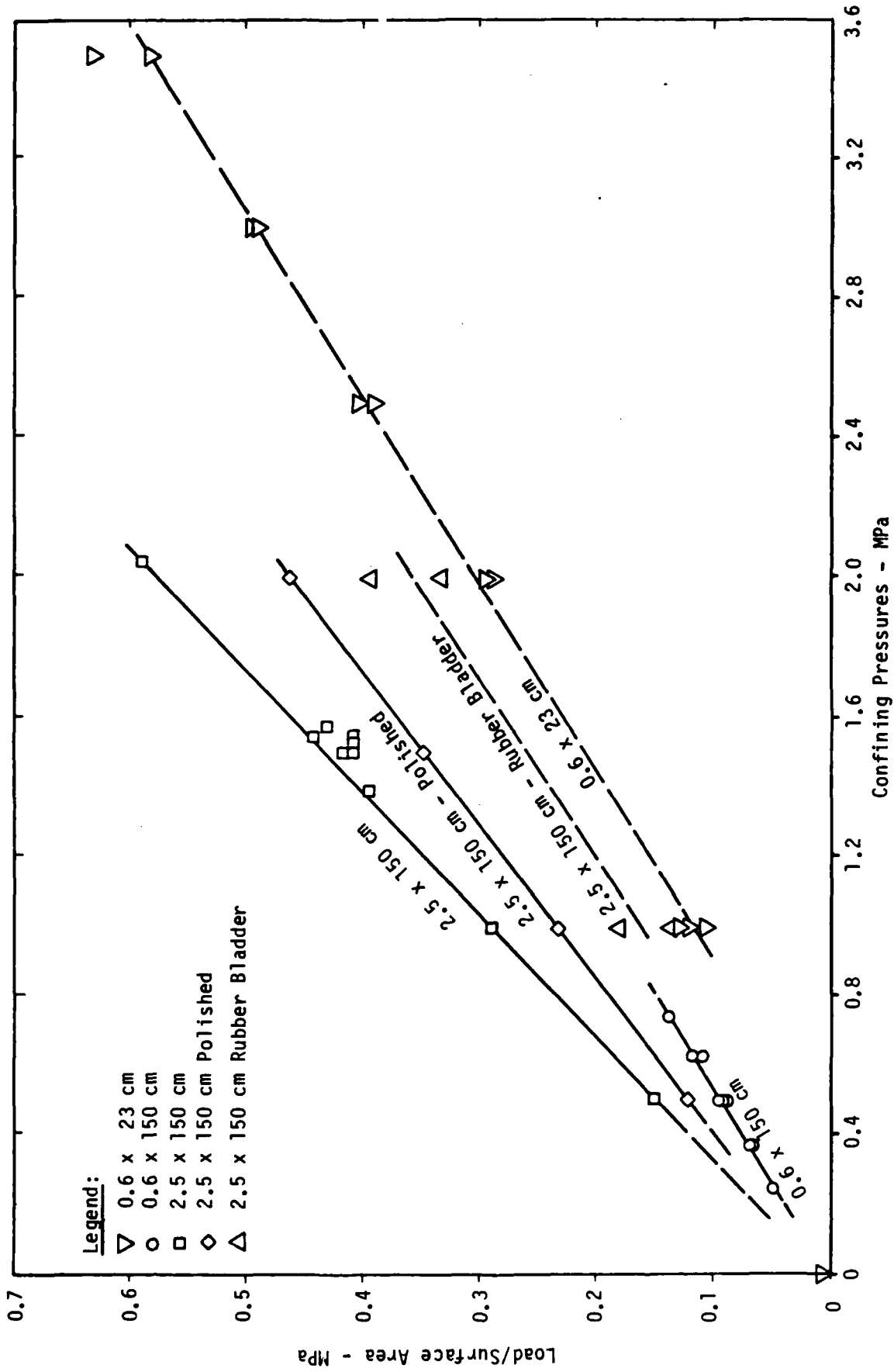


Figure 5.28. Normalized pullout load versus confining pressure.

## SECTION 6

### DISCUSSION OF SHEAR TEST RESULTS

The first conduit specimen tested in the single shear tester was a 5.5 m unjointed length of 4 in. ductile iron pipe as described in Section 3. Figure 6.1 illustrates the deformed shape of the specimen at six load steps as determined from the various displacement gages. The left and right portions of the figure are plotted at different scales to highlight both the overall shape and the region where the greatest curvature developed. The left end of the specimen underwent minimal displacement and is thus excluded from the figure.

The strain data indicate a maximum flexural strain of  $3341 \mu\text{m/m}$  and a maximum tensile strain of  $231 \mu\text{m/m}$ . Both strain peaks occurred 15 cm from the shear plane toward the moving end. They occurred just after the peak total load of 53.8 kN was reached. Since no strain gages were placed precisely at the shear plane it is possible that the peaks recorded were exceeded slightly at another location.

The suggested yield stress in flexure for design is 48,000 psi or 331 MPa, and the modulus of elasticity is 166,000 MPa (Reference 17). From these values, a minimum yield strain of  $1990 \mu\text{m/m}$  is obtained, which of course is much less than the peak measured strain. Since the last value is derived from a design value, it is assumed that the average expected yield strain is significantly higher. Therefore, the apparent indication of yielding in the test based on strains is probably greatly exaggerated. In fact, in spite of apparent severe deformation at peak load, when the tested specimen was removed and examined, no permanent deformation could be measured. If any yielding occurred during the test, it must have been quite superficial and had minimal permanent effect on the pipe.

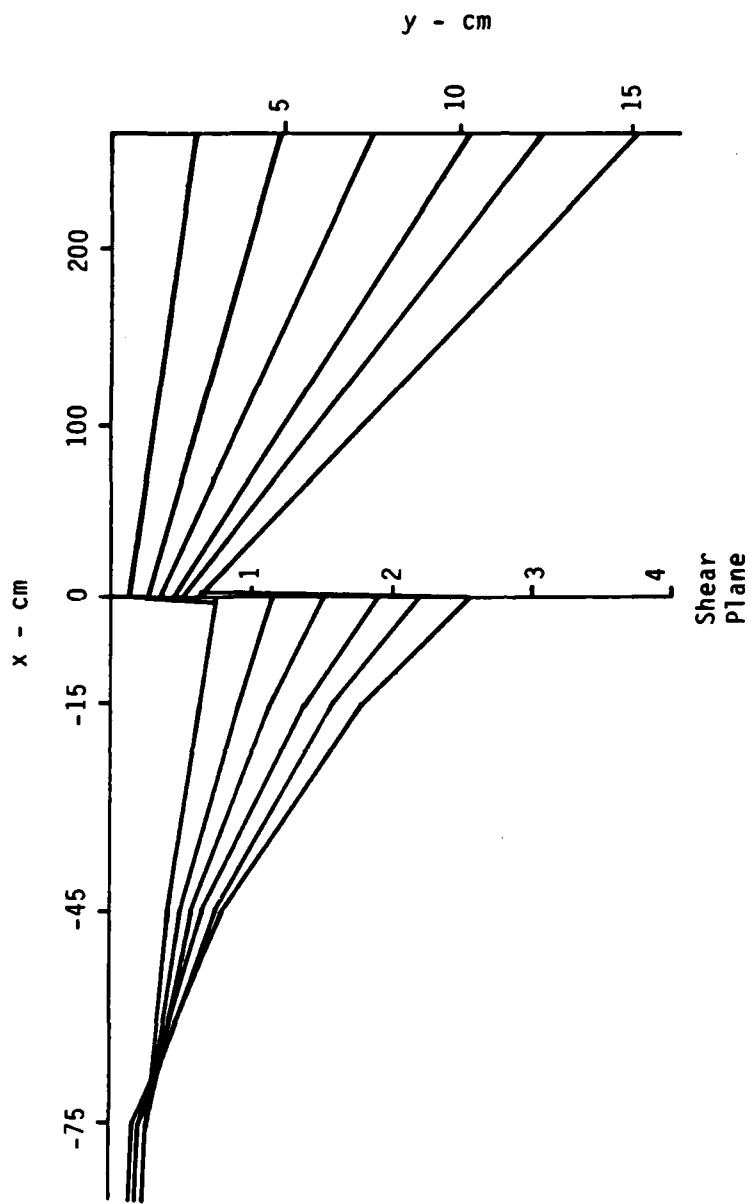


Figure 6.1. Ductile iron pipe shear test deformation.

Table 6.1 summarizes strain and displacement data between 15 and 75 cm from the shear plane (fixed soil bin side). These can provide a reasonableness check from the following relationships.

Neglecting the second order tangential strain

$$E\epsilon_f = \sigma_f = \frac{Mc}{I} \quad (6-1)$$

and

$$M = EIy'' \quad (6-2)$$

so that

$$E\epsilon_f = \frac{EIcy''}{I} \quad \text{or} \quad \epsilon_f = cy'' \quad (6-3)$$

in which  $E$  = modulus of elasticity,  $I$  = moment of inertia,  $c$  = distance from centroidal axis to extreme fiber = outside radius,  $M$  is moment,  $\sigma_f$  is maximum flexural stress,  $\epsilon_f$  is maximum flexural strain, and  $y''$  is the curvature as approximated normally for small strains as the second derivative of the displacement with respect to the axial dimension.

From a numerical differentiation of the deflections twice, an approximation to  $y''$  is obtained which can be converted to strain by multiplying by the radius of 6.1 cm. The table indicates that for most displacement values, the calculated strains are some 30% greater than measured. This is good agreement considering the approximations and error sources involved especially in numerical integration of the relatively coarse deflection data.

Converse to the approach used above, integration of strains could be used to estimate slopes and displacements. Such an approach was not applied here since

Table 6.1. Selected shear test displacements and strains.

Value	x (cm)	Main Displacement - cm					
		<u>2.45</u>	<u>4.86</u>	<u>7.43</u>	<u>10.28</u>	<u>12.39</u>	<u>15.04</u>
y-cm	15	0.650	0.925	1.150	1.400	1.575	1.800
100 y'	30	0.750	1.417	1.917	2.500	2.750	3.333
y-cm	45	0.425	0.500	0.575	0.650	0.750	0.800
10,000 y''-1/cm	45	0.833	1.946	2.780	3.333	3.057	4.166
$\epsilon$ - $\mu$ strain	45	508	1187	1696	2033	1865	2541
$\epsilon$ measured*	45	601	967	1297	1558	1721	1931
100 y'	60	0.500	0.833	1.083	1.500	1.833	2.083
y-cm	75	0.275	0.250	0.250	0.200	0.200	0.175

$$y' = \frac{y_1 - y_0}{\Delta x}$$

$$y'' = \frac{y'_1 - y'_0}{\Delta x}$$

$$\epsilon = ry''$$

$$r = \text{outside radius of pipe} = 6.1 \text{ cm}$$

\* Interpolated from measurements at x = 30 cm and x = 60 cm

only four strain points were available and appropriate boundary conditions were lacking.

Prior to the test it was expected that a symmetric deformation pattern would result. It was soon clear that the presence of compressible pressurization bladders was causing asymmetry in the deformations. While this may model some real conduit installations fairly accurately, pre-test anticipation of the asymmetry would probably have dictated a different instrumentation plan. Additional strain gages would be useful in future tests of this type, especially if the absence of plastic strains permits reuse of the specimen. Different placement, and possibly omission for some tests, of the pressurizing bladders should also be considered.

In an attempt to understand the test results better, several simple load distribution models for the pipe were examined. These models are shown in Figure 6.2. In these representations, the extreme left end is considered fixed (i.e. slope and displacement equal zero), the extreme right end is free (moment equals zero), with the fixed soil bin to the left and the movable bin to the right. Distributions (a) and (b) use linear load functions while (c), (d), and (e) are based on sine or cosine functions. In view of their simplicity it is not surprising that none of the models achieved a good fit of all measured data. The general shape of measured data was best matched by the function in (e).

Figure 6.3 illustrates the integration of the Figure 6.2e loading to obtain shear, moment, slope, and displacement. At a maximum shear of 10 kN, midpoint and maximum displacements of 2.5 cm and 16.7 cm agree very well with measured displacements shown in Figure 6.1. However, 10 kN is substantially less than the estimated peak load of 40 kN derived from Figure 6.4 (allowing approximately

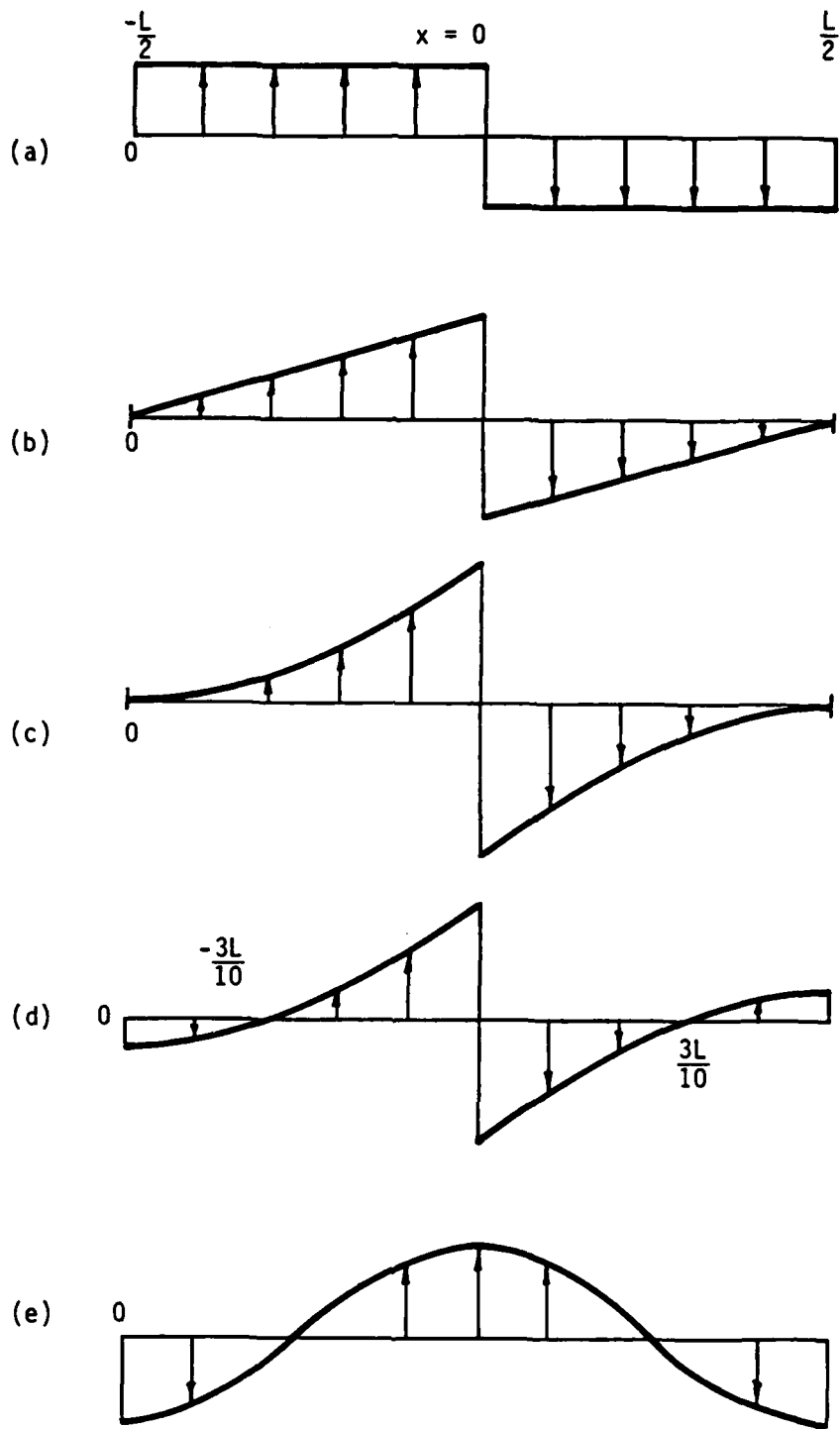


Figure 6.2. Load distribution models for DIP shear test.

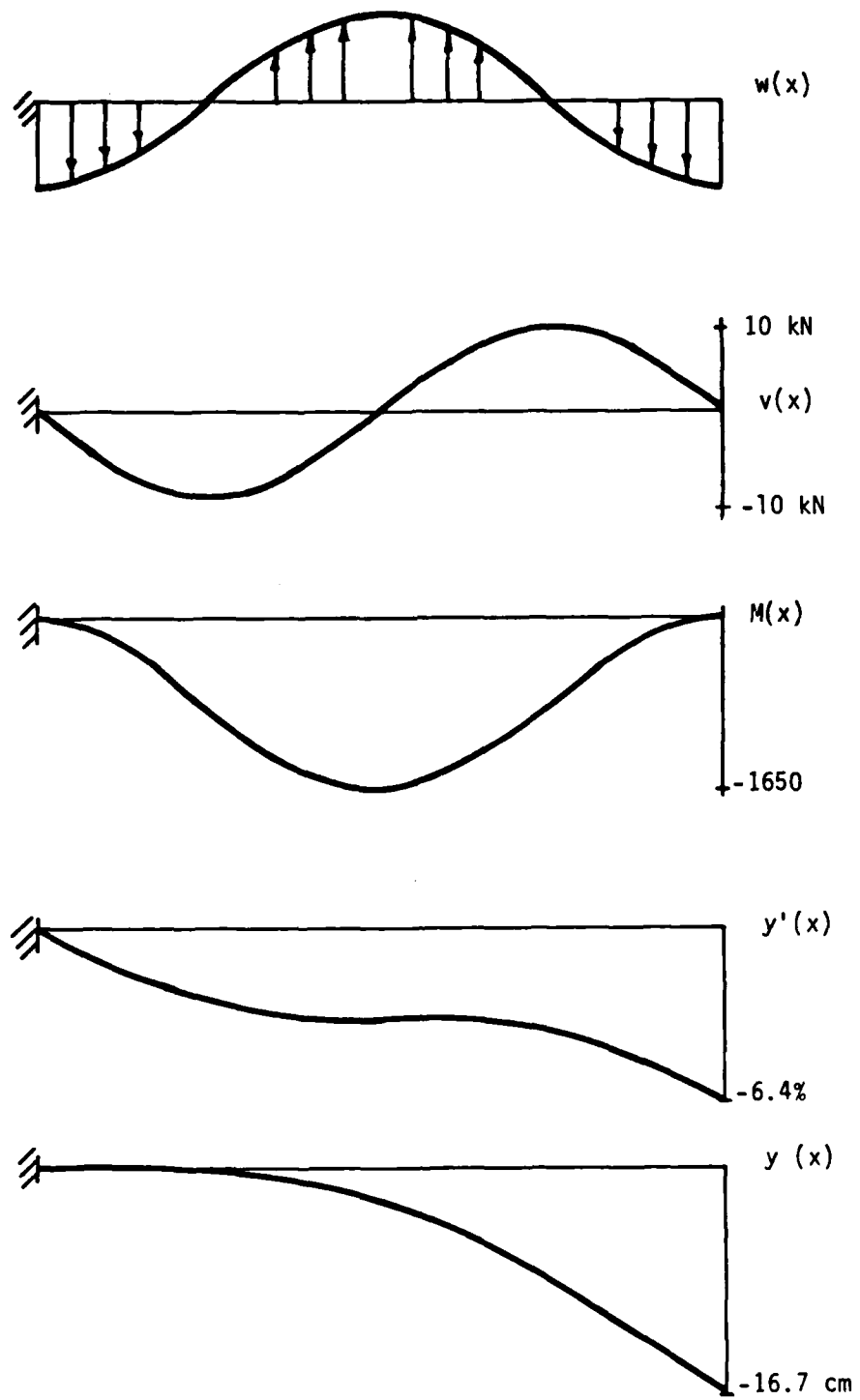


Figure 6.3. Beam functions for assumed load distribution.

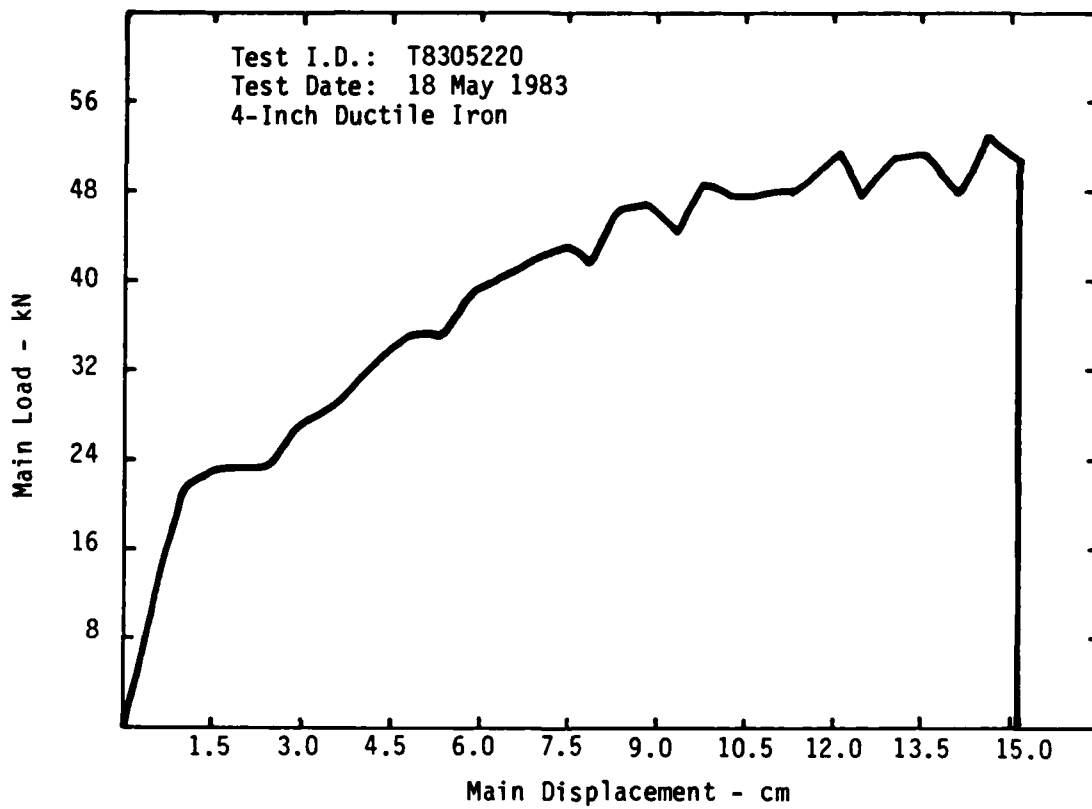


Figure 6.4. 4-inch ductile iron pipe shear test.

10 kN for fixture and sand). Using  $E = cy^n$  with  $c = 6.1$  cm this model produces a peak strain of 1519 which is about one-half the measured peak strain.

In spite of the obvious imperfection of this model in terms of function magnitudes, the shapes of the displacement, slope, and moment functions agree very well with the measured data. It thus seems safe to use the model to make some inferences regarding the shear and load functions as is done in Figure 6.3. The load function obtained indicates that the load is imposed mainly on the ends of the pipe and is reacted by the sand under the center portion. This further indicates that the presence of compressible bladders on the top prevented the sand from gripping and loading the pipe uniformly. As a further consequence of this, the resulting shear diagram reflects minimal shear at the shear plane where one might expect maximum shear. Several variations of the pressurizing bladder system have been considered for future tests in order to simulate the performance of pipelines at depth more accurately.

The first shear test of 4 in. vitrified clay pipe (VCP), number 223, was so dramatically different from the ductile iron pipe test that the test was repeated in number 224. In both of the VCP tests, the pipe fractured at a main shear displacement of less than 0.5 cm. In each test, a second fracture occurred which was generally symmetric about the shear plane compared to the first break. Both of these second breaks occurred at main displacements below 1.0 cm.

While a more brittle behavior, compared to ductile iron, was anticipated, it was believed that the presence of quite flexible joints in the VCP at 0.9 m each side of the shear plane would allow for more than 0.5 cm of displacement prior to failure. The joints were included in the VCP tests as that pipe comes only in 6 foot maximum lengths.

After the failures occurred, the pipe quickly filled with sand, which blocked the view through the pipe. Since the displacement measurements were dependent on seeing through the pipe and since no strain measurements were included in the tests, these tests were terminated following the second break.

## SECTION 7

### CONCLUSIONS AND RECOMMENDATIONS FOR ADDITIONAL RESEARCH

During this program, over 100 laboratory tests were conducted to investigate the performance of buried lifeline/instrumentation conduits. Also, two new, specialized test fixtures were constructed and operated. One of these fixtures was used to investigate the pullout characteristics of lifelines embedded in a pressurized sand backfill. The other fixture was used to study the performance of larger lifeline specimens in single shear while embedded in sand. The pullout tests produced considerable data about sand/conduit frictional characteristics and resulted in a much better understanding of the conduit slip mechanism.

The pullout tests were performed to investigate conduit/backfill axial slip characteristics as a function of backfill confining pressure, conduit diameter and conduit length. A limited number of tests were also performed to assess the effects of moisture content in the backfill as well as loading rate. The behavior was evaluated in terms of pullout force versus slip displacement measured at the far end of the conduit. These results indicated a linear relationship between pullout load and backfill confining pressure at confining pressures below 4 MPa. Computed coefficients of sliding friction ranged between 0.17 to 0.20 for the 1 in. conduit and 0.07 to 0.13 for the 1/4 in. conduit. At higher confining pressures, the friction coefficient increased more rapidly to a value of about 0.29 at 8 MPa (1 in. conduit). The presence of moisture in the backfill caused a decrease in the frictional resistance of nearly thirteen percent.

Repeated testing using the same test specimen resulted in a marked increase in the effective frictional resistance of the sand/conduit interface, regardless of

whether the backfill was wet or dry. In fact, a completely saturated backfill test produced nearly a two-fold increase in functional resistance after the specimen had been cycled 18 times. This phenomenon is attributed to conduit surface preconditioning caused by sand grain embedment in the steel surface. Cycling of the conduit resulted in an increase in the depth and number of striations of the steel surface, thereby increasing the coefficient of friction between the sand and conduit. Since the laboratory conduit specimens are relatively smooth as compared to field conditions, the higher values obtained after cycling may be more realistic. Hence, the smooth conduit results may be interpreted as a lower bound.

The shear tests conducted revealed dramatically different performance between relatively stiff and flexible conduits. The DIP, partly due to the sand confining method, demonstrated a capacity to redistribute a shear-intensive loading into a primarily flexural deformation due to its strength and flexibility compared to the surrounding sand. This test then showed the DIP performs extremely well in shear-flexure, at least in a backfill of fairly low stiffness.

The VCP, conversely, showed very little tolerance to shearing deformations even in the presence of close, apparently quite flexible joints, having sustained complete transverse fractures at small shear offsets. In spite of this susceptibility to shear-flexure failure, it cannot be concluded that VCP, especially in gravity flow sanitary sewer installations, is unsuitable for use in known seismic regions. It may be that such fractures could occur with little or no degradation of conduit servicability if the total offset at each fracture remained small.

Further tests of conduits in single shear would be very valuable now that basic characterization of conduits in this load configuration has been completed. Two

other areas deserving future test effort are additional study of backfill moisture content, and basic pullout tests on a 4 in. size DIP and VCP. But most importantly, similar tests of conduits in other soil types (e.g. clay) are mandatory if a comprehensive understanding of conduit behavior is to be achieved.

The program was originally planned using two materials; sand and clay. However, the estimated cost was relatively high due to the inclusion of two materials. Because of the budgetary constraints, it was decided to reduce the program to approximately half the estimated cost, but in the process, one material had to be eliminated to retain a logical program. For reasons of efficiency the decision was made to retain sand, for which frictional characteristics dominate, in the initial effort. Testing of clay was delayed.

The tests which have been completed in sand reinforce the original thesis that data are needed for the limiting types of behavior: (a) where friction and probably discrete grains control (sand) and, (b) where grain size and friction are probably less important (clay). Having data for these limits will provide fundamental information from which behavior of conduits surrounded by any natural soil can be deduced. Perhaps the most significant finding to date from the tests completed is that initial slippage of a conduit being forced longitudinally through sand occurs in the sand, not at the sand-conduit boundary. This phenomenon will probably not occur in clay, but the fundamental behavior in clay is totally unknown. Future work should address this last problem generally; it should also address the integration of data from the tests in sand and the new tests in clay.

Also significant is the experience, momentum and investment existing from the current program. Now that design and check-out of all specialized devices and

techniques are complete, a natural momentum has developed which increases the efficiency of performing and interpreting experiments. Through the existing program there is not only the vesting of this experience but also a substantial investment in specialized test fixtures. It would be opportune to further capitalize on these resources.

Finally, the potential for analytical studies drawing upon these results is great and should be exploited as well.

## SECTION 8

### LIST OF REFERENCES

1. Ariman, T., editor, "Earthquake Behavior and Safety of Oil and Gas Storage Facilities, Buried Pipelines and Equipment," (Presented at the 1983 International Symposium on Lifeline Earthquake Engineering, the 4th National Congress on Pressure Vessel and Piping Technology, Portland, Oregon, 19-24 June, 1983), American Society of Mechanical Engineers Publication PVP - Vol. 77.
2. Morrill, K.B., Davis, H.C., and Hartenbaum, B.A., "Tests of Subterranean Instrumentation and Communication Cable Conduits Subjected to Large Amplitude Shear Offsets," DNA 5641F, Merritt CASES, Inc. and H-Tech Laboratories, Inc., 1 January 1981.
3. Isenberg, J. and Wright, J.P., "Survey of Existing Underground Water Pipelines with Emphasis on Their Seismic Resistance," Interim Grant Report IR-1, NSF Grant No. ENV P76-9838, Weidlinger Associates, 1 July 1977.
4. Salvadori, M.G. and Singhal, A., "Strength Characteristics of Jointed Water Pipelines," Interim Grant Report No. IR-3, NSF Grant No. ENV P76-9838, Weidlinger Associates, July 1977.
5. Weidlinger, P., "Behaviour of Underground Lifelines in Seismic Environment," Interim Grant Report No. IR-4, NSF Grant No. ENV P76-9838, Weidlinger Associates, July 1977.
6. Kratky, R.G. and Salvadori, M.G., "Strength and Dynamic Characteristics of Mechanically Jointed Cast-Iron Water Pipelines," Grant Report No. 3a, NSF Grant No. ENV P76-9838, PFR 78-15049, Weidlinger Associates, June 1978.
7. Weidlinger, P. and Nelson, I., "Seismic Analysis of Pipelines with Interference Response Spectra," Grant Report No. 7, NSF Grant No. ENV P76-9838, PFR 78-15049, Weidlinger Associates, June 1978.
8. Parnes, R., "Static Analysis of an Embedded Pipe Subjected to Periodically Spaced Longitudinal Forces," Grant Report No. 12, NSF Grant No. PFR 78-15049, Weidlinger Associates, August 1979.
9. Nelson, I. and Baron, M.L., "Earthquakes and Underground Pipelines - An Overview," Grant Report No. 17, NSF Grant No. PFR 78-15049, Weidlinger Associates, June 1981.
10. Kennedy, R.P., Darrow, A.C., and Short, S.A., "Seismic Design of Oil Pipeline Systems," Journal of the Technical Councils of ASCE, Vol. 105, No. TC1, April 1979, pp. 119-134.
11. Kubo, K., Katayama, T., and Ohashi, M., "Lifeline Earthquake Engineering in Japan," Journal of the Technical Councils of ASCE, Vol. 105, No. TC1, April 1979, pp. 221-238.
12. Lund, L., "Earthquake Effects on Water Meters and Services," A Technical Note in Journal of the Technical Councils of ASCE, Vol. 105, No. TC1, April 1979, pp. 253-257.

13. Wang, L.R.L., Pikul, R.R., and O'Rourke, M.J., "Imposed Ground Strain and Buried Pipelines," A Technical Note in Journal of the Technical Councils of ASCE, Vol. 108, No. TC2, November 1982, pp. 259-263.
14. Sweet, J., "SATURN - A Multi-Dimensional Two-Phase Computer Program which Treats the Nonlinear Behavior of Continua Using the Finite Element Approach," Report No. JSA-79-016, Joel Sweet and Associates, September 1979.
15. Seed, H.B. and Idriss, I.M., "Soil Moduli and Damping Factors for Dynamic Response Analyses," Report No. EERC-70-10, University of California at Berkeley, 1970.
16. A personal communication with S.L. Paul, University of Illinois at Urbana-Champaign, Department of Civil Engineering, 12 September 1983.
17. Handbook. Ductile Iron Pipe. Cast Iron Pipe, Fifth Edition, Cast Iron Pipe Research Association, Oak Brook, Illinois, 1978.

APPENDIX A -

BIBLIOGRAPHY

Ali-Akbarian, M., "Oblique Incidence of Plane Stress Waves on a Circular Tunnel," Ph.D Thesis, University of Illinois at Urbana, 1967.

Ariman, T., editor, "Earthquake Behavior and Safety of Oil and Gas Storage Facilities, Buried Pipelines and Equipment," (Presented at the 1983 International Symposium on Lifeline Earthquake Engineering, the 4th National Congress on Pressure Vessel and Piping Technology, Portland, Oregon, 19-24 June, 1983), American Society of Mechanical Engineers Publication PVP - Vol. 77.

Baboiian, R., et al., "Galvanic and Pitting Corrosion -- Field and Laboratory Studies," (Presented at Materials Engineering Congress, Detroit, Michigan, 22-23 October 1974), American Society for Testing and Materials Special Technical Publication 576.

Baron, M.L. and Matthews, A.T., "Diffraction of a Pressure Wave by a Cylindrical Cavity in an Elastic Medium," Transactions of the ASME, Journal of Applied Mechanics, Vol. 28, September 1961.

Baron, M.L. and Matthews, A.T., "Diffraction of a Shear Wave by a Cylindrical Cavity in an Elastic Medium," Transactions of the ASME, Journal of Applied Mechanics, Vol. 29, March 1962.

Blume, J.A. and Stauduhar, M.H., editors, "Thessaloniki, Greece Earthquake, June 20, 1978," Reconnaissance Report, Earthquake Engineering Research Institute, January 1979.

Britz, K.I., Edelstein, P.H. and Oppenheim, I.J., "Measurement of Earthquake Performance of Transportation Systems," The Current State of Knowledge of Lifeline Earthquake Engineering, Proceedings of Technical Council on Lifeline Earthquake Engineering, Specialty Conference, University of California, Los Angeles, 30-31 August, 1977, pp. 252-265.

Campbell, K.W., Eguchi, R.T. and Duke, C.M., "Reliability in Lifeline Earthquake Engineering," Journal of the Technical Councils of ASCE, Vol. 105, No. TC2, December 1979, pp. 259-270.

"Cast-in-Place Unreinforced Concrete Pipe," Salt River Project, Phoenix, Arizona, March 1960.

Cevallos-Candau, P.J. and Hall, W.J., "The Commonality of Earthquake and Wind Analysis," Civil Engineering Studies, Structural Research Series No. 472, (UILU-ENG-80-2002), University of Illinois at Urbana, January 1980.

"Chloride Corrosion of Steel in Concrete," (Symposium presented at the 79th Annual Meeting of ASTM, Chicago, Illinois, 27 June - 2 July 1976), American Society for Testing and Materials Special Technical Publication 629.

Cocks, F.H., Manual of Industrial Corrosion Standards & Controls, American Society for Testing and Materials, Philadelphia, Pennsylvania, 1963.

"Concrete Pipe and the Soil-Structure System," (Symposium presented at the 79th Annual Meeting of ASTM, Chicago, Illinois, 27 June - 2 July 1976), American Society for Testing and Materials Special Technical Publication 630.

"Damage Assessment Plan for Volunteer Engineers," Office of Emergency Services, Sacramento, California, May 1978.

Davis, R.E., Bacher, A.E., and Obermuller, J.C., "Concrete Pipe Culvert Behavior -- Part 1" and "Part 2," ASCE Journal of Structural Engineering, Vol. 100, No. ST3, March 1974, pp. 599-630.

"Disaster Preparedness Report to the Congress," Vols. 1, 2 and 3, Office of Emergency Preparedness, Washington, D.C., January 1972.

"Earthquake Damage Evaluation and Design Consideration for Underground Structures," a Public Service Paper, Los Angeles Section, ASCE, Los Angeles, California, February 1974.

"Earthquake Hazards Reduction: Issue for an Implementation Plan," Working Group on Earthquake Hazards Reduction, Office of Science and Technology Policy, Executive Office of the President, 1978.

"Earthquake Resistant Design Requirements for VA Hospital Facilities," Office of Construction, Veterans Administration, Handbook H-08-0, Washington, D.C., June 1973 (revisions March 1974 and May 1977).

"Earthquake Resistant Design Requirements for VA Hospital Facilities, Office of Construction, Veterans Administration, Report of the Earthquake and Wind Forces Committee, Washington, D.C., March 1975.

"Earthquake Resistant Regulations, A World List 1973" and the "1976 Supplement," International Association for Earthquake Engineering, Tokyo.

"Engineering Features of the San Fernando Earthquake of February 9, 1971," EERL 71-02, California Institute of Technology, Pasadena, June 1971.

Erel, B., et al., "Measuring the Earthquake Performance of Urban Water Systems," The Current State of Knowledge of Lifeline Earthquake Engineering, Proceedings of Technical Council on Lifeline Earthquake Engineering, Specialty Conference, University of California, Los Angeles, 30-31 August 1977, pp. 183-198.

Freund, L.B., Li, V.C.F., and Parks, D.M., "An Analysis of a Wire Wrapped Mechanical Crack Arrestor for Pressurized Pipelines," Transactions of the ASME, Journal of Pressure Technology, Vol. 101, February 1979, pp. 51-58.

Galbraith, F.W., "Damage Survey, 9 February 1971, San Fernando Valley Earthquake," California State College, Long Beach, March 1971.

Gray, B.H., Williamson, G.R., and Batson, G.B., "Fibrous Concrete Construction Materials for the Seventies," Conference Proceedings M-28, Construction Engineering Research Laboratory, Champaign, Illinois, December 1972.

"The Great Alaska Earthquake of 1964," Summary and Recommendations, Committee on the Alaska Earthquake of the Division of Earth Sciences, National Research Council, Washington, D.C., 1973.

"Guide for the Protection of Concrete Against Chemical Attack by Means of Coatings and Other Corrosion Resistant Materials," Journal of the American Concrete Institute Proceedings, Vol. 63, No. 12, December 1966.

Hall, W.J. and Newmark, N.M., "Seismic Design Criteria for Pipelines and Facilities," Journal of the Technical Councils of ASCE, Vol. 104, No. TC1, November 1978, pp. 91-107.

Hamilton, R.M., "Earthquake Hazards Reduction Program -- Fiscal Year 1978 Studies Supported by the U.S. Geological Survey," Geological Survey Circular 780, 1978.

Handbook. Ductile Iron Pipe. Cast Iron Pipe, Fifth Edition, Cast Iron Pipe Research Association, Oak Brook, Illinois, 1978.

Hartenbaum, B.A., "The Design of Subterranean Instrumentation Cables to Survive Large Amplitude Ground Motions," DNA 4636F, H-Tech Laboratories, Inc., July 1978.

Hoff, G.C., "Research and Development of Fiber-Reinforced Concrete in North America," WES MP-C-74-3, U.S. Army Waterways Experiment Station, February 1974.

Hollis, E.P., "Earthquake Damage - Dams and Related Structures, Including Water Supply and Irrigation Systems," Bibliography of Earthquake Engineers, Sec. 7.7, Oakland, California, 1971.

Housner, G.W., "Dynamic Pressures on Accelerated Fluid Containers," Bulletin of the Seismological Society of America, January 1957, pp. 15-35.

Hung, S.J., Merritt, J.L. and Seifert, K.D., "Feasibility of Using HE in Model Tests of Structures," DNA 4219F, Merritt CASES, Inc., 1 April 1977.

Ingold, T.S., "A Laboratory Investigation of Grid Reinforcements in Clay," ASTM Geotechnical Testing Journal, Volume 6, Number 3, September 1983, pp. 112-119.

Ingold, T.S., "Laboratory Pull-Out Testing of Grid Reinforcements in Sand," ASTM Geotechnical Testing Journal, Volume 6, Number 3, September 1983, pp. 101-111.

Isenberg, J., "The Role of Corrosion in the Seismic Performance of Buried Steel Pipelines in Three United States Earthquakes," Grant Report No. 6, NSF Grant No. ENV P76-9838, PFR 78-15049, Weidlinger Associates, June 1978.

Isenberg, J., "Seismic Performance of Underground Water Pipelines in the Southeast San Fernando Valley in the 1971 San Fernando Earthquake," Grant Report No. 8, NSF Grant No. PFR 78-15049, Weidlinger Associates, September 1978.

Isenberg, J. and Wright, J.P., "Survey of Existing Underground Water Pipelines with Emphasis on Their Seismic Resistance," Interim Grant Report IR-1, NSF Grant No. ENV P76-9838, Weidlinger Associates, 1 July 1977.

Johnson, A.M. and Hess, J.D., "Load Testing of No-Joint Cast-In-Place Concrete Pipe," a Cooperative Project of the City of Phoenix, and Salt River Project, Phoenix, Arizona, January 1963.

Katona, M.G. and Smith J.M., "A Modern Approach for Structural Design of Pipe Culverts," Civil Engineering Laboratory, Port Heuneme, California, 1976.

Kennedy, R.P., Chow, A.W., and Williamson, R.A., "Fault Movement Effects on Buried Oil Pipelines," ASCE Journal of Transportation Engineering, Vol. 103, No. TE5, September 1977, pp. 617-633.

Kennedy, R.P., Darrow, A.C., and Short, S.A., "Seismic Design of Oil Pipeline Systems," Journal of the Technical Councils of ASCE, Vol. 105, No. TC1, April 1979, pp. 119-134.

Kienow, K.E. and Kienow, K.K., "Performing Cost-Effective Analysis for Alternative Interceptor Sewer Designs," Water and Sewage Works, October 1978.

Kienow, K.E. and Kienow, K.K., "Predicting Sulfide in Force Mains," Water and Sewage Works, December 1978.

Kienow, K.K., "Concrete Interceptor Sewer Corrosion Protection - A State-of-the-Art Report," presented at the Third International Conference on the Internal and External Protection of Pipes, Imperial College, London, England, 5 - 7 September 1979.

Kienow, K.K. and Kienow, K.E., "Computer Predicts Pipe Corrosion," Water and Sewage Works, September 1978.

Kienow, K.K. and Pomeroy, R.D., "Corrosion Resistant Design of Sanitary Sewer Pipe," presented at the ASCE Convention and Exposition, Chicago, Illinois, October 1978.

Kingston, W.L., "Soil Cement Slurry Backfill," (Presented at the 1973 fall convention of the American Water Works Association, Oakland, California, 27 September 1973), Department of Water and Power.

Kratky, R.G. and Salvadori, M.G., "Strength and Dynamic Characteristics of Gasket-Jointed Concrete Water Pipelines," Grant Report No. 5, NSF Grant No. ENV P76-9838, PFR 78-15049, Weidlinger Associates, June 1978.

Kratky, R.G. and Salvadori, M.G., "Strength and Dynamic Characteristics of Mechanically Jointed Cast-Iron Water Pipelines," Grant Report No. 3a, NSF Grant No. ENV P76-9838, PFR 78-15049, Weidlinger Associates, June 1978.

Kratky, R.G., et al., "Suggested Experiments on Straight Pipes in Air and in Soil," Grant Report No. 9, NSF Grant No. PFR 78-15049, Weidlinger Associates, January 1979.

Kubo, K., Katayama, T., and Ohashi, M., "Lifeline Earthquake Engineering in Japan," Journal of the Technical Councils of ASCE, Vol. 105, No. TC1, April 1979, pp. 221-238.

"Learning from Earthquakes," 1977 Planning and Field Guides, Earthquake Engineering Research Institute.

"Learning from Earthquakes," Project Report 1973-1979, Earthquake Engineering Research Institute.

Leeds, D.J., editor, "Earthquake in Romania, March 4, 1977," Preliminary Report, Newsletter, Vol. 11, No. 3B, Earthquake Engineering Research Institute, May 1977.

Leeds, D.J., editor, "The Guatemala Earthquake of February 4, 1976," Preliminary Report, Newsletter, Vol. 10, No. 2B, Earthquake Engineering Research Institute, March 1976.

Leeds, D.J., editor, "The Island of Hawaii Earthquake of November 29, 1975," Newsletter, Vol. 10, No. 1B, Earthquake Engineering Research Institute, February 1976.

Lew, H.S., Leyendecker, E.V., and Dikkins, R.D., "Engineering Aspects of the 1971 San Fernando Earthquake," National Bureau of Standards BSS 40, December 1971.

Lund, L., "California Water & Power Earthquake Engineering Forum," The Current State of Knowledge of Lifeline Earthquake Engineering, Proceedings of Technical Council on Lifeline Earthquake Engineering, Specialty Conference, University of California, Los Angeles, 30-31 August 1977, pp. 459-461.

Lund, L., "Earthquake Effects on Water Meters and Services," A Technical Note in Journal of the Technical Councils of ASCE, Vol. 105, No. TC1, April 1979, pp. 253-257.

Lund, L., "Impact of Earthquakes on Service Connections and Water Meters," The Current State of Knowledge of Lifeline Earthquake Engineering, Proceedings of Technical Council on Lifeline Earthquake Engineering, Specialty Conference, University of California, Los Angeles, 30-31 August 1977, pp. 161-167.

Marsh, H.N., Jr. and Clarke, L.L., Jr., "Glass Fibers in Concrete," Proceedings of the ACI International Symposium on Fiber Reinforced Concrete, Ottawa, Ontario, Canada, 11 October 1973, American Concrete Institute Publication SP-44.

Meehan, J.F., et al., "Managua, Nicaragua Earthquake of December 23, 1972," Reconnaissance Report, Earthquake Engineering Research Institute, May 1973.

Merritt, J.L., et al., "Preliminary Studies of Buried Concrete Circular Pipe," Briefing to Los Angeles County Flood Control personnel, Los Angeles, California, November 13, 1975.

Moran, D., et al., "Engineering Aspects of the Lima, Peru Earthquake of October 3, 1974," Reconnaissance Report, Earthquake Engineering Research Institute, May 1975.

Morrill, K.B., "A Biaxial Inelastic Moment-Curvature Relation for a Reinforced Concrete Section," M.S. thesis, University of California, Los Angeles, 1975.

Morrill, K.B., Davis, H.C., and Hartenbaum, B.A., "Tests of Subterranean Instrumentation and Communication Cable Conduits Subjected to Large Amplitude Shear Offsets," DNA 5641F, Merritt CASES, Inc. and H-Tech Laboratories, Inc., 1 January 1981.

Nelson, I., "Axial Vibrations of A Fluid Filled Pipe," Technical Note No. 1, NSF Grant No. PFR 78-15049, Weidlinger Associates, November 1978.

Nelson, I. and Baron, M.L., "Earthquakes and Underground Pipelines - An Overview," Grant Report No. 17, NSF Grant No. PFR 78-15049, Weidlinger Associates, June 1981.

Nelson, I. and Weidlinger, P., "Development of Interference Response Spectra for Lifelines Seismic Analysis," Interim Grant Report No. IR-2, NSF Grant No. ENV P76-9838, Weidlinger Associates, 1 July 1977.

Nelson, I., and Weidlinger, P., "Dynamic Seismic Analysis of Long Segmented Lifelines," Grant Report No. 10, NSF Grant No. PFR 78-15049, Weidlinger Associates, November 1978.

Newmark, N.M., et al., "Earthquake Prediction and Hazard Mitigation Options for USGS and NSF Programs," NSF-USGS Publication, 15 September 1976.

Oppenheim, I.J., "Economic Analysis of Earthquake Engineering Investment," Proceedings of the 2nd U.S. National Conference on Earthquake Engineering, 22-24 August, 1979, Stanford University, California, pp. 467-476.

Oppenheim, I.J., "Simulation of Water System Seismic Risk," Journal of the Technical Councils of ASCE, Vol. 105, No. TC2, December 1979 (and Preprint No. 3349, October 1979).

Oppenheim, I.J., "Vulnerability of Transportation and Water Systems to Seismic Hazard Methodology for Hazard Cost Evaluation," The Current State of Knowledge of Lifeline Earthquake Engineering, Proceedings of Technical Council on Lifeline Earthquake Engineering, Specialty Conference, University of California, Los Angeles, 30-31 August, 1977, pp. 394-409.

O'Rourke, M.J., "Axial Soil Strain Due to Seismic Wave Propagation," (Presented at the User's Panel Meeting for Merritt CASES, Inc. DNA/NSF Research Project, Reno, Nevada, 10 February 1983) Rensselaer Polytechnic Institute.

O'Rourke, M.J., Singh, S. and Pikul, R., "Seismic Behavior of Buried Pipelines," Lifeline Earthquake Engineering - Buried Pipelines, Seismic Risk and Instrumentation, (Presented at the Third National Congress on Pressure Vessels and Piping, San Francisco, California, 25-29 June 1979, American Society of Mechanical Engineers Publication PVP-34, pp. 49-61.

Parker, M.E., "Pipeline Corrosion and Cathodic Protection," Gulf Publishing Company, Houston, Texas, 1962.

Parmelee, R.A. and Corotis, R.B., "Analytical and Experimental Evaluation of Modulus of Soil Reaction," Geometric Highway and Culvert Design, Transportation

Research Record 518, Transportation Research Board, National Research Council, Washington, D.C., 1974.

Parmelee, R.A. and Corotis, R.B., "The Iowa Deflection Formula: An Appraisal," Soil-Structure Interaction, A Symposium, Highway Research Record Number 413, Highway Research Board, National Research Council, Washington, D.C., 1972.

Parnes, R., "Static Analysis of an Embedded Pipe Subjected to Periodically Spaced Longitudinal Forces," Grant Report No. 12, NSF Grant No. PFR 78-15049, Weidlinger Associates, August 1979.

Parnes, R. and Weidlinger, P., "Dynamic Response of an Embedded Pipe Subjected to Periodically Spaced Longitudinal Forces," Grant Report No. 13, NSF Grant No. PFR 78-15049, Weidlinger Associates, August 1979.

Paul, S.L., "Interaction of Plane Elastic Waves with a Cylindrical Cavity," Ph.D Thesis, University of Illinois at Urbana, 1963.

Peck, R.B., "Deep Excavation and Tunneling in Soft Ground," University of Illinois at Urbana.

"Prediction of Sulfide Generation and Corrosion in Sewers," (A Case Study prepared for American Concrete Pipe Association), J.B. Gilbert & Associates, Sacramento, California, April 1979.

"Proceedings of the 2nd U.S. National Conference on Earthquake Engineering," sponsored by the Earthquake Engineering Research Institute, Stanford University, California, 22-24 August 1979.

"Proceedings of the World Conference on Earthquake Engineering," sponsored by the Earthquake Engineering Research Institute and the Department of Engineering, University Extension, University of California at Berkeley, California, June 1956.

Redekop, D. and Schroeder, J., "Approximate Prediction of Hoop Stresses at Major Sections of Tee Intersections of Cylindrical Shells Subjected to Internal Pressure," Transactions of the ASME, Journal of Pressure Vessel Technology, Vol. 101, August 1979, pp. 186-193.

"Research Needs in Lifeline Earthquake Engineering," Journal of the Technical Councils of ASCE, Vol. 105, No. TC2, December 1979, pp. 343-362.

Salvadori, M.G. and Singhal, A., "Strength Characteristics of Jointed Water Pipelines," Interim Grant Report No. IR-3, NSF Grant No. ENV P76-9838, Weidlinger Associates, July 1977.

"San Fernando, California, Earthquake of February 9, 1971," Vol. II, Utilities, Transportation and Sociological Aspects, U.S. Department of Commerce, Washington, D.C., 1973.

Schiff, A.J., "Affecting Improved Power System Seismic Resistance," Journal of the Technical Councils of ASCE, Vol. 105, No. TC2, December 1979, pp. 337-341.

Schiff, A.J. and Newson, D.E., "Fragility of Electrical Power Equipment," Journal of the Technical Councils of ASCE, Vol. 105, No. TC2, December 1979, pp. 451-465.

Seed, H.B. and Idriss, I.M., "Soil Moduli and Damping Factors for Dynamic Response Analyses," Report No. EERC-70-10, University of California at Berkeley, 1970.

"Seismic Vulnerability Study. U.S. Air Force Satellite Test Center, Sunnyvale, California. Volume I - Seismic Criteria, Volume II - Structural Evaluation," SAMSO Contract: F04701-73-C-0313, John A. Blume & Associates, July 1974.

Shinozuka, M. and Kawakomi, H., "Ground Characteristics and Free-Field Strains," Technical Report No. CU-2, NSF Grant No. ENV-76-09838, Columbia University, New York, New York, August 1977.

Shinozuka, M. and Kawakomi, H., "Underground Pipe Damages and Grout Characteristics," Technical Report No. CU-1, NSF Grant No. ENV-76-09838, Columbia University, New York, New York, June 1977.

Shinozuka, M. and Koike, T., "Estimation of Structural Strains in Underground Lifeline Pipes," Technical Report No. CU-4, NSF Grant No. PFR-78-15049, Columbia University, New York, New York, March 1979.

Sobel, L.H. and Newman, S.Z., "Plastic Buckling of Cylindrical Shells under Axial Compression," Transactions of the ASME, Journal of Pressure Vessel Technology, Vol. 102, February 1980, pp. 40-44.

Spannagel, D.W., Davis, R.E., and Backer, A.E., "Structural Behavior of a Flexible Metal Culvert Under a Deep Earth Embankment Using Method A Backfill," State of California, Business and Transportation.

"Standard Specifications for Public Works Construction," Building News, Inc., Los Angeles, California, 1973.

Stratta, J.L. and Wyllie, L.A., Jr., "Friuli, Italy Earthquakes of 1976," Reconnaissance Report, Earthquake Engineering Research Institute, August 1979.

Stratta, J.L., et al., "Mindanao, Philippines Earthquake, August 17, 1976," Reconnaissance Report, Earthquake Engineering Research Institute, August 1977.

"Stress Corrosion Cracking of Metals - A State-of-the-Art Report," (Presented at the American Society for Metals Conference, Detroit, Michigan, 18 October 1971), American Society for Testing and Materials Special Publication 518.

"Surveillance of the Seismic Study, Air Force Satellite Test Center, Sunnyvale, California, Summary Report," prepared for SAMSO, Karagozian & Case, July 1974.

Sweet, J., "SATURN - A Multi-Dimensional Two-Phase Computer Program which Treats the Nonlinear Behavior of Continua Using the Finite Element Approach," Report No. JSA-79-016, Joel Sweet and Associates, September 1979.

"Symposium on Creep of Concrete," American Concrete Institute Special Publication SP-9, 1964.

Szilard, R. and Wallevik, O., "Effectiveness of Concrete Cover in Corrosion Protection of Prestressing Steel," Corrosion of Metals in Concrete, American Concrete Institute Special Publication SP-49, 1975.

"Tentative Provisions for the Development of Seismic Regulations for Building, A Cooperative Effort with the Design Professions, Building Code Interests and the Research Community," prepared by Applied Technology Council, associated with the Structural Engineers Association of California, ATC 3-06, NBS Special Publication 510, NSF Publication 78-8, June 1978.

Terzaghi, K., Theoretical Soil Mechanics, John Wiley & Sons, Inc., New York, New York, 1943.

Terzaghi, K. and Peck, R.B., Soil Mechanics in Engineering Practice, John Wiley & Sons, New York, New York, 1967.

Wang, L.R.L. and O'Rourke, M.J., "State-of-the-Art of Buried Lifeline Earthquake Engineering," The Current State of Knowledge of Lifeline Earthquake Engineering, Proceedings of Technical Council on Lifeline Earthquake Engineering Specialty Conference, University of California, Los Angeles, 30-31 August 1977, pp. 252-265.

Wang, L.R.L., Pikul, R.R., and O'Rourke, M.J., "Imposed Ground Strain and Buried Pipelines," A Technical Note in Journal of the Technical Councils of ASCE, Vol. 108, No. TC2, November 1982, pp. 259-263.

Warren, G.D. II, and Tchobanoglous, G., "A Study of the Use of Concrete Pipe for Trunk Sewers in the City of Delano, California," a report prepared for California Precast Concrete Pipe Association, University of California, Davis, California, September 1976.

Weidlinger, P., "Behavior of Underground Lifelines in Seismic Environment," Interim Grant Report No. IR-4, NSF Grant No. ENV P76-9838, Weidlinger Associates, July 1977.

Weidlinger, P. and Nelson, I., "Seismic Analysis of Pipelines with Interference Response Spectra," Grant Report No. 7, NSF Grant No. ENV P76-9838, PFR 78-15049, Weidlinger Associates, June 1978.

White, G.F. and Haas, J.E., "Assessment of Research on Natural Hazards," The MIT Press Environmental Studies Series, MIT Press, Cambridge, Massachusetts and London, England, 1975.

Womack, D.E. and Kirdan, E., "Loads and Minimum Cover for Cast-In-Place, Unreinforced Concrete Pipe," Salt River Valley Water Users' Association, Phoenix, Arizona, November 1960.

Yanev, P.I., "The Lice, Turkey, Earthquake of September 6, 1975," Reconnaissance Report, Newsletter, Vol. 9, No. 6B, Earthquake Engineering Research Institute, November 1975.

Young, F.M. and Hunter, S.E., "Hydraulic Transients in Liquid-Filled Pipelines During Earthquakes," Lifeline Earthquake Engineering - Buried Pipelines, Seismic Risk and Instrumentation, (Presented at the Third National Congress on Pressure Vessels and Piping, San Francisco, California, 25-29 June 1979), American Society of Mechanical Engineers Publication PVP-34, pp. 143-151.

## APPENDIX B

### LIST OF SYMBOLS

A	Cross sectional area of conduit
$D_\gamma$	Relative density
E	Modulus of elasticity
E'	Modulus of elasticity in plane stress
$E_s$	Modulus of elasticity of steel tube
F	Axial force in conduit
$F_n$	Sand/conduit normal force
$F_t$	Sand/conduit tangential force
G	Shear modulus
I	Moment of inertia
K	Bulk modulus
L	Length
M	Moment
P	External normal pressure on the conduit
$P_c$	Backfill lateral confining stress
$P_o$	Pressure of confining oil
a	Internal radius of cylinder
$a_s$	Internal steel tube radius
b	External radius of cylinder
$b_s$	External steel tube radius
c	Distance from centroidal axis to extreme fiber
k	Friction coefficient
$p_i$	Internal cylinder pressure
$p_e$	External cylinder pressure
$p_s$	External steel tube pressure

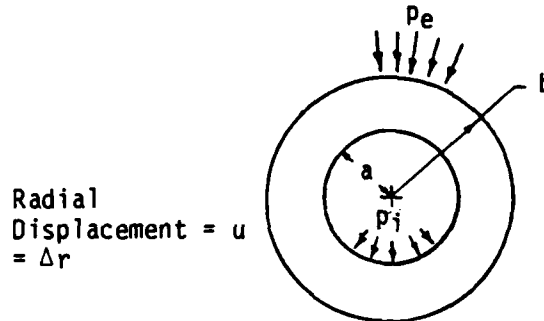
$r$	Radius
$r_1$	Inside radius of conduit
$r_0$	Outside radius of conduit
$u$	Radial displacement
$u_s$	Radial displacement of steel tube
$v$	Shear
$w$	Uniform load magnitude per length
$x$	Horizontal dimension
$y$	Vertical displacement
$y'$	Vertical slope
$y'_0$	Vertical slope at point 0
$y'_1$	Vertical slope at point 1
$y''$	Vertical curvature
$y_0$	Vertical displacement at point 0
$y_1$	Vertical displacement at point 1
$\Delta r$	Radius change
$\Delta x$	Difference of $x$ values
$\alpha$	Drucker-Prager yield parameter
$\epsilon$	Strain
$\epsilon_f$	Flexural strain
$\epsilon_z$	Axial strain
$\epsilon_\theta$	Tangential conduit strain
$\nu$	Poisson's ratio
$\nu'$	Plane stress Poisson's ratio
$\nu_s$	Poisson's ratio of steel tube
$\sigma_{kk}^o$	Mean stress

$\sigma_f$  Flexural stress  
 $\sigma_r$  Radial stress  
 $\sigma_z$  Axial stress  
 $\sigma_\theta$  Tangential stress  
 $\tau_{max}$  Maximum shearing stress (yield stress for simple tension)  
 $\phi$  Angle of internal friction

APPENDIX C

CONDUIT RADIAL DISPLACEMENT

For a thick walled cylinder as shown:



$$u = \frac{r}{E} \left[ \frac{a^2 p_i - b^2 p_e}{b^2 - a^2} (1 - \nu) + \frac{(p_i - p_e) a^2 b^2 (1 + \nu)}{b^2 - a^2} \frac{1}{r^2} - \nu \sigma_z \right] \quad (C-1)$$

Assume plane strain case,  $\epsilon_z = 0$  and  $E' = \frac{E}{1 - \nu^2}$ ; and  $\nu' = \frac{\nu}{1 - \nu}$ .

For sand around a steel tube,  $u$  must be equal at interface.

For steel tube, let  $p_i = 0$ , and  $p_e = p_s$  in Equation (C-1). When  $r = b_s$

$$u_s = \frac{b_s}{E_s} \left[ \frac{-b_s^2 p_s (1 - \nu_s')}{b_s^2 - a_s^2} - \frac{p_s a_s^2 (1 + \nu_s')}{b_s^2 - a_s^2} \right] \quad (C-2)$$

This expression is readily evaluated for given values of  $a_s$ ,  $b_s$ ,  $E_s$ ,  $\nu_s$ , and  $p_s$  (see Table C.1).

For the sand let  $p_i = p_s$  and let  $b^2 - a^2 \approx b^2$  since  $a \ll b$ . When  $r = a$ , Equation (C-1) gives

$$u \approx \frac{a}{E'} \left[ \frac{a^2 p_s - b^2 p_e}{b^2} (1 - \nu') + (p_s - p_e) (1 + \nu') \right] \quad (C-3)$$

(Non-subscripted variables refer to sand).

Table C.1. Conduit deformation due to external radial pressure.

$$u_s = \frac{b_s p_s}{E'_s} \left[ \frac{-b_s^2 (1 - \nu'_s) - a^2 (1 + \nu'_s)}{b_s^2 - a_s^2} \right]$$

$$E'_s = 218,400 \text{ MPa}; \nu'_s = .408$$

$p_s$ (MPa)	$u_s$ (cm) 1/4 in. conduit $a_s = 0.246 \text{ cm}; b_s = 0.3175 \text{ cm}$	$u_s$ (cm) 1 in. conduit $a_s = 0.965 \text{ cm}; b_s = 1.27 \text{ cm}$
1	$5.228 \times 10^{-6}$	$1.933 \times 10^{-5}$
2	$1.05 \times 10^{-5}$	$3.87 \times 10^{-5}$
5	$2.61 \times 10^{-5}$	$9.66 \times 10^{-5}$
10	$5.23 \times 10^{-5}$	$1.933 \times 10^{-4}$
15	$7.84 \times 10^{-5}$	$2.90 \times 10^{-4}$
20	$1.05 \times 10^{-4}$	$3.87 \times 10^{-4}$

Since  $a^2$  is small,  $u$  can be written

$$u \approx \frac{a}{E'} \left[ (p_s - p_e) (1 + \nu') - p_e (1 - \nu') \right] \quad (C-4)$$

solving for  $p_e$

$$p_e = \frac{1}{2} \left[ (1 + \nu') p_s - \frac{E'}{a} u \right] \quad (C-5)$$

for (1)  $\nu' = .333$ ,  $a = 0.3175$  cm,  $E' = 1509$  MPa

(2)  $\nu' = .333$ ,  $a = 1.27$  cm,  $E' = 1509$  MPa

let  $p_s = 20$  MPa and solve for  $p_e$ .

$$(1) p_e = 0.667 \times 20 \text{ MPa} - (2376 \times 1.05 \times 10^{-4}) \text{ MPa} = 13.33 - .25 = 13.08 \text{ MPa}$$

$$(2) p_e = 0.667 \times 20 \text{ MPa} - (594 \times 3.87 \times 10^{-4}) \text{ MPa} = 13.33 - .23 = 13.10 \text{ MPa}$$

so that the  $\frac{E'}{a} u$  term is negligible.

Hence,  $p_e = \frac{(1 + \nu')}{2} p_s$  or  $p_s = 1.5 p_e$

## APPENDIX D

### FINITE ELEMENT MODELING OF CONDUIT PULLOUT TESTS

The conduit pullout tests were modeled analytically using the SATURN finite element computer code (Reference 14). The results of 29 runs (A-AK) are summarized in Table D.1. They consist of one linear material model, 21 Drucker-Prager material models, and 7 von Mises material models.

The problem configuration appears in Figure D.1. The case considered here is the 1 in. conduit with a length of 23 cm. The wall thickness is assumed to be 0.4 cm. The outside diameter of the soil is 10.54 cm.

The SATURN runs were performed with the axisymmetric assumption. The lateral confining stress  $P_c$  is first applied and then the force,  $F$  is incremented until the conduit is slipping at all node locations in contact with the soil.

The displacement of the end of the conduit as a function of the axial force,  $F$  appears in Figure D.2 for a linear material (Run A). The development of the slip along the conduit as a function of axial load appears in Figures D.3 through D.13 for various axial loads, again for Run A. These displacements are magnified by a factor of 100 in the longitudinal direction.

Plots of the end displacement versus end load for the runs listed in Table D.1 appear in Figures D.14 through D.42. Since these runs are force-controlled, the solution becomes unstable after slip occurs along the total length of the conduit. Figure D.43 illustrates the modified mesh used for run AK which provided a more detailed sand mesh near the interface.

Table D.1. Summary of 'SATURN' runs.

Run	Sand * Failure Model	Friction Coef., k	Conf. Press., P <sub>c</sub> , MPa	Max. End Displ., mm	Max. End Force, kN	No. of Plastic Elements	Remarks
A	1	.30	3.0	.0124	24.6	0	
B	2	.30	3.0	.0131	23.9	16	
C	3	.30	3.0	.0142	24.5	35	
D	4	.30	3.0	.0206	23.5	52	
E	5	.30	3.0	.0375	25.3	76	
F	6	.30	3.0	.151	30.7	114	
G	3	.25	3.0	.0102	19.2	11	
H	3	.35	3.0	.0218	29.8	33	
I	3	.40	3.0	.0207	31.3	33	
J	3	.20	3.0	.0091	16.9	7	
K	3	.30	4.0	.0180	31.6	28	
L	3	.25	4.0	.0133	25.4	9	
M	3	.35	4.0	.0312	37.8	35	
N	3	.40	4.0	.0263	38.5	32	
O	3	.20	4.0	.0120	21.4	3	
P	3	.30	2.0	.0095	17.1	16	
Q	3	.25	2.0	.0068	13.6	8	
R	3	.35	2.0	.0106	18.7	33	
S	3	.40	2.0	.0168	23.6	31	
T	3	.20	2.0	.0050	11.4	6	
U	5	.25	3.0	.0154	19.0	60	
V	5	.35	3.0	.049	27.7	80	
W	5	.40	3.0	.0801	32.0	90	
X	5	.20	3.0	.0114	16.4	60	
Y	3	.40	3.0	.093	40.0	85	
Z	7	.30	3.0	.0137	24.5	15	
AE	8	.30	3.0	.043	25.1	83	
AF	9	.30	3.0	.033	24.5	14	
AK	3	.30	3.0	.014	24.3	32	New mesh

1. Linear
2. Drucker-Prager,  $\phi = 32^\circ$
3. Drucker-Prager,  $\phi = 30^\circ$
4. Von Mises,  $\tau_{\max} = 1$  MPa
5. Von Mises,  $\tau_{\max} = 0.6$  MPa
6. Von Mises,  $\tau_{\max} = 0.2$  MPa
7. Drucker-Prager,  $\phi = 30^\circ$  with Associated Flow Rule
8. Drucker-Prager,  $\phi = 8^\circ$
9. Drucker-Prager,  $\phi = 30^\circ$ ,  $K = 236$  MPa,  $G = 142$  MPa

\* Unless noted otherwise all sand models have elastic constants of:  
 $K = 943$  MPa,  $G = 566$  MPa,  $\nu = 0.25$

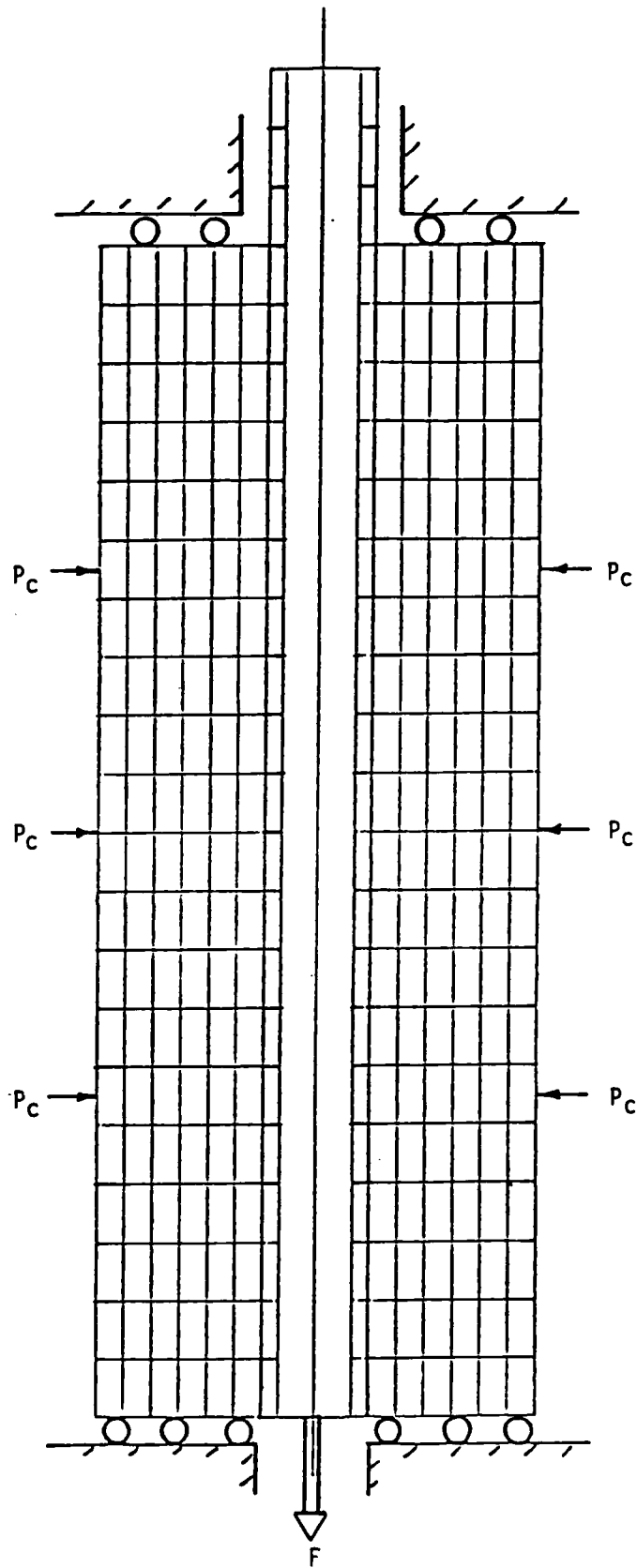


Figure D.1. Finite element idealization.

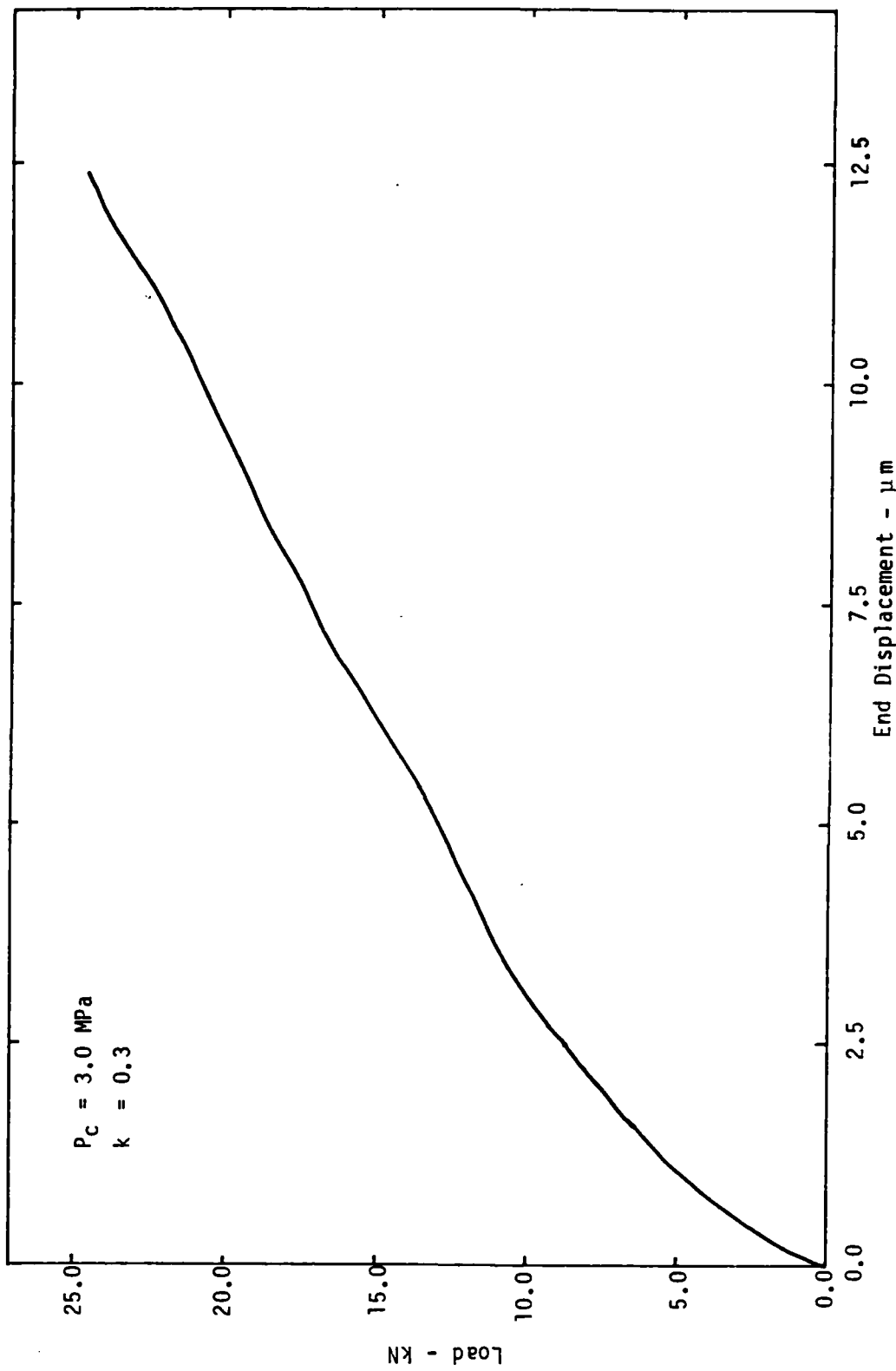


Figure D.2. Calculated load/slip behavior (linear material).

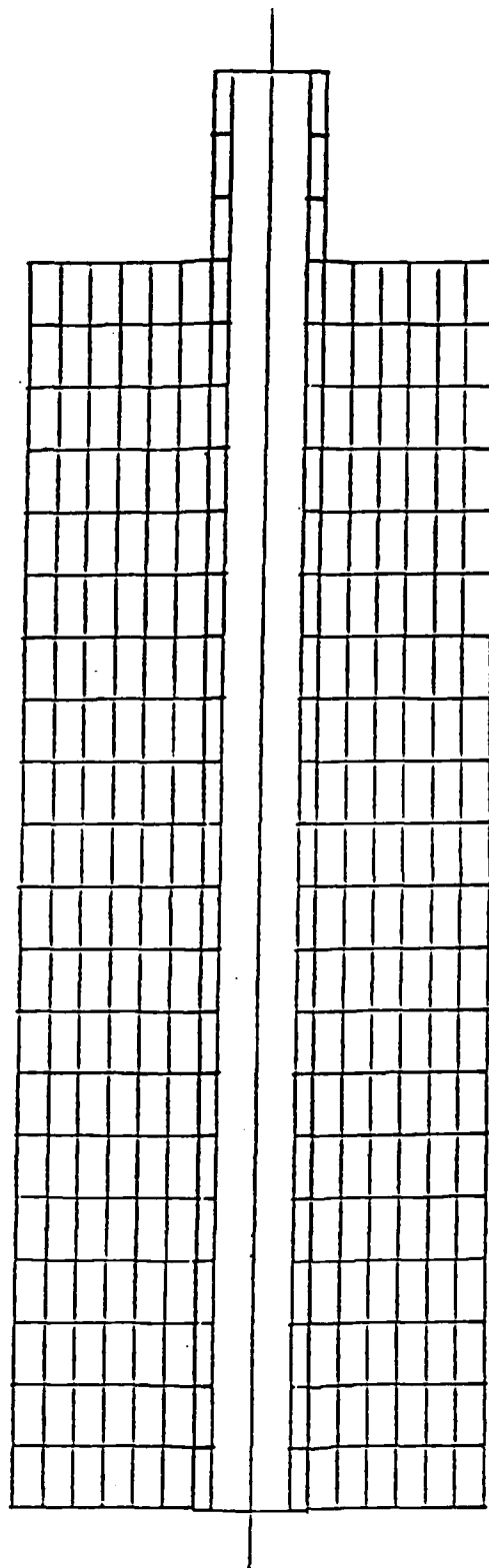


Figure D.3. Slip development along conduit  
at pullout load of 1.8 kN.

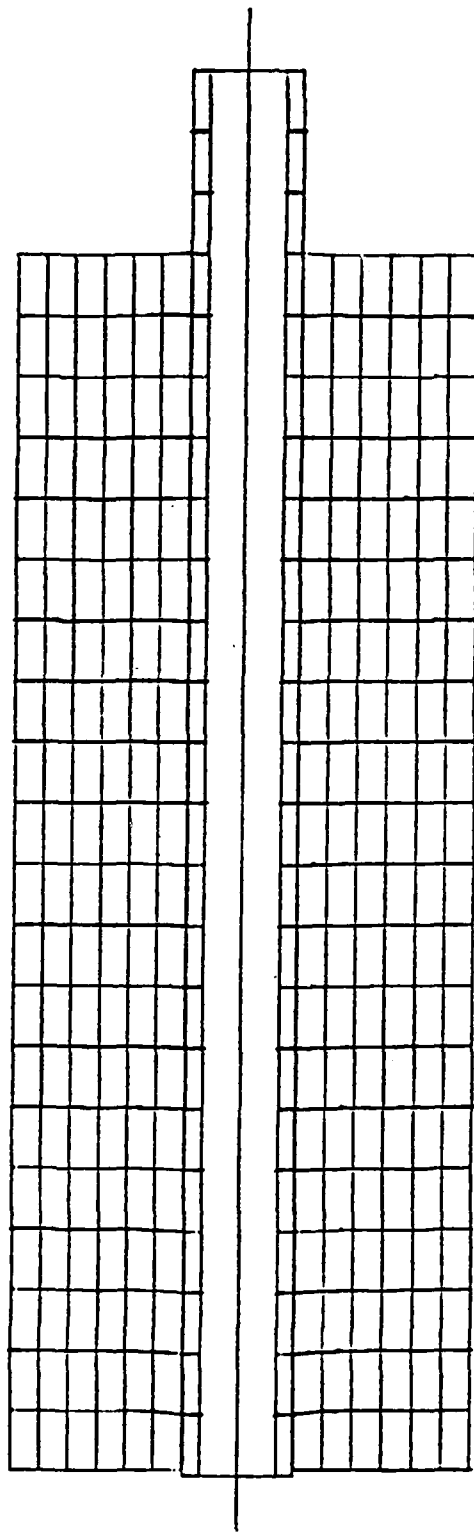


Figure D.4. Slip development along conduit  
at pullout load of 3.6 kN.

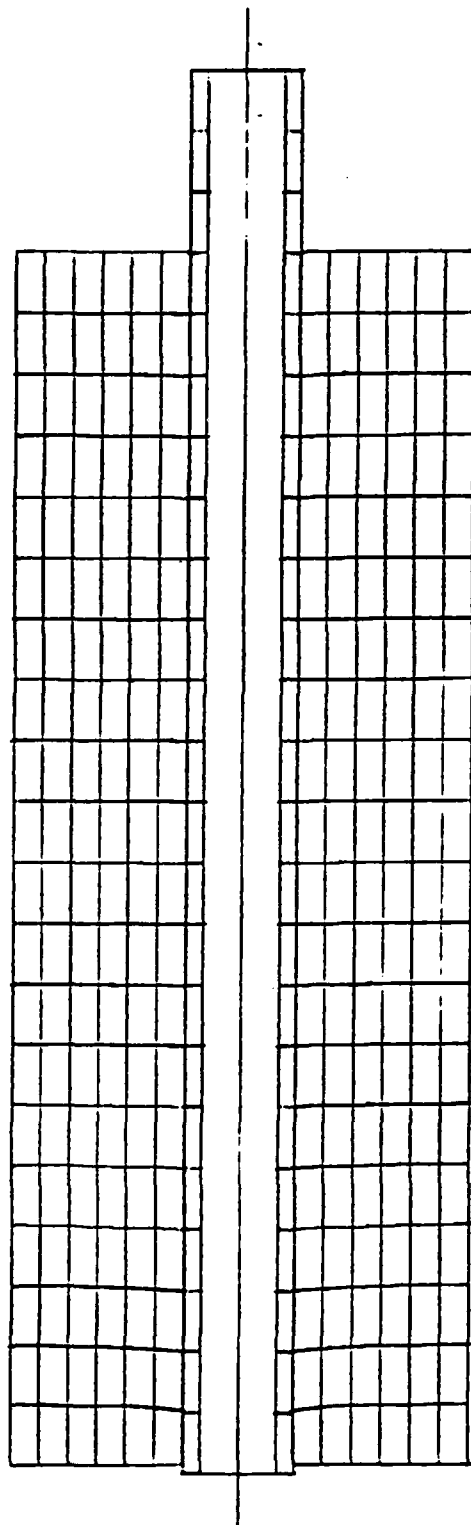


Figure D.5. Slip development along conduit  
at pullout load of 5.5 kN.

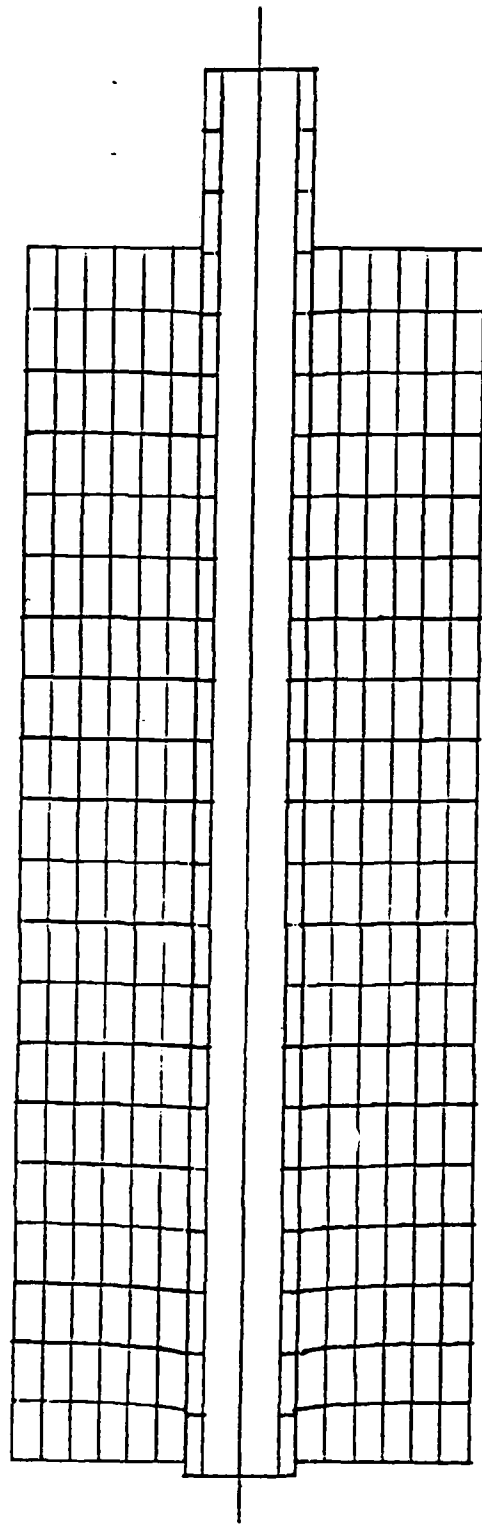


Figure D.6. Slip development along conduit at pullout load of 7.3 kN.

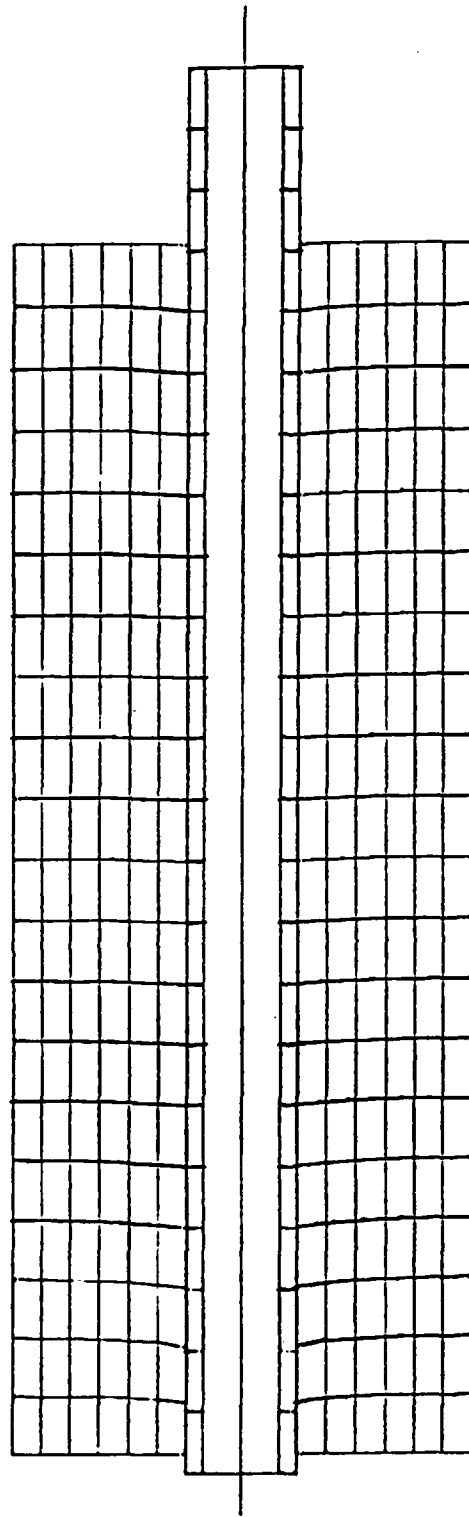


Figure D.7. Slip development along conduit at pullout load of 9.1 kN.

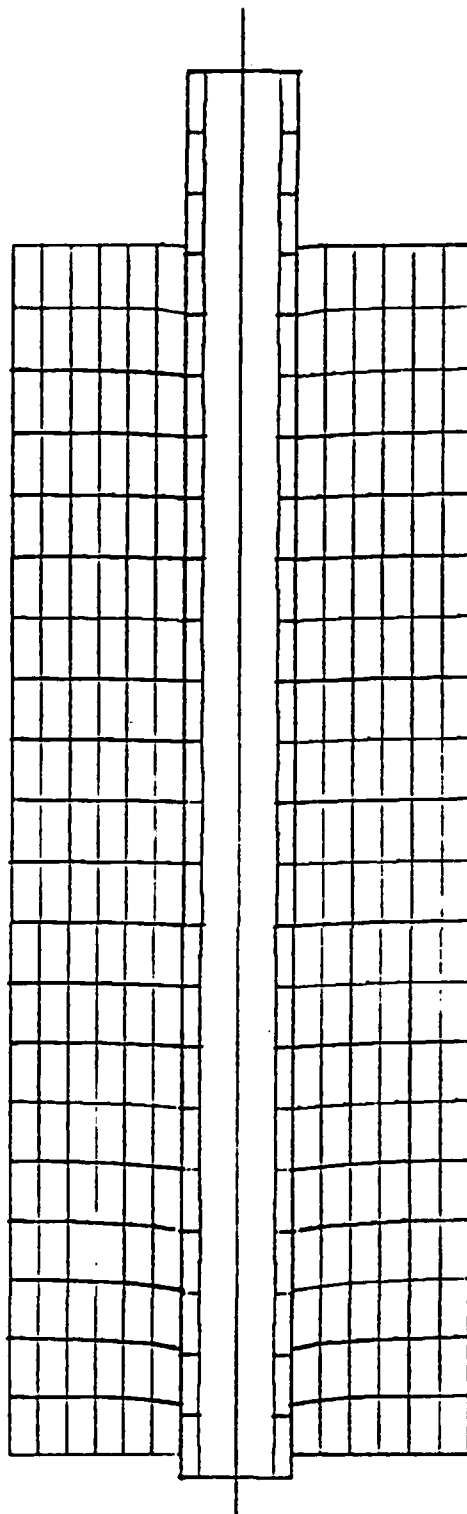


Figure D.8. Slip development along conduit at pullout load of 10.9 kN.

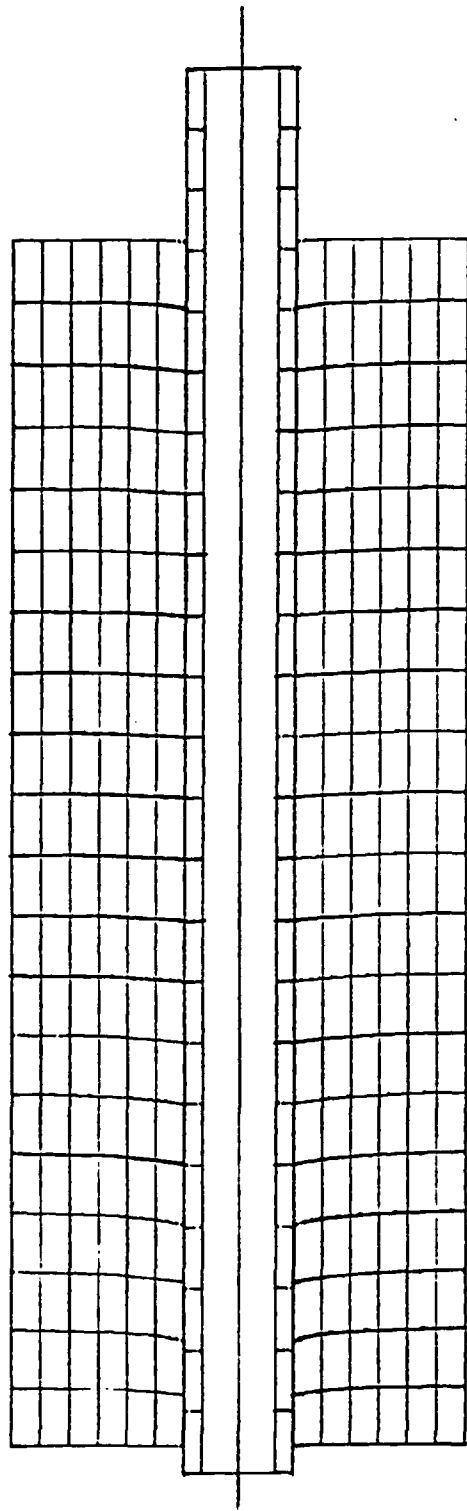


Figure D.9. Slip development along conduit  
at pullout load of 12.8 kN.

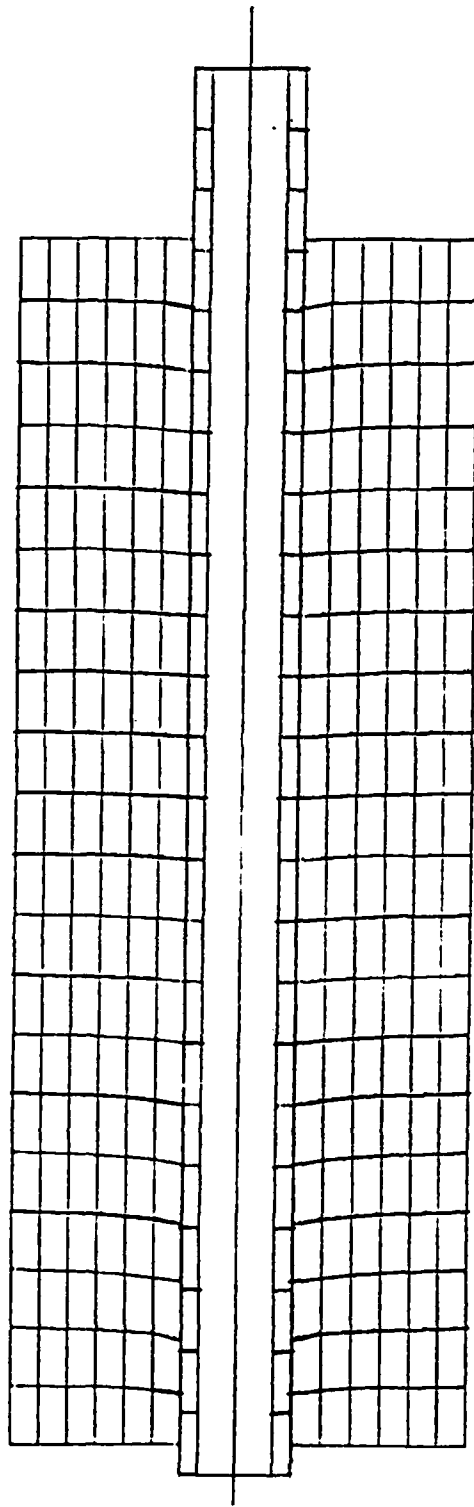


Figure D.10. Slip development along conduit at pullout load of 14.6 kN.

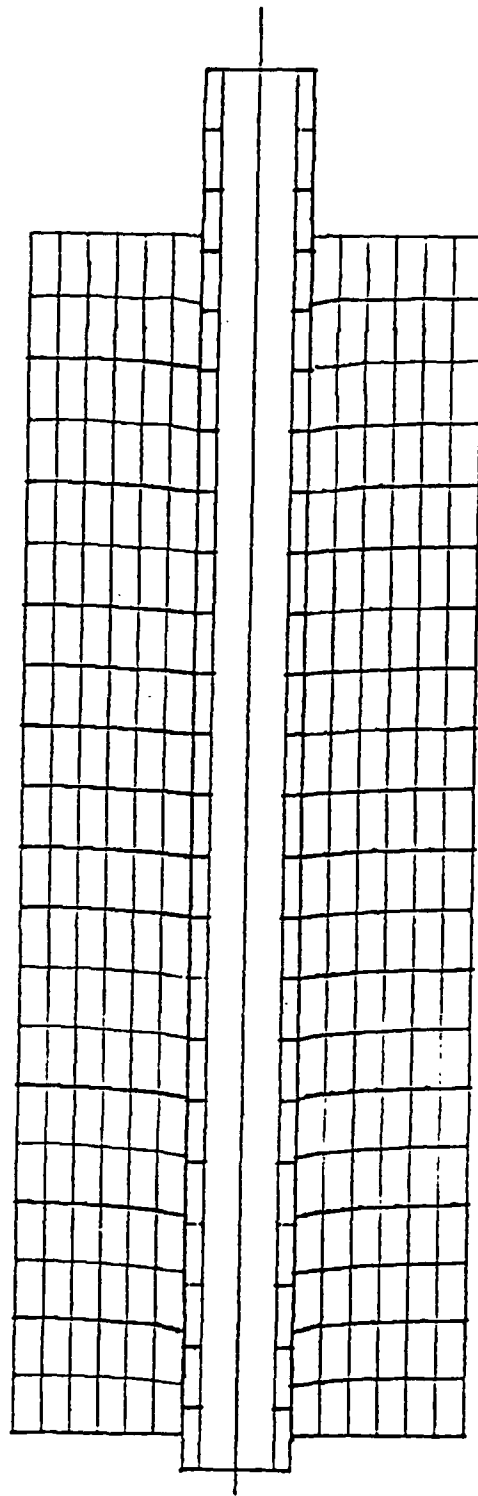


Figure D.11. Slip development along conduit  
at pullout load of 16.4 kN.

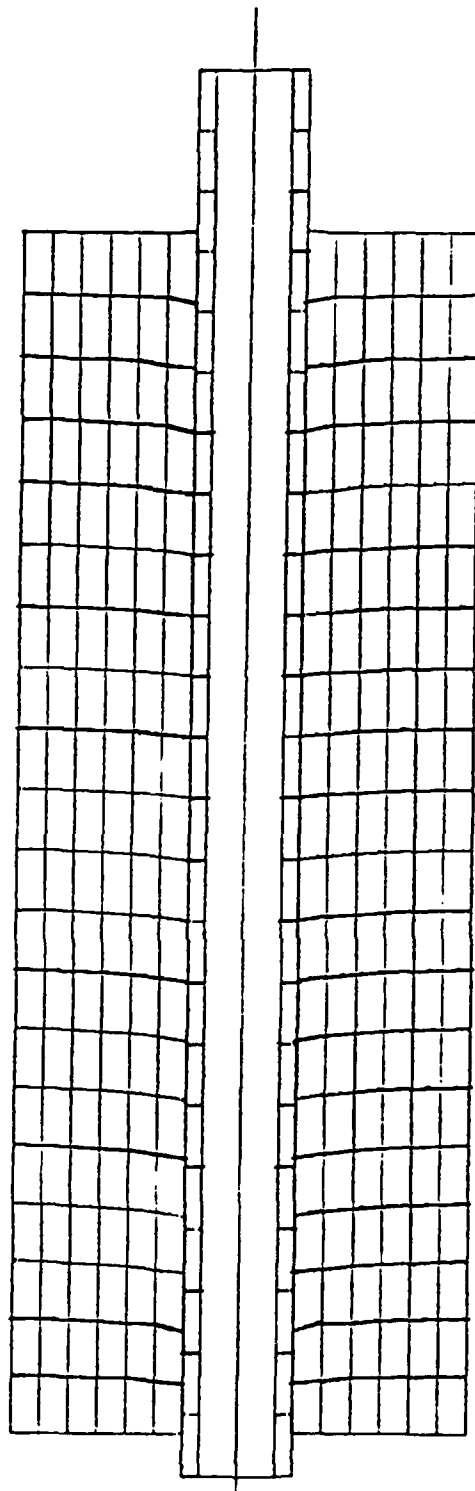


Figure D.12. Slip development along conduit  
at pullout load of 18.2 kN.

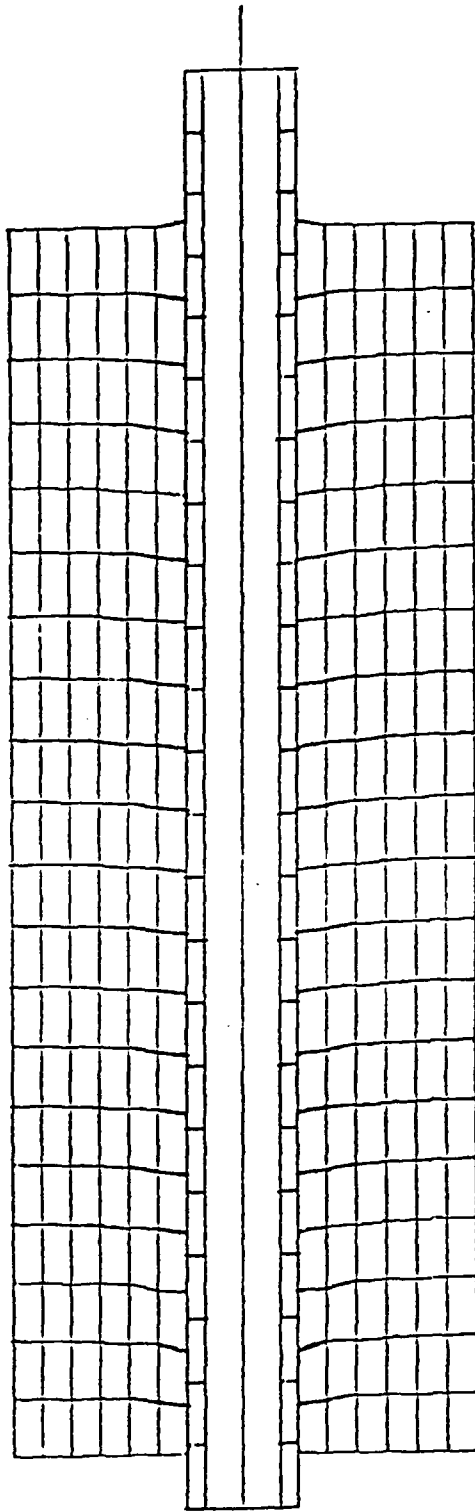


Figure D:13. Slip development along conduit  
at pullout load of 20 kN.

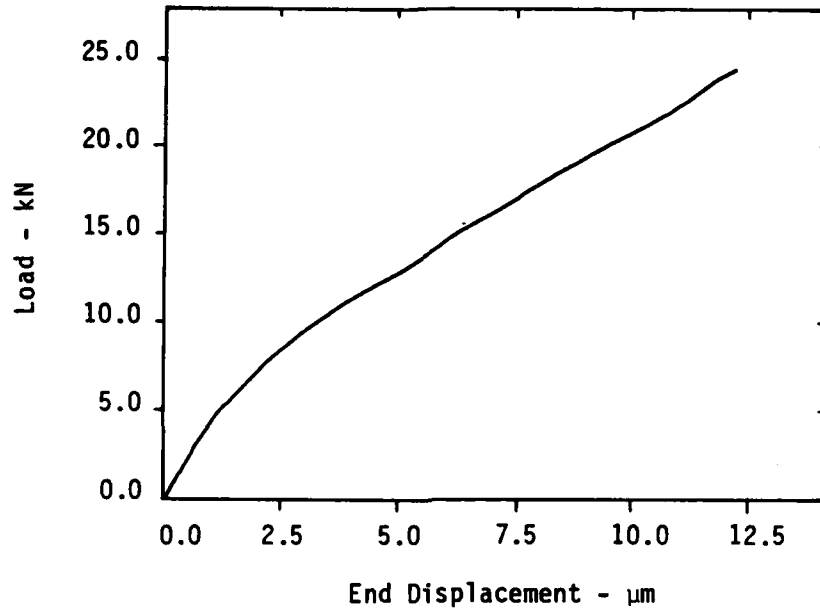


Figure D.14. End displacement versus pullout load, Run A.

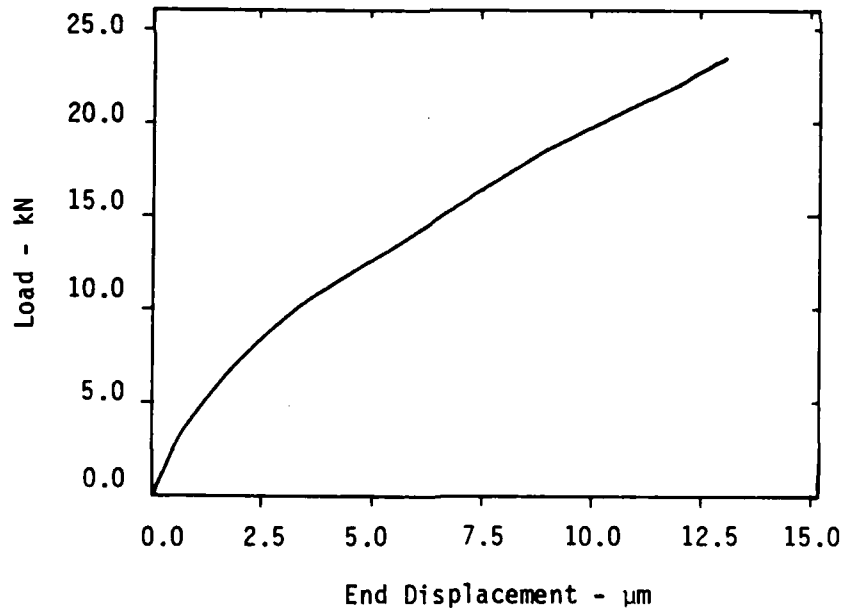


Figure D.15. End displacement versus pullout load, Run B.

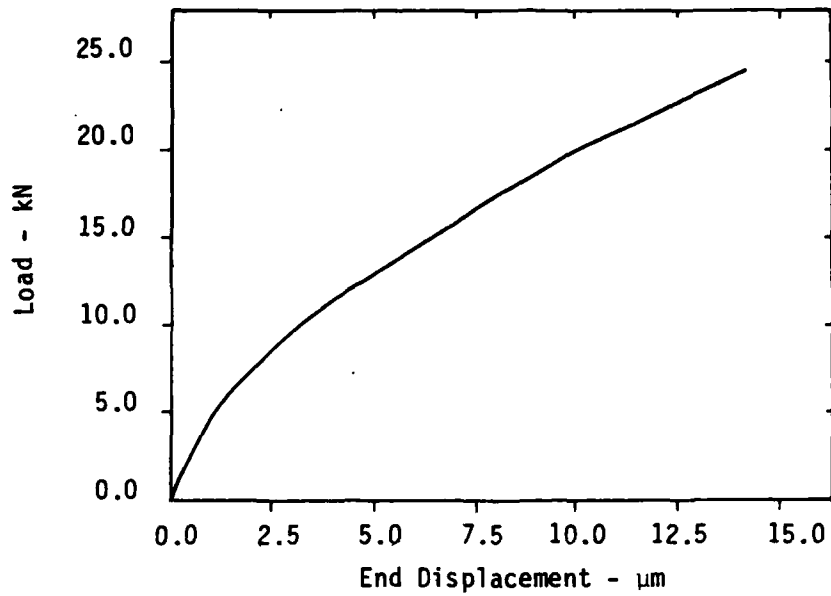


Figure D.16. End displacement versus pullout load, Run C.

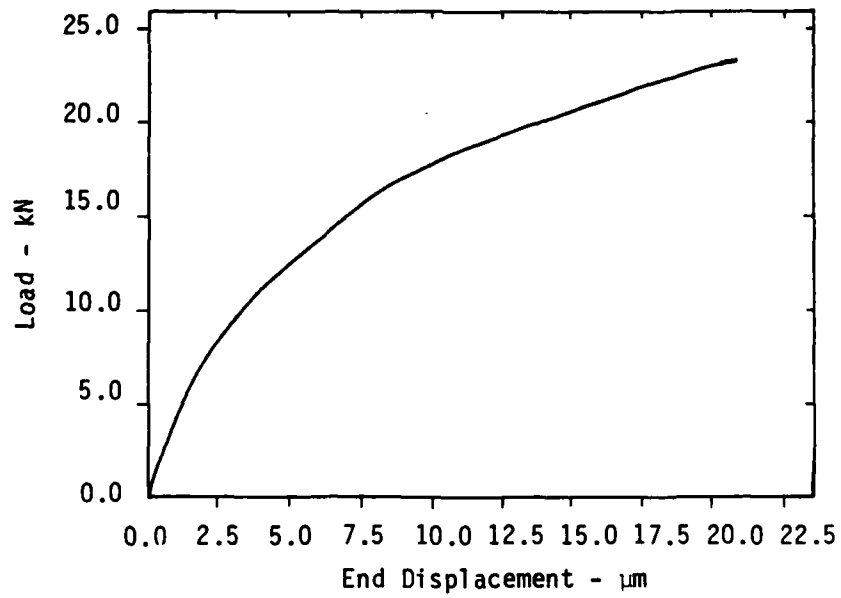


Figure D.17. End displacement versus pullout load, Run D.

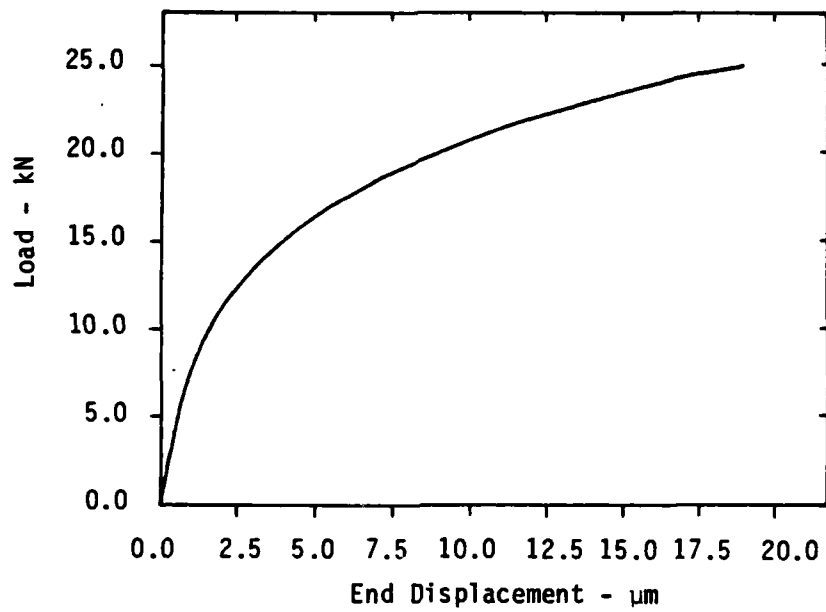


Figure D.18. End displacement versus pullout load, Run E.

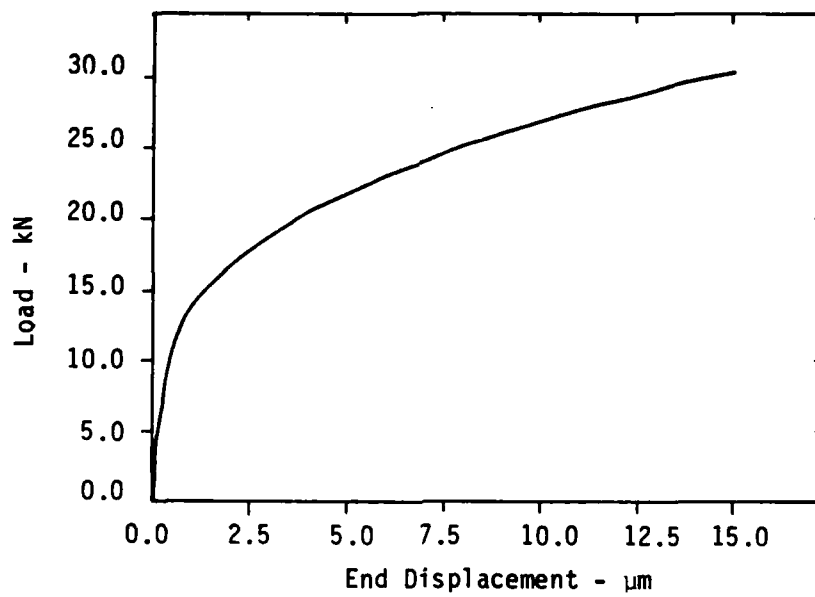


Figure D.19. End displacement versus pullout load, Run F.

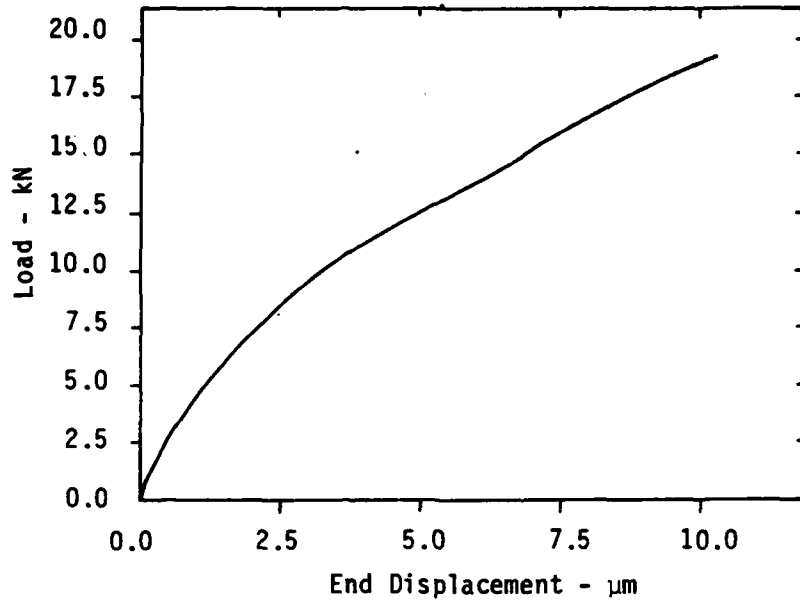


Figure D.20. End displacement versus pullout load, Run G.

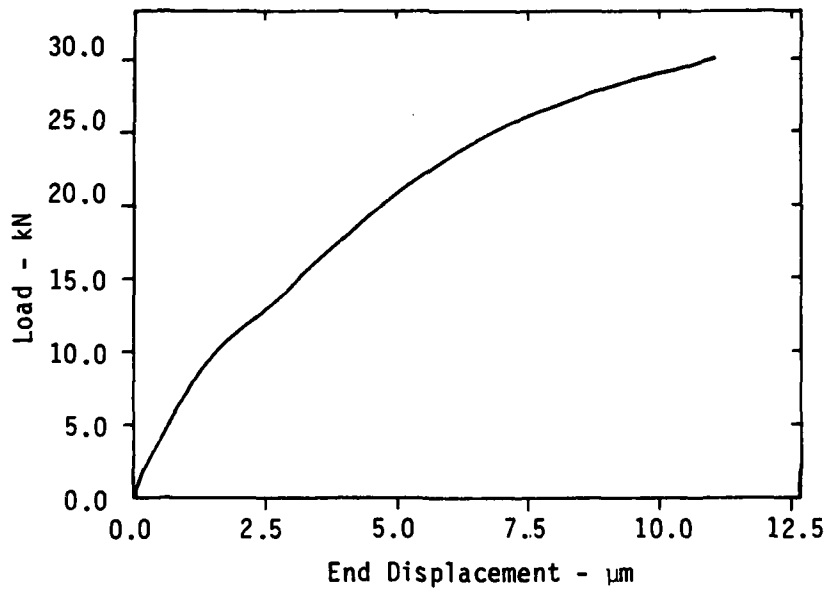


Figure D.21. End displacement versus pullout load, Run H.

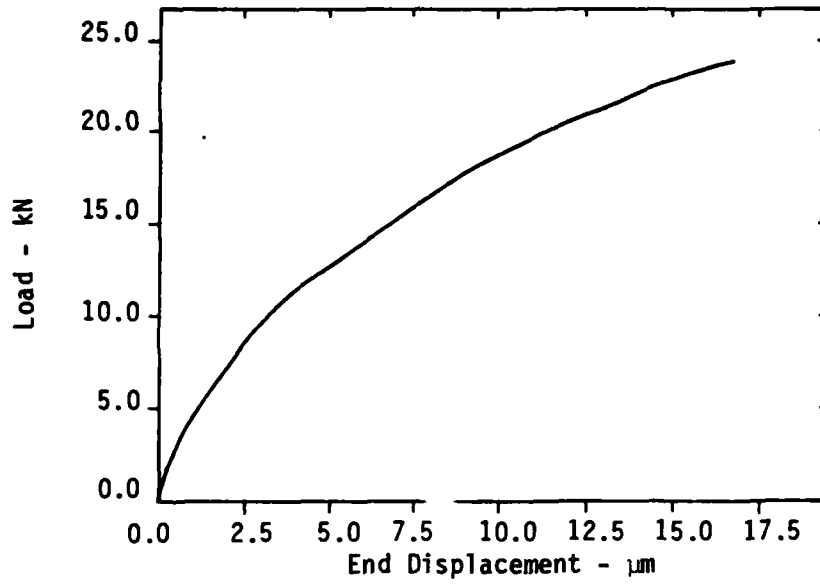


Figure D.22. End displacement versus pullout load, Run I.

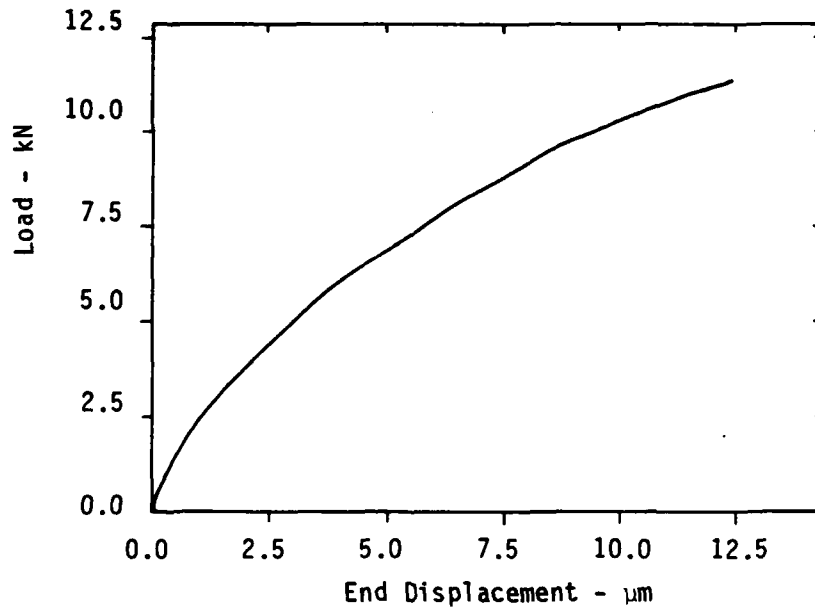


Figure D.23. End displacement versus pullout load, Run J.

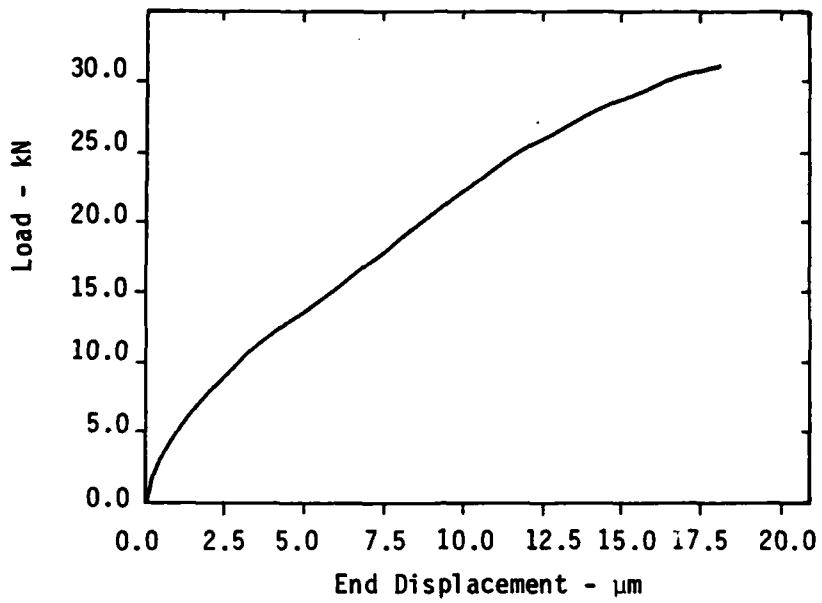


Figure D.24. End displacement versus pullout load, Run K.

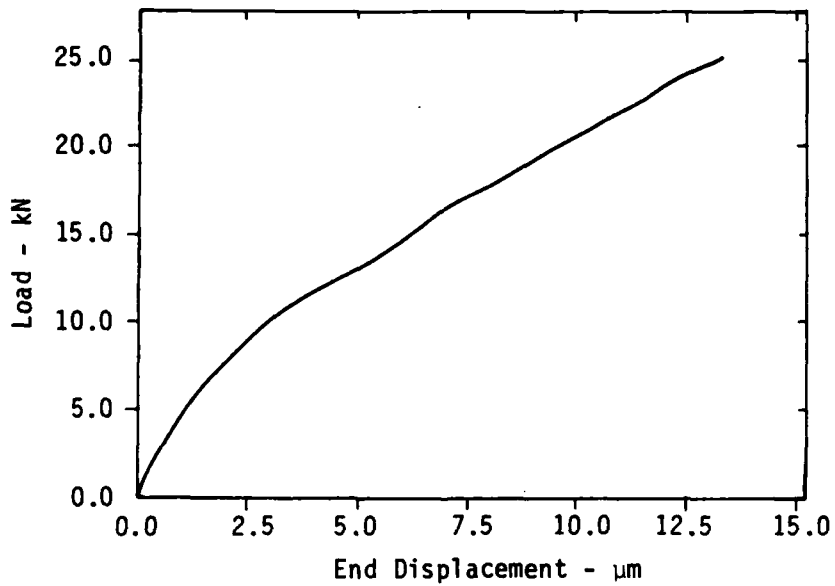


Figure D.25. End displacement versus pullout load, Run L.

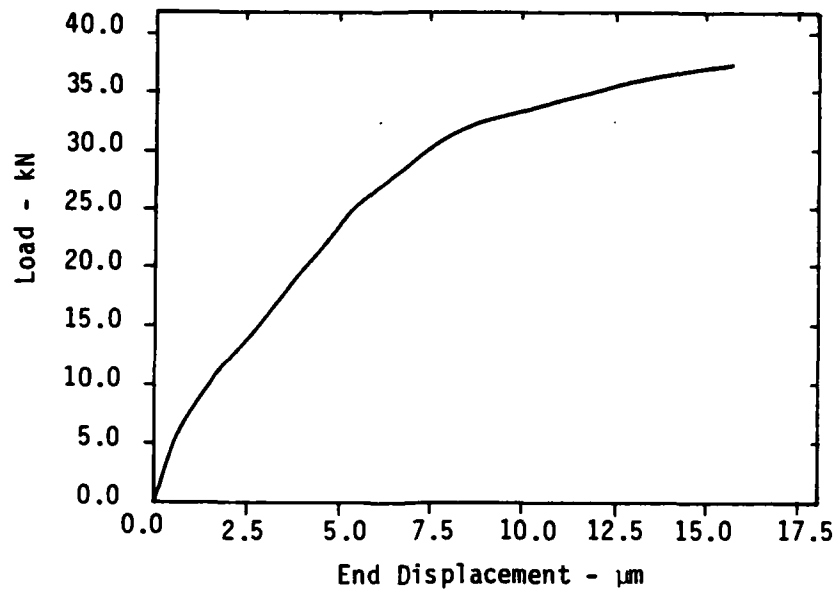


Figure D.26. End displacement versus pullout load, Run M.

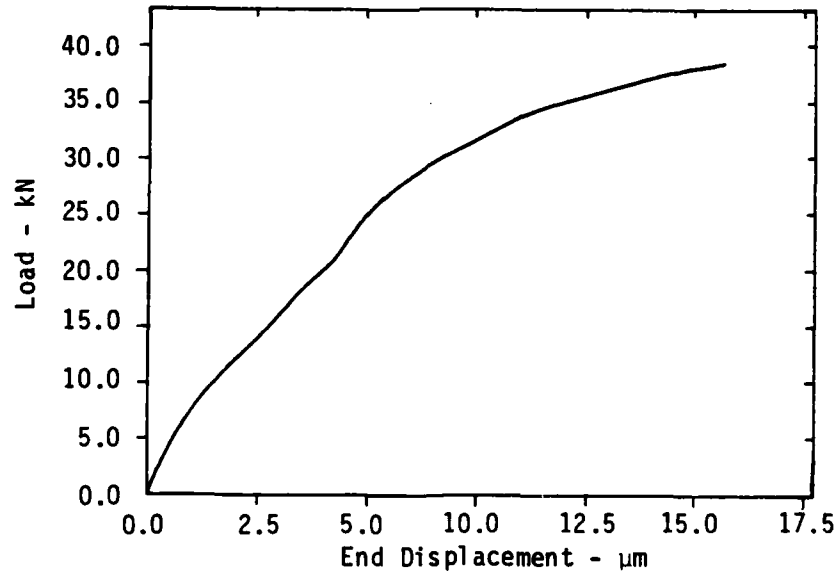


Figure D.27. End displacement versus pullout load, Run N.

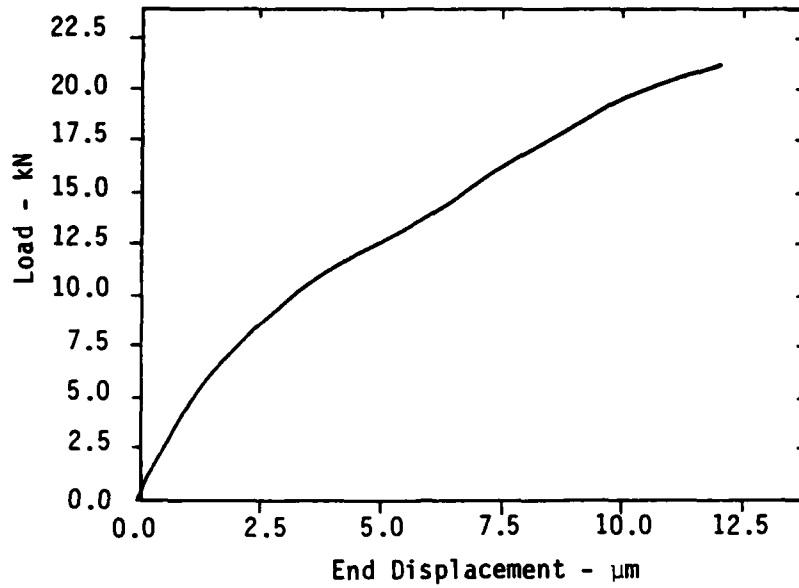


Figure D.28. End displacement versus pullout load, Run 0.

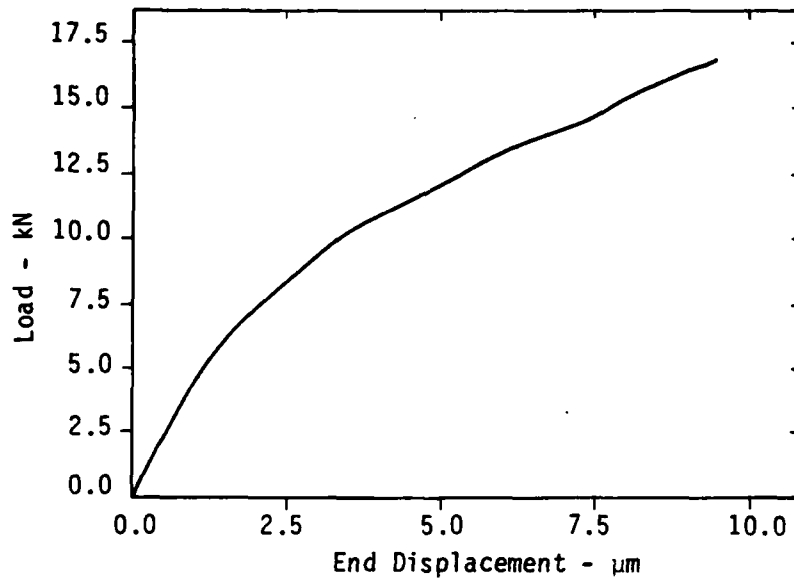


Figure D.29. End displacement versus pullout load, Run P.

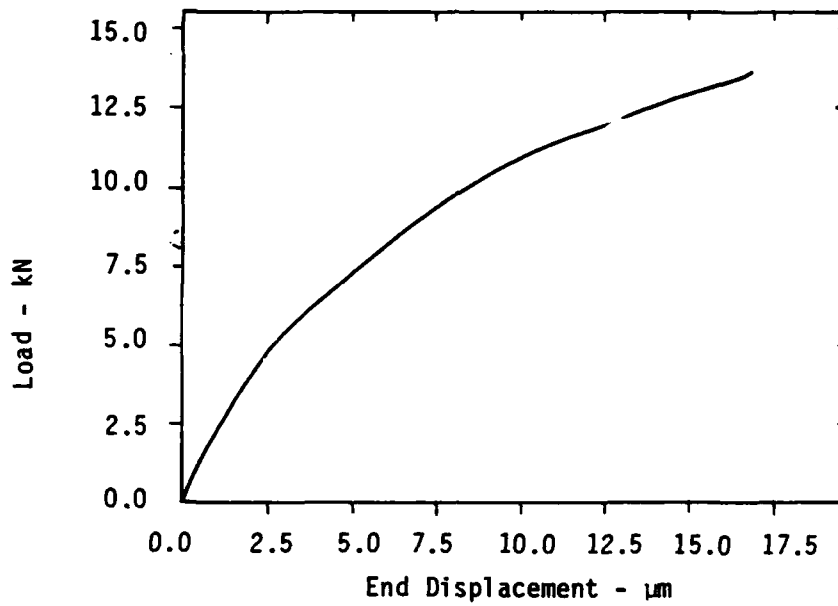


Figure D.30. End displacement versus pullout load, Run Q.

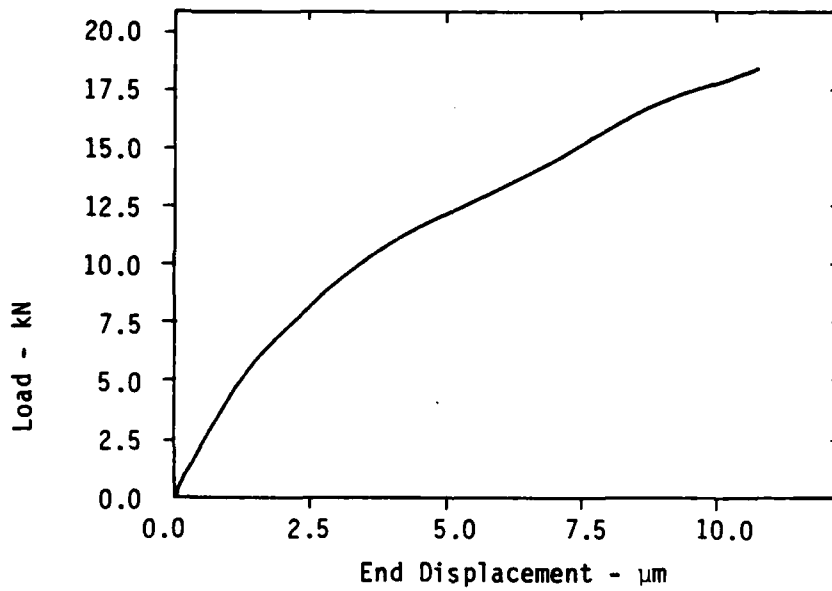


Figure D.31. End displacement versus pullout load, Run R.

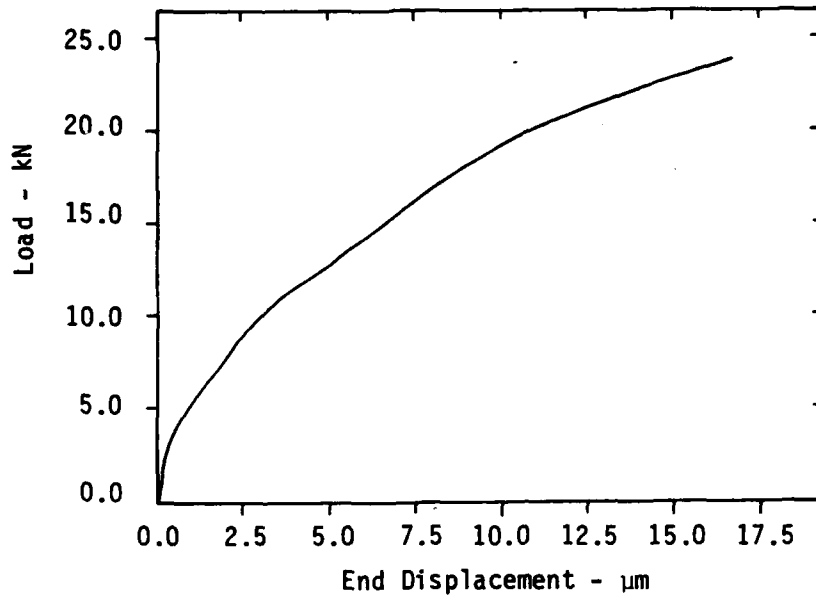


Figure D.32. End displacement versus pullout load, Run S.

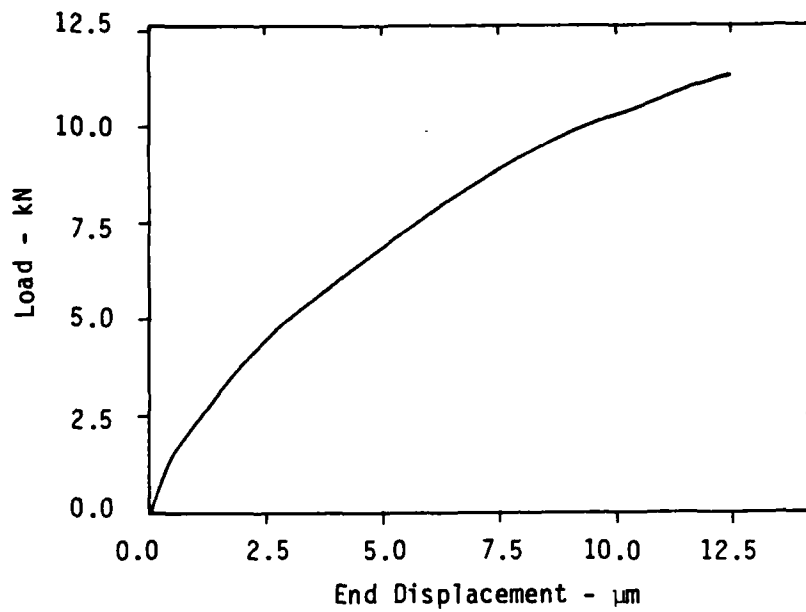


Figure D.33. End displacement versus pullout load, Run T.

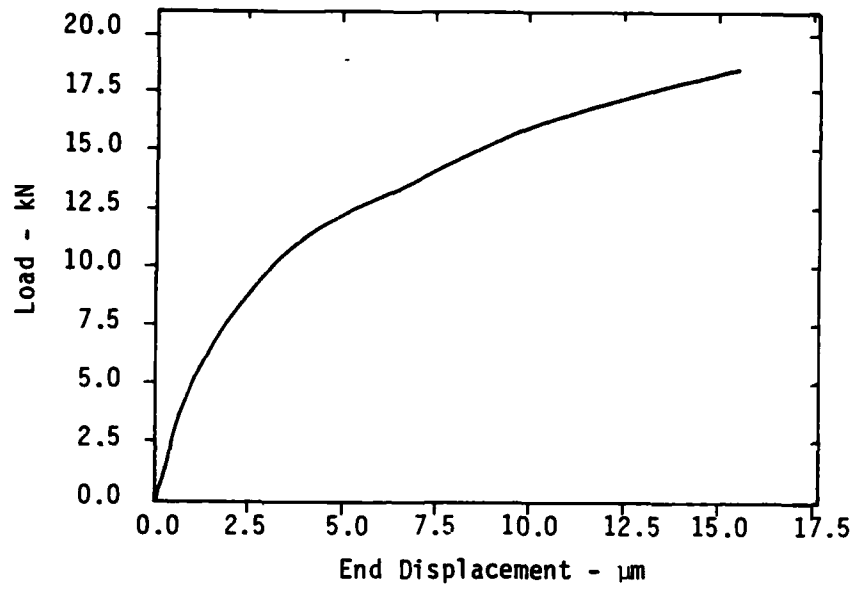


Figure D.34. End displacement versus pullout load, Run U.

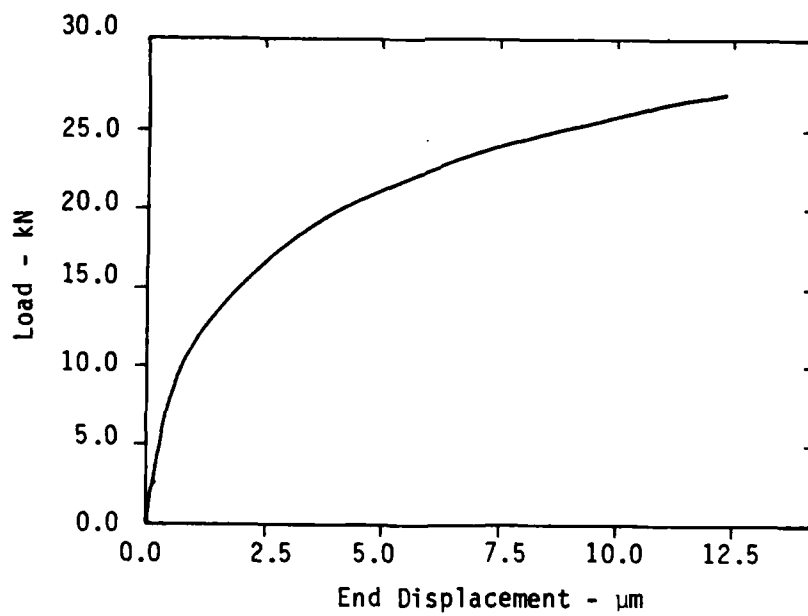


Figure D.35. End displacement versus pullout load, Run V.

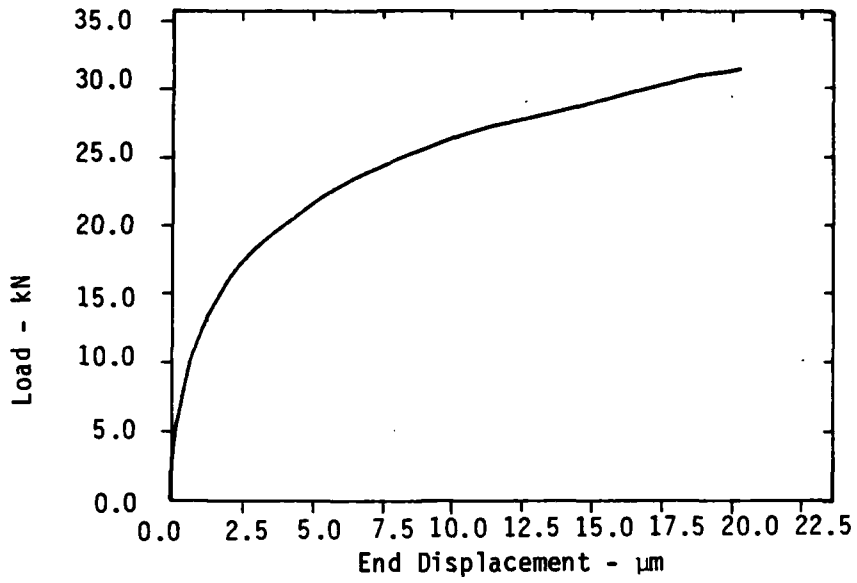


Figure D.36. End displacement versus pullout load, Run W.

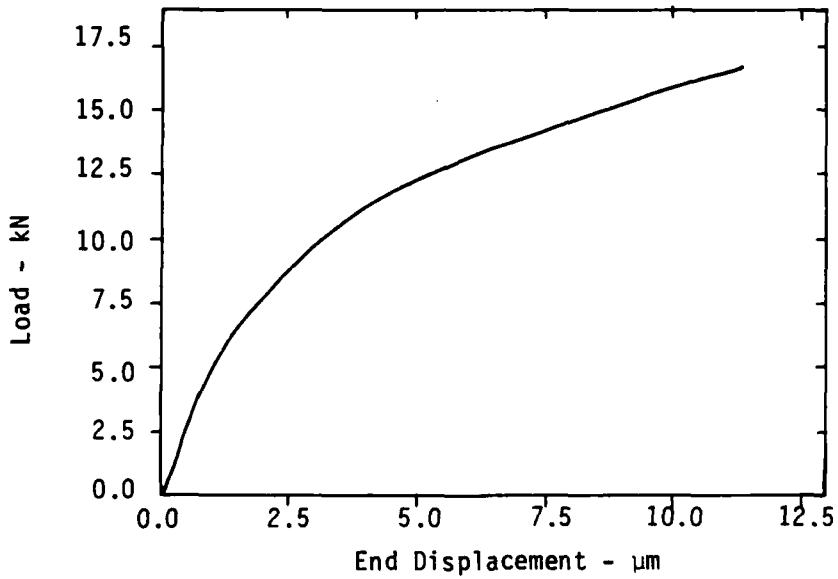


Figure D.37. End displacement versus pullout load, Run X.

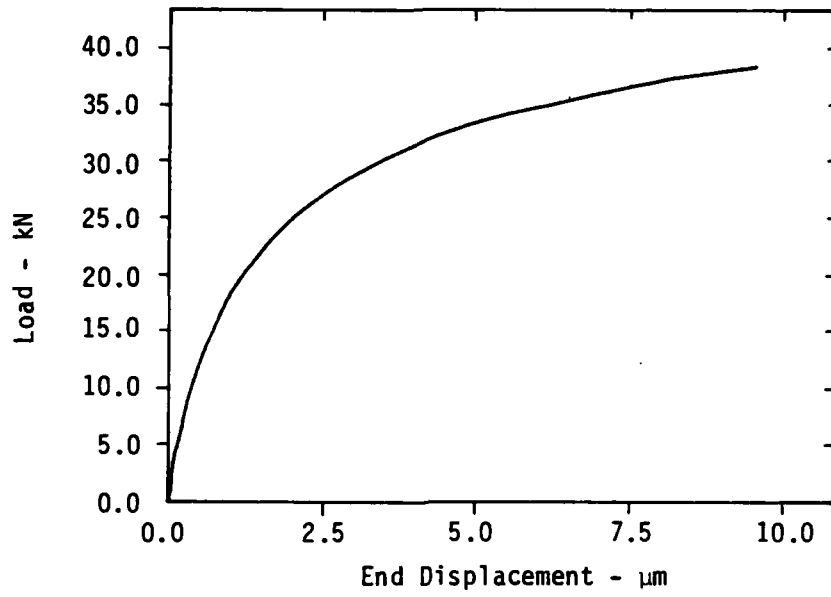


Figure D.38. End displacement versus pullout load, Run Y.

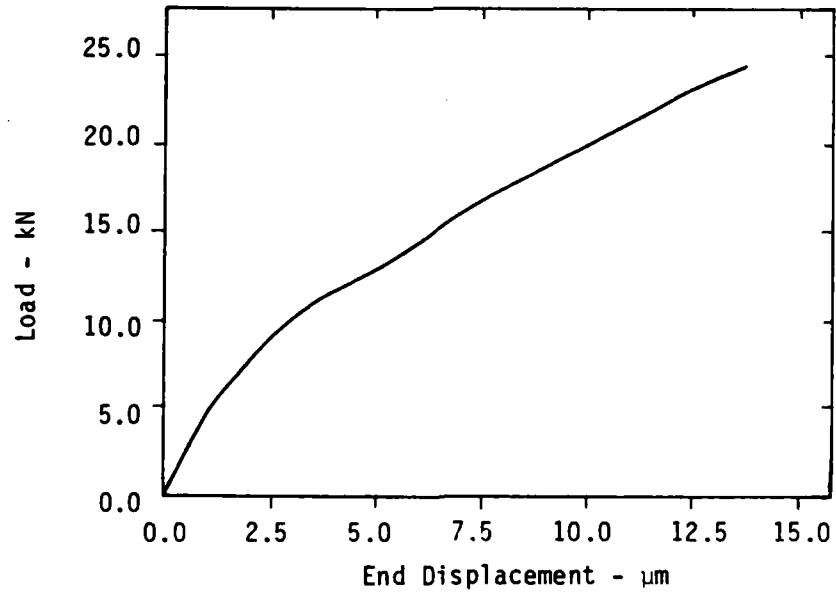


Figure D.39. End displacement versus pullout load, Run Z.

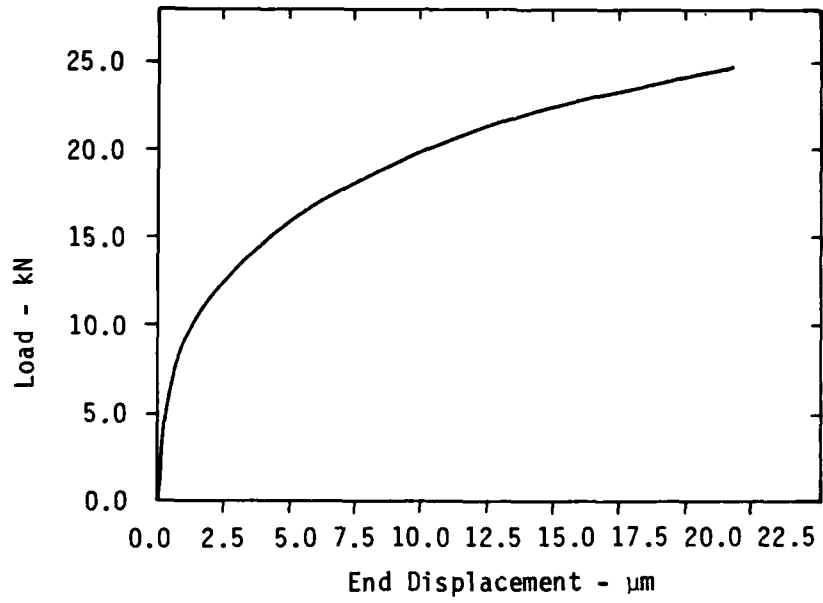


Figure D.40. End displacement versus pullout load, Run AE.

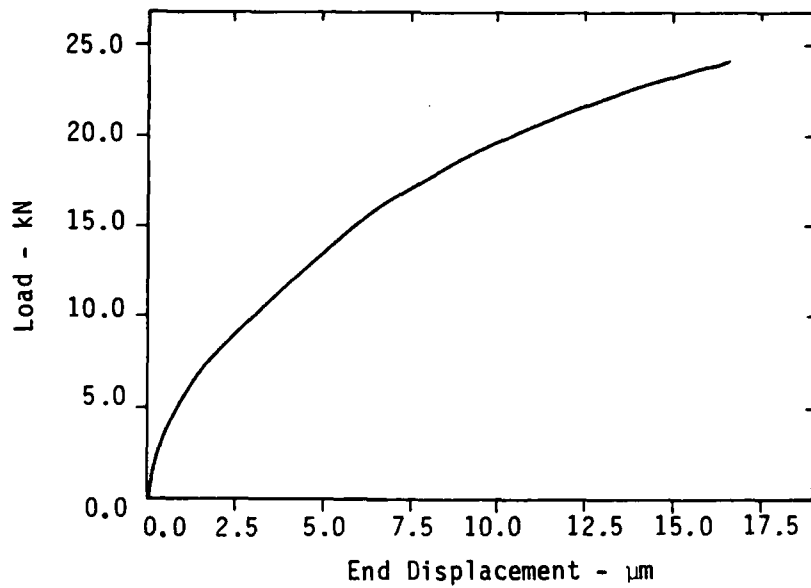


Figure D.41. End displacement versus pullout load, Run AF.

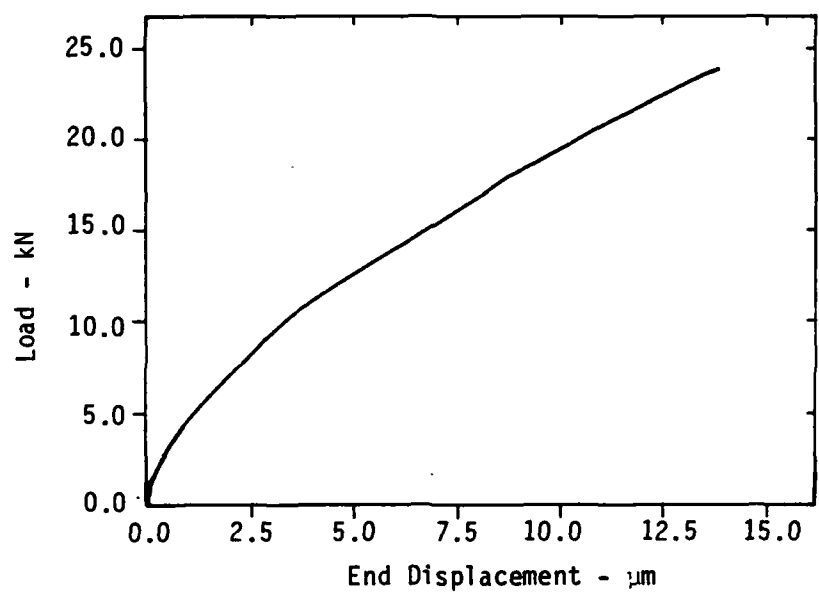


Figure D.42. End displacement versus pullout load, Run AK.

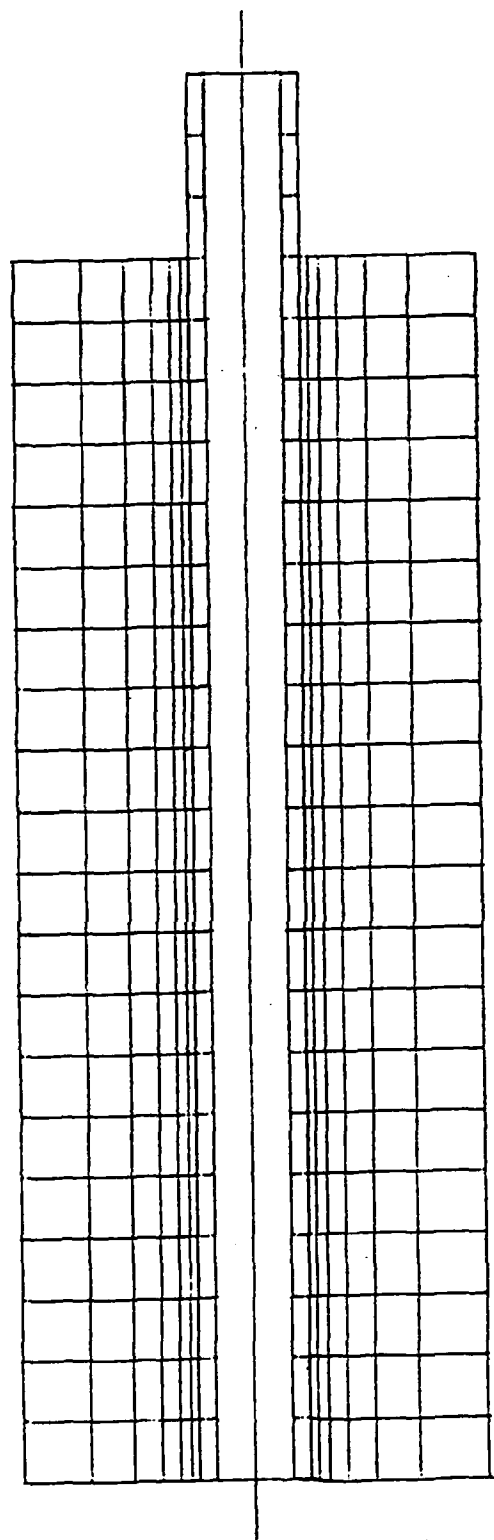


Figure D.43. Modified mesh used in Run AK.

## APPENDIX E

### SUMMARY OF USER'S PANEL MEETINGS

#### 1982 User's Panel Meeting

The first meeting of the User's Panel was held at the San Francisco Airport Hilton on 25 February 1982. This meeting date was selected to coincide with the Earthquake Engineering Research Institute (EERI) meeting at the same location.

In attendance at this meeting were:

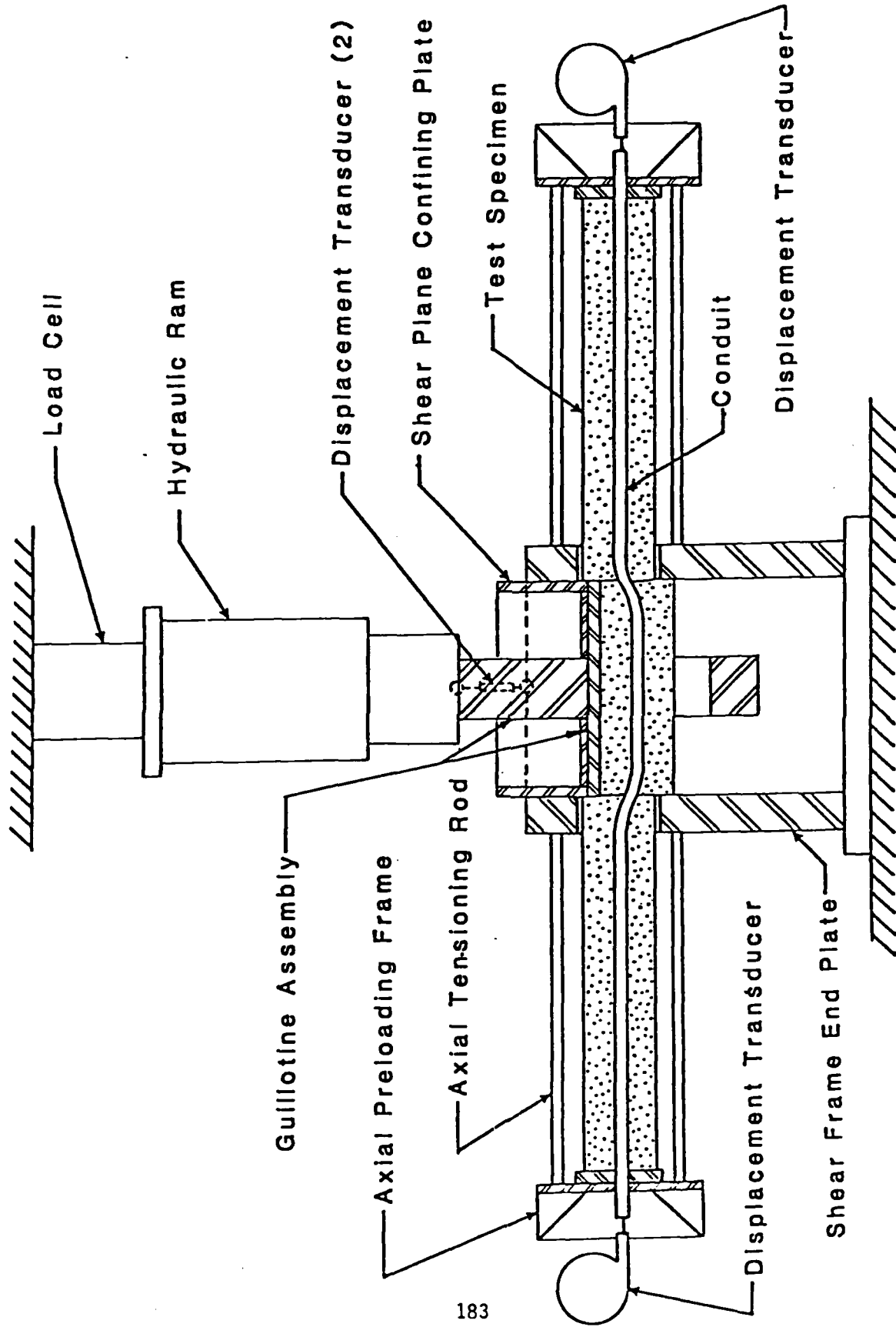
- Dr. William J. Hall, University of Illinois
- Dr. Jeremy Isenberg, Weidlinger Associates
- Dr. R.A. Parmelee, Northwestern University
- Dr. M.J. O'Rourke, Rensselaer Polytechnic Institute
- Dr. Irving J. Oppenheim, Carnegie-Mellon University

Also in attendance were H.C. Davis, J.L. Merritt and K.B. Morrill of Merritt CASES, Inc. and Dr. William Hakala of the National Science Foundation. Dr. Hakala and Dr. Hall were only in attendance for part of the meeting, due to prior commitments. Dr. Liu of NSF, Dr. Goering of DNA, Dr. Hartenbaum of H-Tech Laboratories and Mr. Lund of the Los Angeles Department of Water and Power had indicated before the meeting that they would be unable to attend due to unavoidable conflicts.

All prior work in related research at CASES as well as a description of the current test program, were reviewed at this all-day meeting; the test results to date were also presented. After a presentation of the future test plans was made the meeting was opened for general discussion. Several recommendations were made and conclusions drawn either in support of the existing plans or with some alterations. It was suggested that since the Panel would not meet again

for approximately one year, it might be advisable to contact individual members to obtain their opinion on key points in the program, if that seemed indicated during the ensuing test program. A summary of key points discussed with the Panel follows.

1. Shear failures are more important than axial failures. However, axial effects (friction and slip characteristics between pipe and backfill) influence the shear behavior of the pipe. This is particularly true of the proposed laboratory shear tests using a scaled-up version (to accommodate larger samples of pipe) of the test configuration shown in Figure E.1.
2. Careful consideration should be given to the boundary conditions at the two ends of the test specimen. We could run tests with no restraint and then similar tests with full restraint (to simulate an infinite length of pipe) and therein bracket the actual conditions. In this regard, jointed pipe may be the easier test. Consideration should also be given to the implications of double shear (current test configuration) versus single shear (actual condition).
3. We should expand our pullout test program to define the end restraint conditions for the shear tests. Pullout test data is also valuable design information in itself to define the friction and slip characteristics between the pipe and backfill under axial deformation. The amount of backfill material required in the laboratory tests can be reduced by applying a controlled amount of radial pressure to the outside of the test specimen to simulate the effects of in situ confinement due to overburden stress. We also should probably plan to include additional materials in the pullout test series. These might include coated pipes or wrapped pipes. We should



183

Figure E.1. Double shear test apparatus.

also conduct pull tests on concrete pipe even though unreinforced pipe is the only type available in a 4 in. size. Since the surface condition is the only characteristic which should affect the friction and slip, the internal make-up of the pipe specimen can be disregarded. This assumes that the ultimate strength is not a factor in conducting the pullout tests.

4. The 4 in. ductile iron pipe and the 4 in. vitrified clay pipe, both jointed and unjointed, are suitable materials for conducting the test program.
5. We should look into the possibility of using acoustic emission as a tool for detecting and interpreting movement of the pipe or backfill during the test program.
6. We should conduct pullout tests on longer specimens to evaluate the effect of an increase in the length on the slip characteristics.
7. We should conduct pullout tests using both wet and dry soil to evaluate and quantify the difference in slip characteristics.
8. We should pressurize the jointed pipe specimens during testing to properly simulate an underground condition. It was felt the internal pressure will change the reaction at the joint and it would be important to maintain the pressurized condition. This is particularly true with ductile iron pipe which is capable of containing higher pressures than the vitrified clay pipe.
9. The axial tension and compression tests planned for the 4 in. pipe specimens were considered the least important in the program. It was felt if any segment of the testing should be deleted, those tests would be the most logical choice.

10. It was felt the program would be of most benefit if the tests were planned for providing practical results or design information rather than for building a data base or striving for analytical information.
11. It was suggested that push tests also be included in the pullout test series to establish what difference may exist when the loading condition is reversed.
12. We should contact two individuals who have done significant work in the past and are still involved in defining pipe and soil interface characteristics. They are A. Singhal of Arizona State University and T. O'Rourke of Cornell University.
13. It was agreed that we would provide the User's Panel with interim results consisting of a summary of current tests and proposed future tests.
14. It was suggested that we prioritize experiments to allow for shifts in emphasis arising from significant test results.

#### 1983 User's Panel Meeting

The User's Panel meeting was conducted at the MGM Grand Hotel in Reno, Nevada on February 10, 1983. In attendance at the meeting were H.C. Davis, CASES; B.A. Hartenbaum, H-Tech Laboratories, Inc.; Toshio Mayeda, Los Angeles Department of Water and Power (LADWP); J.L. Merritt, CASES; K.B. Morrill, CASES; I.J. Oppenheim, Carnegie-Mellon University; and M.J. O'Rourke, Rensselaer Polytechnic Institute. The agenda for this meeting is attached. The conclusions and recommendations that resulted from the discussions are detailed below.

AGENDA

SECOND MEETING OF USER'S GROUP

DNA/NSF TESTS OF BURIED LIFELINES AND INSTRUMENTATION/COMMUNICATION CONDUITS

10 February 1983  
MGM Grand Hotel, Reno, Nevada

9:00 a.m. - Noon:

- I. Program Review - CASES
- II. Summary of Test Results to Date - CASES
- III. Single Shear Test Fixture Design, Checkout and Testing Procedures - CASES

LUNCH

1:30 p.m. - 5:00 p.m.

- IV. User's Group Presentations
  - A. Discussion on Calculation of Pipe Strains - M.J. O'Rourke
  - B. Other Presentations - Users
- V. Planned Future Testing - CASES
  - A. Description of 4 in. Diameter Pipe Specimens
  - B. Push/Pullout Tests
  - C. Single Shear Tests
  - D. Ancillary Tests (Beam Tests - Material Tests)
- VI. Proposed Measurements and Instrumentation - CASES
- VII. General Discussion - All
- VIII. Plans and Recommendations for Follow-On Work - All

## General Summary

All work performed to date was summarized for participants in the User's Panel. Results of the pullout tests were specifically reviewed and discussed. It was generally agreed that these tests provided basic data on conduit/sand slip-behavior useful in understanding the characteristics of this interaction. The successful methods used in the conduct of these tests also provided confidence that the same procedures could be used to evaluate larger pipe specimen slip-behavior as well as assist in the interpretation of the proposed single shear tests.

In reviewing the proposed schedule of testing for the remainder of the contract, the Panel emphasized the shear tests were most important. The Panel cautioned that because the single shear test fixture was a new piece of equipment, the variables evaluated during testing should be kept to a minimum. Once confidence in the performance of the device has been achieved, additional parametric testing would be desirable. Some important variables to be considered in the future include:

1. Wet/dry sand
2. Soil cement (LADWP)
3. Wrapped pipe
4. Joint types/configurations
5. Pressurized pipe
6. Overburden stress (magnitude and orientation)

### Specific Meeting Highlights

1. Some concern was expressed for the effect of end conditions in the pullout tests to date.
2. Participants were interested in seeing what pullout test conduit striations would look like with various strength materials and conversely how different strength materials would react to similar pullout test conditions.
3. Pullout tests on concrete pipe or concrete coated pipe or other materials was generally supported as a worthwhile investigation.
4. The interesting observation of our wet sand maintaining its shape after removal of the conduit from the pressure tester was discussed at length. It was felt this phenomenon may be worth further lab study even at the expense of future experiments. All seemed to feel that additional study should be considered on wet sand characteristics.
5. There was concern that friction at the shear plane in the new fixture may not be suitably calibrated out; it was suggested we may need to calibrate the device with a shearing material such as the bearing pad material used on bridges. Use of an elastomer for this purpose was suggested.
6. It was theorized that the friction calibration of the shear plates might extrapolate downward through a point representing the hold-up weight of the box. This might be verified with future data.
7. There was a comment that we might possibly consider more representative soil types in a future test program instead of Lapis Lustre sand.

8. Dry sand as the soil medium for remaining tests on this program was generally supported. It was agreed we should consider these tests as a look into the fundamental behavior of underground lifelines.
9. It was felt we should not complicate the test program until we can fully investigate and understand the operation and capability of the new shear tester. There seemed to be general agreement on this. For instance, do not worry about pressurizing the conduits internally during testing.
10. It was pointed out that the shear tests are breaking new ground and could involve considerable effort to properly investigate the operation and results. Push/pullout tests should be more routine and predictable.
11. Our approach to end restraint, no restraint to full restraint, as a bracketing of the problem, was again supported by the group.
12. We should not try to adhere to the proposed test schedule but rather let the program steer itself based on the progression of test results. All agreed.
13. We should concentrate on testing of Tyton joints in ductile iron pipe rather than mechanical joints because of wider usage and more susceptibility to problems.
14. We should be concerned with properly raining-in the sand to achieve uniformity in the soil boxes. No specific suggestions were made on a method to use for sand raining except the general opinion that some control would need to be employed. The use of superlean grout to assure uniform loading was also offered as an alternate method.
15. The question was raised, "How do we determine when to stop the test?" We will need to monitor the shear test closely to detect early failures.

16. It was suggested we consider using a borescope to monitor shear and joint displacements.
17. It was also suggested we might want to consider using an advanced technology concept for monitoring the shear offset such as microwave, sonic, radar, etc.
18. Consensus seemed to be for bladders to be placed at the top only for confinement. It was noted that we might want to locate the bladders on one side and assume it to be the top. Then the shear would simulate a lateral shear.
19. After some discussion it was generally concluded we should try one bladder placement and stick with it for the duration of the existing program and concentrate on making the machine perform satisfactorily. It was also felt in this remaining program and any follow on, that we should place most emphasis on continuing the shear tests and make the push/pullout tests a lower priority.
20. Toshio Mayeda pointed out that cemented soils are being used in Los Angeles more and more in new pipe installations. At our request, he provided the soil cement specifications and the steel pipeline specifications currently being used by the Los Angeles Department of Water and Power.
21. It was noted we should try to publish the results of our investigations on lifelines in technical journals to support the NSF goals of distributing their program data.

## DISTRIBUTION LIST

### DEPARTMENT OF DEFENSE

Defense Intelligence Agency  
ATTN: RTS-2B

Defense Nuclear Agency  
ATTN: SPTD  
3 cys ATTN: SPSS  
4 cys ATTN: STTI-CA

Defense Technical Information Center  
12 cys ATTN: DD

### DEPARTMENT OF THE ARMY

US Army Ballistic Research Lab  
ATTN: DRDAR-BLA-S, Tech Lib

US Army Engr Waterways Exper Station  
ATTN: Library

US Army Nuclear & Chemical Agency  
ATTN: Library

### DEPARTMENT OF THE NAVY

Naval Surface Weapons Center  
ATTN: Code F31

### DEPARTMENT OF THE AIR FORCE

Air Force Institute of Technology  
ATTN: Library

Air Force Weapons Laboratory  
ATTN: NTE, M. Plamondon  
ATTN: SUL

Ballistic Missile Office/DAA  
2 cys ATTN: ENSH

### DEPARTMENT OF ENERGY

University of California  
Lawrence Livermore National Lab  
ATTN: Tech Info Dept Library

Sandia National Laboratories  
ATTN: Library & Security Classification Div

Sandia National Laboratories  
ATTN: Tech Lib 3141

### OTHER GOVERNMENT AGENCIES

Federal Emergency Management Agency  
ATTN: Ofc of Rsch/NP, D. Benson

Los Angeles Dept of Water and Power  
ATTN: Mr. Lund  
ATTN: Mr. Mayeda

National Bureau of Standards  
ATTN: Dr. R. Wright III

National Science Foundation  
ATTN: Dr. W. Hakala  
5 cys ATTN: Dr. K. Thirumalai

### DEPARTMENT OF DEFENSE CONTRACTORS

Aerospace Corp  
ATTN: Library Acquisition M1/199

Agabian Associates  
ATTN: M. Agabian

Applied Research Associates, Inc  
ATTN: D. Piepenburg

Arizona State University  
ATTN: A. Singhal

BDM Corp  
ATTN: Corporate Lib

Boeing Co  
ATTN: Aerospace Library

California Research & Technology, Inc  
ATTN: K. Kreyenhagen

California Research & Technology, Inc  
ATTN: F. Sauer

California Institute of Technology  
ATTN: C. Babcock

Carnegie Mellon University  
ATTN: I. Oppenheim

University of Colorado  
ATTN: S. Datta

Cushing Associates  
ATTN: V. Cushing

Ductile Iron Pipe Research Association  
ATTN: D. Ford

GTE  
ATTN: R. Sullivan

H-TECH Labs, Inc  
ATTN: B. Hartenbaum

IIT Research Institute  
ATTN: Documents Library

University of Illinois  
ATTN: W. Hall

Kaman Sciences Corp  
ATTN: Library

Kaman Tempo  
ATTN: DASIAC  
ATTN: J. Shoutens

Kaman Tempo  
ATTN: DASIAC

Merritt CASES, Inc  
ATTN: Library  
2 cys ATTN: G. Wintergerst  
2 cys ATTN: H. Davis  
2 cys ATTN: J. Merritt  
2 cys ATTN: K. Morrill

DEPARTMENT OF DEFENSE CONTRACTORS

University of New Mexico  
ATTN: N. Baum

Northwestern University  
ATTN: Dr. R. Parmelee

Nyman Associates  
ATTN: Dr. D. Nyman

University of Oklahoma  
ATTN: L. Ru-Liang Wang

R & D Associates  
ATTN: J. Lewis  
ATTN: Technical Information Center

R & D Associates  
ATTN: G. Ganong

Rensselaer Polytechnic Institute  
ATTN: ATTN: Dr. M. O'Rourke

S-CUBED  
ATTN: Library

Science & Engrg Assoc, Inc  
ATTN: B. Chambers

Science Applications Intl Corp  
ATTN: Technical Library

Science Applications Intl Corp  
ATTN: W. Layson

Pacific-Sierra Research Corp  
ATTN: H. Brode, Chairman SAGE

DEPARTMENT OF DEFENSE CONTRACTORS

SRI International  
ATTN: G. Abrahamson

Stanford University  
ATTN: Dr. Shih-Chi-Liu

Structural Mechanics Associates, Inc  
ATTN: R. Kennedy

Terra Tek, Inc  
ATTN: S. Green

TRM Electronics & Defense Sector  
ATTN: Technical Information Center  
2 cys ATTN: N. Lipner

TRM Electronics & Defense Sector  
ATTN: P. Dai

University of Tulsa  
ATTN: Dr. T. Ariman

Weidlinger Assoc, Consulting Engrg  
ATTN: T. Deevy

Weidlinger Assoc, Consulting Engrg  
ATTN: M. Baron

Weidlinger Assoc, Consulting Engrg  
ATTN: J. Isenberg

Cornell University  
ATTN: T. O'Rourke